

A new morphological dataset reveals a novel relationship for the adzebills of New Zealand (*Aptornis*) and provides a foundation for total evidence neoavian phylogenetics

GRACE M. MUSSER¹ AND JOEL CRACRAFT²

ABSTRACT

Relationships among Neoaves, a group comprising approximately 95% of all extant birds, are difficult to resolve because of multiple short internodes presumably created by a rapid evolutionary radiation around the K/Pg boundary. This difficulty has plagued both morphological and molecular studies. Compared with molecular studies with extensive taxon and character sampling, morphological datasets have largely failed to provide insight into the phenotypic evolutionary transitions of the neoavian radiation. Extinct neoavian taxa remain an understudied but critical key to resolving relationships among these problematic stem lineages and understanding evolutionary changes in structure and function. Adzebills (*Aptornis*), some of the most phylogenetically controversial fossil neoavians, are extinct terrestrial birds endemic to New Zealand since at least the early Miocene. Past morphological studies have placed adzebills as a sister taxon to the flightless Kagu of New Caledonia (*Rhynochetos jubatus*) or to the land- and waterfowl group Galloanseres. Recent molecular studies reveal the Kagu and Sunbittern (*Eurypyga helias*) to be sister taxa, whereas adzebills have been postulated to be within Rallidae (rails, gallinules, and coots) or the sister taxon of Sarothruridae (flufftails) or Ralloidea (finfoots, flufftails, and rails). To better resolve the position of adzebills and begin constructing a fine-scale total evidence phylogenetic dataset for the base of Neoaves, we constructed a new and more comprehensive morphological dataset of 368 discrete osteological characters for 38 extant

¹ The University of Texas at Austin, the Jackson School of Geosciences.

² Department of Ornithology, American Museum of Natural History.

and two extinct taxa that includes extensive sampling of nearly all neoavian stem lineages. We then combined this dataset with 32 DNA sequences of the slowly evolving nuclear RAG1 and RAG2 genes. Morphological results place adzebills as the sister taxon of trumpeters (*Psophia*) within core Gruiformes and confirm strong support for a Kagu+Sunbittern sister group (99% bootstrap value). Results for analyses of the combined data were identical, and the adzebill+trumpeter clade was supported by a 99% Bayesian clade credibility value. Although the Kagu+Sunbittern sister group is consistent with recent molecular hypotheses, the adzebill+trumpeter group is novel.

INTRODUCTION

Proposed phylogenetic relationships at the base of Neoaves, a group comprising approximately 95% of all extant bird lineages, conflict across numerous molecular and morphological studies of Neoaves (Jarvis et al., 2014; Prum et al., 2015; Reddy et al., 2017). This uncertainty is generally attributed to a rapid evolutionary radiation that occurred around the K-Pg mass extinction event approximately 66 million years ago (mya), with stem lineages of Neoaves diversifying over a short 5 to 8 million year window (Livezey and Zusi, 2007; Jarvis et al., 2014; Prum et al., 2015; Claramunt and Cracraft, 2015). The short internodes created by this radiation have led to difficulties in resolving the stem lineages of modern birds, especially at the base of the tree of Neoaves.

The problematic consequences of these short internodes are further exacerbated by the questionable positions of many neoavian taxa represented by fossils. Past morphological studies including these extinct taxa tend to have limited taxon sampling and/or be based on preconceptions regarding neoavian phylogeny. At the same time, increased focus on molecular data has limited insight into the placement of these extinct taxa and has dramatically slowed construction of comprehensive neoavian morphological studies (Cracraft and Clarke, 2001; Mayr and Clarke, 2003; Livezey and Zusi, 2007; Jarvis et al., 2014; Prum et al., 2015). As a result, little is understood regarding the early phenotypic transitions among neoavian lineages.

An important key to resolving the base of the neoavian tree and uncovering neoavian phenotypic transitions may be in understanding relationships among taxa that at one time were grouped into Gruiformes (now limited to rails, cranes, and allies), as many of these are now known to have close affinities with multiple basal neoavian clades. Gruiformes were first established by Max Fürbringer (1888) and came to comprise many families, including Rallidae (rails, gallinules, and coots), Gruidae (cranes), Otidae (bustards), Mesitornithidae (mesites), Rhyonchetidae (the Kagu), Turnicidae (button quails), Aramidae (the Limpkin), Psophiidae (trumpeters), Heliornithidae (finfoots), Eurypygidae (the Sunbittern), Cariamidae (cariamias), Sarothruridae (flufftails), and Pedionomidae (the Plains-wanderer). Multiple 20th-century studies subsequently suggested that most of these families are distantly related to one another (Olson and Steadman, 1981; Olson, 1985; Sibley and Ahlquist, 1990 [with removal of Turnicidae]; Houde et al., 1997). Twenty-first century morphological and molecular studies have supported several of these later hypotheses and confirmed that the historic “Gruiformes” is not monophyletic (Fain and Houde, 2004; Fain et al., 2007; Ericson et al., 2006; Livezey and Zusi,

2007; Hackett et al., 2008; Jarvis et al., 2014; Prum et al., 2015). It is now generally accepted that monophyletic “core Gruiformes,” or Gruiformes sensu stricto, comprise Aramidae, Rallidae, Gruidae, Psophiidae, Heliornithidae, and Sarothruridae. The relationships of families that historically were included within the order have remained problematic, and some relationships within Gruiformes sensu stricto remain controversial, especially those within Ralloidea (Livezey, 1998; Livezey and Zusi, 2007). Phylogenetic resolution and morphological analysis of “historic” and core Gruiformes have important implications for neoavian temporal history, as many of these taxa have a rich Paleogene fossil record and are of global significance for understanding neoavian biogeographic history. The strange New Zealand extinct taxon *Aptornis* is positioned in the middle of many arguments about the relationships of former and current gruiform taxa and thus may play an important role in understanding early evolution of neoavian stem lineages.

To better resolve the phylogenetic placement of *Aptornis* (adzebills) and further elucidate evolutionary phenotypic transitions within basal Neoaves, we created a new morphological dataset that provides a foundation for analyzing phenotypic transitions within Neoaves and total-evidence basal neoavian phylogenetics. Resolving the phylogenetic placement of adzebills and elucidating their phenotypic evolution in the context of other basal lineages has important implications for understanding the evolution and biogeographic history within Neoaves broadly.

THE ADZEBILLS (*APTORNIS*)

Aptornis (adzebills), a genus comprising extinct terrestrial birds endemic to the North and South islands of New Zealand from at least the early Miocene to the 13th century (Wilmhurst et al., 2008; Wood et al., 2017), is a problematic gruiformlike fossil taxon that has eluded phylogenetic placement since its first description by Owen (1843). Owen (1843) described *Aptornis* from a tibiotarsus and originally identified the remains as a new species of moa, *Dinornis otidiformis*. After more osteological elements of *Aptornis* were discovered, Mantell (1848) and then Owen (1849) renamed the genus *Aptornis* based on unique metatarsal and cranial characters to distinguish the taxon from *Dinornis* (Giant Moa) and *Palapteryx* (Giant Moa, now included in *Dinornis*). *Aptornis* had been spelled in a previous publication as *Apterornis* (Hesse, 1990); however, it is believed that this spelling was erroneous (Weber and Krell, 1995) and that this is likely due to *Apterornis* having been used by several authors to denote other genera, including a genus of dodos (Sélys Longchamps, 1848) and a subgenus of *Porphyrio* (swamphen) (Fürbringer, 1888). Since Owen (1843), *Aptornis* has been the prevailing name used for the genus.

Most workers currently recognize two species of adzebills, *Aptornis defossor* (South Island Adzebill) and *Aptornis otidiformis* (North Island Adzebill) (Owen, 1849). Body height of both species was approximately 80 cm; however, more robust specimens with a body weight closer to 19 kg are often categorized as South Island Adzebills, while smaller and more gracile specimens weighing around 16 kg are typically assigned to the North Island species (Worthy and Holdaway, 2002). Worthy et al. (2011) described a third adzebill species, *A. proasciarostratus*, based on two thoracic vertebrae from the early Miocene St. Bathans Fauna site in Central Otago (South Island). *A. proasciarostratus* is distinguished from the North and South Island

Adzebills by relatively smaller size, increased pneumaticity of the corpus vertebrae, and unique characteristics found in the processus spinosus and processus transversus; however, no additional individuals representing this species have been recovered to date. W.W. Smith excavated a relatively larger adzebill-like skull at Albury, South Canterbury, around 1888 and Owen designated the taxon *Aptornis bulleri* but never described the species; thus, this name has remained a nomen nudum (Worthy and Holdaway, 2002). Hamilton (1891) suggested that this size difference may have been due to sexual dimorphism.

The fossil record of *Aptornis* suggests a coastal distribution for both species on the North and South islands. The first elements found of *Aptornis*, a tibiotarsus and femur, were found on the east coast of the North Island of New Zealand (Owen, 1843). A complete skeleton of *A. otidiformis* and an almost complete skeleton of *A. defossor* were extracted from a limestone cave at Te Kuiti, a northwestern region of the North Island about 30 km from the western coast, and described by Owen (1849). Owen (1871) reported 105 *A. defossor* bones, representing at least 8 individuals, as found in Sims Cave, Bone Cave, and Earl Grey Cave at an unnamed site in Takaka Hill, near the northern coast of the South Island. A skull, femur, and tibiotarsus of *A. defossor* were subsequently found in a cave about 14 miles from Oamaru and forwarded to Owen in 1863 (Owen, 1879). Elements of *Aptornis* species discovered during the 19th century appear to remain robustly preserved and intact, and many are three-dimensional; nonetheless, Owen (1879) described them as “rare.”

More recent excavation of *Aptornis* has largely been conducted by Australia-based paleozoologist Trevor Worthy. Such excavations have shown that while the Holocene fossil record of *Aptornis* is fairly robust, older specimens are extremely rare and possess comparatively few elements. The oldest-known *Aptornis* specimen was found and described by Worthy et al. (2011) and comprises two early Miocene thoracic vertebrae of the potential *A. proasciarostratus* from the St. Bathans Fauna site in Central Otago, South Island. A distal femur, an additional vertebral fragment, a phalanx, and possibly a tibiotarsal fragment from the site have also been attributed to this species. Worthy and Holdaway (1994) suggested that *Aptornis* remains are rare in sites closer to the coast in Takaka Hill, as only four (undated) *A. defossor* individuals have been subsequently found at that locality. Worthy and Holdaway (1993) excavated four *A. defossor* individuals at Takaka Valley, and commonly found more elements of these species in Otiran glaciation deposits (ca. 13,000–10,000 years old) of Honeycomb Hill Cave in the Oparara (an inland site near the northwestern coast of the South Island). *Aptornis* appeared to prefer habitats located on the eastern coast of the South Island during the Holocene, as fossils have been located within that region (Worthy and Holdaway, 1994), but have not been found in Otiran and other Holocene deposits on the west coast (Worthy and Holdaway, 1993).

It is generally accepted that adzebills were terrestrial, flightless birds, but several aspects of their ecology remain largely unknown (Worthy and Holdaway, 2002; Wood et al., 2017; Worthy et al., 2017). The localities of recovered adzebill remains point to a coastal distribution for both species on the North and South islands. Worthy and Holdaway (2002) proposed that adzebills preferred shrublands and grasslands, as Holocene fossils have been distributed across eastern regions of the North and South islands. More recent evidence from Wood et

al. (2017) suggests that adzebills preferred dry podocarp forests, as most adzebill remains found in the graveyard deposit within the Honeycomb Hill Cave System in Oparara (19+ individuals) were within strata above a pollen sample indicative of mixed podocarp-beech forest (Worthy and Mildenhall, 1989).

Diet may be the facet of adzebill ecology that has garnered the most focus. Owen (1879) hypothesized that the morphology of adzebill skulls suggests a carnivorous diet of earthworms and lepidopteran (moth and butterfly) larvae, especially as its robust but elongate beak may have been used for “thrusting” into the ground, and he believed that the tarsometatarsus possesses digging and scratching adaptations. The limited additional evidence regarding the life history of adzebills has so far been consistent with this original hypothesis. Two almost complete adzebill skeletons at the Otago Museum, New Zealand, contain small gizzard stones (35 stones weighing approximately 16 g and 23 stones weighing approximately 8 g), which supports a strictly carnivorous diet as herbivore remains tend to contain relatively large gizzard stones (Worthy and Holdaway, 2002). Worthy and Holdaway (2002) also found that stable isotope values for ^{15}N within bone gelatin of two North Island Adzebill individuals supported the predator hypothesis, as both specimens exhibited higher levels of ^{15}N than two herbivores (Coastal Moa, *Euryapteryx curtus*; Finsch’s Duck, *Chenonetta finschi*) and one insectivore (New Zealand Owlet Nightjar, *Aegotheles novaezealandiae*). They additionally confirmed that muscle attachment points apparent on the skull and cervical vertebrae coupled with a shortened tarsometatarsus likely allowed adzebills to dig with their rostrum and feet, and suggested that their large lacrimals may indicate nocturnal hunting and emphasis on olfactory prey detection. Most recently, stable isotope analysis of Holocene South Island Adzebill bone implied similar results as high enrichment of ^{15}N strongly suggested a high (predatory) trophic level (Wood et al., 2017). Wood et al. (2017) posited that adzebills consumed a variety of invertebrates and vertebrates by penetrating rotten logs and/or excavating burrowing animals, including bivalves (*tuatua*) and burrow-nesting birds such as kiwis. Relatively lower levels of ^{13}C do not rule out the possibility of marine bird consumption, and the degree of dietary specialization within adzebills remains unknown.

Due to its high trophic level and consequent lack of predators, it is likely that adzebills became extinct due to human activity. Polynesian settlers (*Māori*) arrived in New Zealand during the 13th century (Wilmhurst et al., 2008) and hunted both North and South Island Adzebills. This coupled with habitat loss and possible predation by the introduced Polynesian rat (*Rattus exulans*; *kiore*) and dogs quickly led to the demise of adzebills (Fleming, 1969; Worthy and Holdaway, 2002). When European settlers arrived on the islands in the 17th century, adzebills had already been eliminated.

PROPOSED SISTER RELATIONSHIPS OF ADZEBILLS

It has been hypothesized that the difficulty of placing *Aptornis* arises from its large size and high number of apomorphic characters (Cracraft, 1982a; Livezey, 1998). Early studies of the genus posited that adzebills were either basal members of Gruiformes, basal rails, or most

closely related to *Rhynochetos jubatus* (the Kagu), an extant flightless bird endemic to New Caledonia called “the ghost of the forest” by the Kanak tribe. Following the original assignment of the holotype within the moa genus *Dinornis* and its subsequent placement in the new genus *Aptornis*, Owen (1879) suggested that adzebills may be most closely related to the *takahē* or *Notornis* (*Porphyrio hochstetteri*), a flightless New Zealand rail, due to the large size of the skull, width of the bill, and small brain cavity size. Subsequent comparative studies continued to place adzebills within core Gruiformes. Parker (1866) described the skull of *Aptornis* as having ralline characteristics but as being most morphologically similar to *Psophia* (trumpeters) due to well-developed basitemporal pterygoid processes, a decurved lower mandible, and nearly complete ossification of the interorbital septum. Parker also suggested that *Aptornis* was likely a member of *Notornis*, and even proposed that its name be changed to *Notornis casuarinus*. Beddard (1898) additionally described the skull of *Aptornis* as somewhat ralline but ultimately conceded along with Fürbringer (1888) that *Aptornis* is most closely aligned with *R. jubatus* due to the presence of schizorhinal nostrils and partial ossification of the nasal septum. Lowe (1926) agreed that adzebills shared porphyriine (referring to the genus *Porphyrio*) and ocydromine (referring to the obsolete brevi-pennate rallid genus *Ocydromus*, as detailed in Buller, 1878, now typically placed in *Gallirallus*, *Hypotaenidia*, or *Rallus*, as noted in Hoyo et al., 2019) characteristics, and concluded that the taxon was ultimately “too primitive” to fall within core Gruiformes. Oliver (1945) and Oliver (1955) similarly proposed a close relationship between *Aptornis* and the Rallidae.

Later morphological studies of adzebills have largely placed it as a sister taxon to the Kagu. Cracraft (1982a) found adzebills and Kagu to be sister taxa based primarily on pelvic similarities and recovered both genera within a monophyletic clade exclusive of other core Gruiformes that also included *Psophia*, *Cariama* (seriamas), and *Eurypyga helias* (the Sunbittern). Olson (1987) concurred that adzebills are most closely related to the Kagu. Livezey (1998) and Livezey and Zusi (2007) also found an *Aptornis*+Kagu sister group with strong support (97% bootstrap support, 11 Bremer support value; 86% bootstrap support, 7 Bremer support value, respectively). A morphological study by Weber and Hesse (1995) proposed an adzebill+Galloanseres sister group based on unique articulation of the eminentia articularis of the quadrate with the zygomatic process of the squamosal; however, Worthy and Holdaway (2002) noted that a similar feature can also be seen in the *takahē* (*Porphyrio hochstetteri*). Hesse (1990) also suggested a relationship between adzebills and Galloanseres due to a rostrally open temporal fossa with a bony bridge present between the postorbital and zygomatic processes, the presence of a tuberculum subcapitulare in the quadrate, and a longer femur than tarsometatarsus. Oliver (1945, 1955) suggested a relationship between adzebills and *Diaphorapteryx hawkinsi* (Giant Chatham Island Rail), and Worthy et al. (2011) suggested that adzebills fall within Ralloidea (rails, finfoots, and flufftails); however, these results were based solely on description of adzebill vertebrae and not on phylogenetic analysis.

Many recent neoavian molecular studies have aligned trumpeters as the sister taxon of Aramidae and Gruidae (Fain and Houde, 2004; Fain et al., 2007; Ericson et al., 2006; Hackett et al., 2008; Jarvis et al., 2014; Prum et al., 2015) and have placed the Kagu+Sunbittern sister

group as the joint sister taxon to the tropicbirds, far removed from core Gruiformes (Houde et al., 1997; Fain and Houde, 2004; Ericson et al., 2006; Hackett et al., 2008). Using 673 bp of mtDNA 12S rRNA from *A. defossor*, Houde et al. (1997) placed adzebills as the sister group of Heliornithidae and both, in turn, were placed as the sister to *Psophia*+Rallidae in a parsimony analysis. Houde et al. (1997) also placed *Aptornis* as the sister taxon of rails using maximum-likelihood methods, with *Psophia* forming the sister taxon to an *Aptornis*+Rallidae sister group; thus, their fragmentary data for a single gene pointed to a gruiform relationship for *Aptornis* and did not support affinities to the Kagu. Subsequent molecular studies including adzebills in taxon sampling since Houde et al. (1997) present a similar placement of this taxon; however, these studies only used the Houde et al. (1997) sequence. Most recently, Boast et al. (2019) compiled near-complete mitochondrial genomes of the South Island and North Island Adzebills and recovered an *Aptornis*+Sarothruridae sister group with high support (100% clade credibility).

In summary, the dominant hypotheses proposed for the sister taxon of adzebills comprise the Kagu, Galloanseres, the Ralloidea, or only the Rallidae or Sarothruridae. Resolving the controversial phylogenetic placement of adzebills and elucidating their phenotypic evolution in the context of other basal lineages has important implications for understanding phenotypic evolution and biogeographic history within Neoaves broadly. Here, we investigate the phylogenetic placement of adzebills and further elucidate phylogeny and phenotypic character variation within basal Neoaves.

MATERIALS AND METHODS

MORPHOLOGICAL CHARACTER MATRIX CREATION AND SCORING: The morphological character matrix on which this study is based is available online via Morphobank (O’Leary and Kaufman, 2012; Project 3419, <http://morphobank.org/permalink/?P3419>). Morphological character descriptions are provided in appendix 1. We first created characters de novo without examining published character matrices to avoid preconceptions regarding avian relationships and morphology as much as possible. Characters were excluded if homology issues were perceived a priori (Salisbury, 1999; Livezey and Zusi, 2006), especially when comparing highly autapomorphic taxa such as *Aptornis*. Independence of characters was assessed via logical evaluation of the mutual exclusivity of characters and associated character states, as detailed in Livezey and Zusi (2006). As in this previous study, nonindependent character states were included within a single multistate character when necessary to avoid redundancy of “additive binary” characterization.

Once our original character list was created, we then compared this against published character matrices to address character overlap and add previously created characters that described morphological variation within our taxon sampling. This included reevaluation of all neoavian osteological characters defined by Livezey and Zusi (2006), the largest morphological dataset for Neoaves to date, relevant for our taxon sampling. Incorporated characters are discussed in appendix 1. Criteria for including characters from past analyses comprised

replicability, independence, and discreteness. Polymorphic and juvenile characters were excluded. Characters were coded numerically, with basal absence coded as (0) and nonapplicable and missing data coded identically as (?). Present, derived character states and absences were coded from (1–6). These scorings are not intended to represent an ordered series.

Morphological characters were created through direct study of skeletal specimens from the Departments of Ornithology and Vertebrate Paleontology of the American Museum of Natural History and the Ornithology Collection of the Field Museum of Natural History. The 368 osteological characters in this study comprised 131 characters of the skull, 27 characters of the vertebrae, 33 characters of the sternum and sternal ribs, 14 characters of the coracoid, 5 characters of the scapula, 34 characters of the humerus, 6 characters of the ulna, 4 characters of the carpometacarpus, 43 characters of the pelvis, 1 character of the intratendinous ossification of the hindlimbs, 22 characters of the femur, 25 characters of the tibiotarsus, and 23 characters of the tarsometatarsus.

TAXONOMIC SAMPLING: The South Island Adzebill (*Aptornis defossor*) was the exemplar for adzebills. Material consisted of two individuals from the Vertebrate Paleontology collection at the American Museum of Natural History: one largely complete mandible, rostrum and postcranial skeleton missing some wing and pedal elements (AMNH 7300), as well as a skull (AMNH 60) and mandible (AMNH 61) from another individual. A lithographic plate from Owen (1879: pl. LXXXIII) was also used to code missing or damaged elements of *A. defossor* when necessary and reasonable, and the use of this publication is noted for applicable characters in appendix 1. *Diaphorapteryx hawkinsi* material comprised a skull (AMNH 7424), mandible (AMNH 7425), humerus (AMNH 7426), femur (AMNH 7428), tibiotarsus (AMNH 7429) and pelvis (AMNH 7427). A lithographic plate of several elements of *D. hawksinsi* from Andrews (1896: pl. III) was used to score characters for this taxon when necessary and possible, and such instances have been noted in appendix 1. The giant Chatham Island rail was included as it is considered to be a basal rail, and Houde et al. (1997) found adzebills as the sister taxon of Rallidae or Ralloidea.

Recent molecular studies and past phylogenetic studies of the adzebill guided selection of exemplars for extant taxa, which are detailed in table 1 (Weber and Hesse, 1995; Cracraft, 1982a; Houde et al., 1997; Hackett et al., 2008; Jarvis et al., 2014; Prum et al., 2015; Claramunt and Cracraft, 2015). Complete or largely complete skeletons were examined from the Department of Ornithology Collection at AMNH, and one specimen (*Mentocrex kioloides*) was included from the Ornithology Collection of the Field Museum of Natural History. The Kagu and Sunbittern were included due to conflicting results regarding the relationship of the Kagu to adzebills and multiple studies that have resulted in an *Aptornis*+Kagu sister group (Fürbringer, 1888; Beddard, 1898; Cracraft, 1982a; Olson, 1987; Livezey, 1998; Livezey and Zusi, 2007). Core Gruiformes were included as both gruoid and ralloid taxa have been hypothesized to be sister taxa of *Aptornis* (Parker, 1866; Lowe, 1926; Owen, 1879; Houde et al., 1997; Worthy and Holdaway, 2002). *Porphyrio hochstetteri* (Notornis), *Himantornis haematopus whitesidei* (Nkulengu Rail), *Canirallus oculus batesi* (Grey-throated Rail), *Aramides cajanea* (Grey-necked Wood Rail), *Mentocrex kioloides* (Madagascar Wood-rail) and *Gallirallus* sp. (*Weka*) were specifically included as morpho-

logical and molecular studies have suggested that these species represent the basalmost lineages of rails, and it has repeatedly been suggested that adzebills are most closely related to *Notornis* (Parker, 1866; Lowe, 1926; Owen, 1879; Worthy and Holdaway, 2002). *Mentocrex kiolooides* and the Sarothruridae additionally provide a test of the *Aptornis* + Sarothruridae sister group hypothesis put forth by Boast et al. (2019). Galliform taxa and tinamous were used as outgroups. Galliform taxa also served as a test of the hypothesis put forth by Weber and Hesse (1995) that adzebills are a sister taxon to Galloanseres. Additional comparative taxa included species from Aequornithes, Caprimulgiformes, Charadriiformes, Phaethontidae, Opisthocomidae, Gruoidea, and higher land birds. These were added because of the uncertainty surrounding which groups might be most closely related to historic and core Gruiformes and to test the relationship of *Aptornis* to each of these basal lineages.

Multiple specimens were used to code each exemplar when possible, and the species names and specimen numbers of these exemplars are noted in table 1. Species within the same genus were used to code missing elements of rarer taxa when identical species were not available, and the species name and numbers of these alternative specimens are detailed in table 1. Illustrations of *Podica senegalensis* (African Finfoot) from Beddard (1890) were used to score cranial characters for this taxon when possible, as no skulls were present for AMNH *P. senegalensis* specimens. Such occurrences have been noted in appendix 1.

ANALYSES AND MOLECULAR AND COMBINED MATRICES: The morphological data matrix was created using Mesquite and was analyzed in PAUP* (Swofford, 2002; Version 4.0a, build 161) using heuristic parsimony search methods. No weighting or ordering of characters was employed, and the data were unconstrained. Parsimony settings were default with the exception of using 10,000 random replicates. Default parsimony settings for this version and build of PAUP* included collapsing branches if maximum length was zero; using accelerated transformation for optimizing unordered characters; allowing only states that can be identified as possible shortcuts via the “3+1” test for assignment of states not observed in tips to the internal nodes; interpreting multiple states as uncertainties; using minimum-possible single-character lengths for calculating CI, RI, and RC; and treating gap states as missing data. The default heuristic search settings kept only optimal trees, acquiring starting trees for branch-swapping through stepwise addition, swapping on the best tree only when multiple starting trees are present, using a TBR swapping algorithm with a reconnection limit of 8, and saving multiple trees. Bootstrap support values were calculated from 100 replicates with all heuristic settings default except for the use of 1000 random addition sequence replicates. Only groups with greater than 50% bootstrap values were retained. Monophyly-constraint analyses used the same settings as primary parsimony heuristic analysis with the exception of using 1000 replicates. Optimized synapomorphies were only considered to be evidence for the relationship of a group if both taxa were scored (no missing data was present) and had identical terminal character states for each target taxon. Additional synapomorphies that include missing states or differing terminal states are not detailed as evidence of relationship but are reported in table 2.

The molecular matrix comprised nuclear (RAG1 and/or RAG2) exonic sequences from 32 species that had a maximum final alignment length of 4038 base pairs, with gaps and/or miss-

TABLE 1. Complete list of specimens used to create morphological characters, data matrix and combined data matrix.

Group name	Skeletal specimens	Molecular sequences
Tinamidae	<i>Crypturellus undulatus undulatus</i> (primary: AMNH 2751; secondary: AMNH 6479), <i>Tinamus solitarius</i> (AMNH 21983)	<i>Crypturellus</i> <i>Tinamus guttatus</i>
Galliformes	<i>Lophura bulweri</i> (AMNH 10962, AMNH 16532), <i>Gallus varius</i> (AMNH 16531), <i>Gallus gallus</i> (AMNH 18555, AMNH 4031)	<i>Gallus gallus</i>
Gaviidae	<i>Gavia immer</i> (AMNH 15919)	<i>Gavia immer</i>
Spheniscidae	<i>Pygoscelis antarcticus</i> (AMNH 26159), <i>Spheniscus humboldti</i> (AMNH 4921)	<i>Pygoscelis antarcticus</i> <i>Spheniscus humboldti</i>
Podicipedidae	<i>Podiceps cristatus</i> (AMNH 25241), <i>Podiceps grisegena</i> (AMNH 10743)	<i>Podiceps</i>
Caprimulgidae	<i>Caprimulgus affinis griseatus</i> (AMNH 17746), <i>Lyncornis (Eurostopodus) argus</i> (AMNH 29901)	<i>Caprimulgus longirostrus</i> <i>Lyncornis macrotis</i>
Charadriiformes	<i>Eudromias ruficollis</i> (AMNH 7013), <i>Burhinus bistriatus</i> (AMNH 2630), <i>Charadrius hiaticula semipalmatus</i> (AMNH 9963), <i>Chionis alba</i> (AMNH 549)	<i>Pluvianus aegyptius</i> <i>Burhinus capensis</i> <i>Charadrius vociferous</i> <i>Chionis minor</i>
Opisthocomidae	<i>Opisthocomus hoazin</i> (AMNH 12127)	<i>Opisthocomus hoazin</i>
Phaethontidae	<i>Phaethon aethereus</i> (primary: AMNH 28494; secondary: AMNH 24187, <i>Phaethon lepturus</i>)	<i>Phaethon lepturus</i>
Gruoidea	<i>Psophia obscura</i> (primary: AMNH 2671; secondary: AMNH 29322, <i>Psophia crepitans</i>), <i>Aramus guarana</i> (AMNH 24194), <i>Balearica regulorum</i> (AMNH 10699), <i>Grus japonensis</i> (primary: AMNH 1938; secondary: AMNH 1718)	<i>Psophia crepitans</i> <i>Aramus guarana</i> <i>Grus canadensis</i>
Ralloidea	<i>Podica senegalensis</i> (primary: AMNH 4148; secondaries: AMNH 4208 and AMNH 5268), <i>Sarothrura lugens</i> (primary: AMNH 2417; secondary: AMNH 4235, <i>Sarothrura pulchra</i>), <i>Mentocrex kioloides</i> (FMNH 345622), <i>Himantornis haematopus whitesidei</i> (AMNH 4183), <i>Gallirallus</i> sp. (AMNH 4369), <i>Canirallus oculus batesi</i> (AMNH 4151), <i>Aramides cajanea</i> (AMNH 4343), <i>Rallus elegans</i> (AMNH 16569), <i>Gallinula chloropus</i> (AMNH 28451), <i>Fulica cornuta</i> (AMNH 10207), <i>Porphyrio hochstetteri</i> (AMNH 26211)	<i>Heliornis fulica</i> <i>Sarothrura insularis</i> <i>Mentocrex kioloides</i> <i>Gallirallus sylvestris</i> <i>Aramides ypecaha</i> <i>Rallus limicola</i> <i>Gallinula chloropus</i> <i>Fulica americana</i> <i>Porphyrio alleni</i>
Eurypygidae	<i>Eurypyga helias</i> (primary: AMNH 3750; secondary: AMNH 4293)	<i>Eurypyga helias</i>
Rhynochetidae	<i>Rhynochetos jubatus</i> (primary: AMNH 1326; secondary: AMNH 554)	<i>Rhynochetos jubatus</i>
Higher land birds	<i>Cathartes burrovianus</i> (AMNH 1264), <i>Cariama cristata</i> (primary: AMNH 1722; secondary: AMNH 8646), <i>Leptosomus discolor</i> (AMNH 10083)	<i>Cathartes</i> <i>Cariama cristata</i> <i>Leptosomus</i>
Extinct taxa	<i>Diaphorapteryx hawkinsi</i> (AMNH 7424: largely complete skull including rostrum, AMNH 7425: largely complete mandible, AMNH 7426: complete R humerus, AMNH 7427: complete pelvis, AMNH 7428: complete L femur, AMNH 7429: complete L tibiotarsus), <i>Aptornis defossor</i> (AMNH 7300: largely complete skeleton, AMNH 60: cranium, AMNH 61: complete mandible)	

TABLE 2. Synapomorphies for selected groups within core Gruiformes and groups that have been hypothesized to be the sister taxa of *Aptornis*, except Galloanseres.

Synapomorphies presented are those from tree 1, which is closest to the consensus trees. Synapomorphies are denoted by character number followed by the character state in parentheses. Synapomorphies that contain missing data for *Aptornis* or differing scorings of terminal taxa are annotated with an asterisk. Character descriptions are detailed in appendix 1.

Group name	Branch length range	Unique synapomorphies (CI = 1.0)	Other synapomorphies, tree 1 (CI<1.0)
Core Gruiformes (including <i>Aptornis</i>)	11–87	none	11(2), 15(0), 54(1), 80(3), 84(2), 89(2), 116(2), 150(2), 176(1), 177(1), 195(1), 206(2), 214(2), 225(3), 227(1), 255(3), 260(2), 284(2), 293(1), 300(1), 319(2), 337(1), 345(1), 353(2), 356(1)
<i>Aptornis</i> + <i>Psophia</i>	21–87	none	22(2)*, 30(1)*, 54(2), 90(1)*, 150(1)*, 180(1)*, 182(2), 203(1)*, 206(0), 209(1), 214(1), 252(2)*, 254(3)*, 264(1), 266(3), 278(3), 288(3), 289(3), 290(2), 302(3), 306(2), 349(1), 356(2)
Gruoidea (including <i>Aptornis</i>)	12–87	none	6(1), 69(1), 120(0), 134(1), 135(1), 136(1), 143(1), 147(1), 162(1), 173(6), 183(2), 184(4), 189(1), 191(1), 198(1), 216(1), 243(2), 244(1), 253(2), 254(2), 287(1), 298(1), 308(2), 310(2), 341(2)
Aramidae+Gruidae	12–34	none	2(2), 13(2), 31(2), 32(2), 33(1), 36(2), 68(2), 74(1), 96(2), 145(1), 146(1), 167(1), 178(1), 207(2), 222(1), 223(2), 225(1), 229(2), 237(2), 246(2), 248(2), 250(1), 259(2), 317(2), 331(1), 336(2)
Gruidae	20–34	none	1(1), 18(1), 35(2), 77(2), 82(1), 108(2), 120(1), 122(1), 133(1), 143(0), 149(2), 165(1), 166(1), 172(3), 176(2), 179(1)*, 194(3), 201(3), 227(2), 236(1), 258(2), 294(2), 301(2), 312(1), 319(1), 324(3), 348(1)
Ralloidea	11–38	none	3(1), 31(2), 35(2), 173(3), 184(1), 189(2), 227(2), 232(1), 240(2), 256(1), 259(2), 266(3), 268(3), 274(0), 275(2), 288(1), 312(1), 318(1), 322(2), 329(2), 341(3)
<i>D. hawkinsi</i> + Ralloidea	11–38	272(2)	14(1), 62(2)*, 93(1), 129(1), 133(2)*, 169(2)*, 174(2)*, 187(1)*, 202(2)*, 213(3), 219(1), 251(2)*, 252(3)*, 257(2), 272(2), 277(0), 285(3)*, 299(1), 338(2), 339(2), 352(3)*, 354(3)*
Sarothruridae+ <i>Mentocrex</i>	20–38	none	40(1)*, 62(1)*, 65(1)*, 68(2)*, 70(2)*, 81(2), 84(1), 96(2)*, 137(2), 150(1), 236(1), 240(1), 256(2), 258(3), 265(2), 286(2), 293(3), 296(2), 298(1), 342(1), 361(2)
Sarothruridae+ <i>Himantornis</i> + <i>Mentocrex</i>	20–38	none	29(2), 34(3), 44(1), 80(1), 94(2), 106(2), 116(1), 159(1), 166(1), 206(1), 209(1), 223(2), 249(0), 258(2)* 278(3), 299(2), 310(2), 317(2), 328(3), 368(1)
Rallinae	11–38	none	18(1), 32(1), 33(1), 37(1), 76(2), 184(2), 187(2), 200(1), 229(2), 246(2), 248(2), 290(2), 321(2), 324(3), 347(1), 357(2), 366(2)
<i>R. jubatus</i> + <i>E. helias</i>	23–30	none	4(2), 6(1), 13(2), 16(2), 24(2), 135(1), 139(3), 151(3), 171(1), 173(1)*, 177(1), 179(1), 184(2)*, 185(2)*, 207(2), 212(2), 216(1), 225(2), 227(1), 258(1), 263(2), 274(1), 276(1), 278(3), 289(1), 306(2)

ing data both coded as (?). Included sequences are available on Morphobank (O'Leary and Kaufman, 2012; Project 3419, <http://morphobank.org/permalink/?P3419>), and the identification numbers of each sequence have been provided in table 4. Both the matrix solely containing molecular data and the combined data matrix are available on Morphobank (O'Leary and Kaufman, 2012; Project 3419) as well. Sequences included were matched to the species level where possible; otherwise sequences of taxa within the same genus or family level were used. No molecular data were included for adzebills, as these markers have not currently been recovered for that taxon. Given that these are exonic sequences, they were easily aligned by eye using Geneious, version 6.1.8 (Kearse et al., 2012). The molecular data were analyzed using a GTR + gamma substitution model (Lanave et al., 1984; Yang, 1994, respectively) after Claramunt and Cracraft (2015), in which the RAG1 and RAG2 genes were sampled from a diverse range of neoavian families. Partitions and model settings are detailed in the available matrix files. The Mk model (Lewis, 2001) was used for the morphological data partition within our combined data matrix. Bayesian analysis (Yang and Rannala, 1997) of molecular and morphological data was performed in MrBayes (Huelsenbeck and Ronquist, 2001; Ronquist and Huelsenbeck, 2003; Version 3.2.6).

The combined data matrix can also be found on Morphobank (O'Leary and Kaufman, 2012; Project 3419, <http://morphobank.org/permalink/?P3419>). Default MrBayes settings were used for the combined data, with the exception of running the analysis for 1,100,000 generations, until the average standard deviation of split frequencies was 0.003467. A total of 1652 samples were taken from a total of two runs, with 1101 samples taken per run. Three hot chains and one cold chain were used. The molecular data were also run separately in MrBayes for 2,000,000 generations using the same settings described above.

RESULTS

We first discuss phylogenetic relationships of basal Neoaves. Although the primary aim of this study was to resolve the phylogenetic position of *Aptornis*, our results also provide new information that will aid in better resolving basal neoavian relationships. The morphological results analyzed using parsimony are discussed first, followed by trees resulting from Bayesian analysis of RAG1 and RAG2 genes, and then the results of Bayesian analysis of the combined data. Following these discussions, we present evidence for the phylogenetic placement of *Aptornis* based on morphological and then combined data, including discussion of morphological synapomorphies and monophyly-constraint analyses.

PHYLOGENETIC RELATIONSHIPS OF BASAL NEOAVES RESULTS OF MORPHOLOGICAL DATA ANALYSIS

Unweighted parsimony heuristic searches of morphological data resulted in nine most-parsimonious trees with a score of 2038 steps (see strict consensus tree, fig. 1 and majority-rule consensus tree, fig. 2). A monophyletic neoavian node was recovered with 82% bootstrap sup-

port. Our morphological results recovered Caprimulgiformes (*Caprimulgus affinis griseatus* and *Lyncornis (Eurostopodus) argus*; 100% bootstrap support) as forming the sister group of all other included neoavian taxa, with *Opisthocomus hoazin* and *Cariama cristata* as the sister of the remaining taxa with less than 50% bootstrap support.

The placement of core Gruiformes with respect to other basal neoavian groups was poorly resolved (less than 50% bootstrap support). Core Gruiformes, Charadriiformes, and Aequornithes were monophyletic. The core-gruiform and gruoid nodes received less than 50% bootstrap support. Within Gruoidea, *Psophia obscura*+*Aptornis defossor* were recovered as sister taxa with less than 50% bootstrap support. The Aramididae+Gruidae node received 98% bootstrap support, and Gruidae was assigned 100% bootstrap support. The extant ralloid node received a 63% bootstrap value, with *D. hawkinsi* being aligned as the sister taxon of all other Ralloidea with 63% bootstrap support. Relationships within Ralloidea were generally not well supported, with only a group containing *Canirallus oceleus batesi*, *Aramides cajanea*, and *Gallirallus* sp. and a group comprising *Rallus elegans*, *Gallinula chloropus*, and *Fulica cornuta* receiving approximately 50% bootstrap values (both within Rallidae; 53% and 51%, respectively). *Podica senegalensis* was resolved as the sister taxon of a *Rhynochetos jubatus*+*Eurypyga helias* sister group with less than 50% bootstrap support, with the nongruiform *R. jubatus*+*E. helias* sister group receiving 99% bootstrap support.

Additional neoavian relationships were generally not well supported by our morphological results, which may be due to taxon sampling limits and/or a lack of key characters needed to locate more robust relationships. Charadriiformes were recovered as forming the sister taxon of all other included neoavian taxa with less than 50% bootstrap support. *Chionis alba* was aligned as the sister taxon of all other included Charadriiformes with 64% bootstrap support. Remaining charadriiform relationships comprised *Burhinus bistriatus* as the sister taxon of a *Eudromias ruficollis*+*Charadrius hiaticula semipalmatus* sister group (these nodes earned 100% and 92% bootstrap support, respectively). *Phaethon aethereus* was aligned as the sister taxon of Aequornithes (*Gavia immer*, Podicipedidae, and Spheniscidae) with 81% bootstrap support. Aequornithes received 95% bootstrap support, with the nodes of Podicipedidae and Spheniscidae receiving 100% bootstrap support. A *Cathartes burrovianus*+*Leptosomus discolor* sister group was recovered with 51% bootstrap support.

RESULTS OF MOLECULAR (RAG1 AND RAG2) ANALYSIS

The resulting tree from Bayesian analysis of RAG1 and RAG2 sequences was largely congruent with those of the morphological and total evidence analyses (RAG1 and RAG2 sequence results are detailed in fig. 3A). Robust neoavian relationships recovered by molecular data comprised core Gruiformes (100% clade credibility support), Spheniscidae (*Pygoscelis antarcticus*+*Spheniscus humboldti*; 100%); Caprimulgiformes (*Caprimulgus longirostris*+*Lyncornis macrotis*; 100%); Charadriiformes (100%); and a *Phaethon lepturus*, *E. helias*, and *R. jubatus* clade (100%).

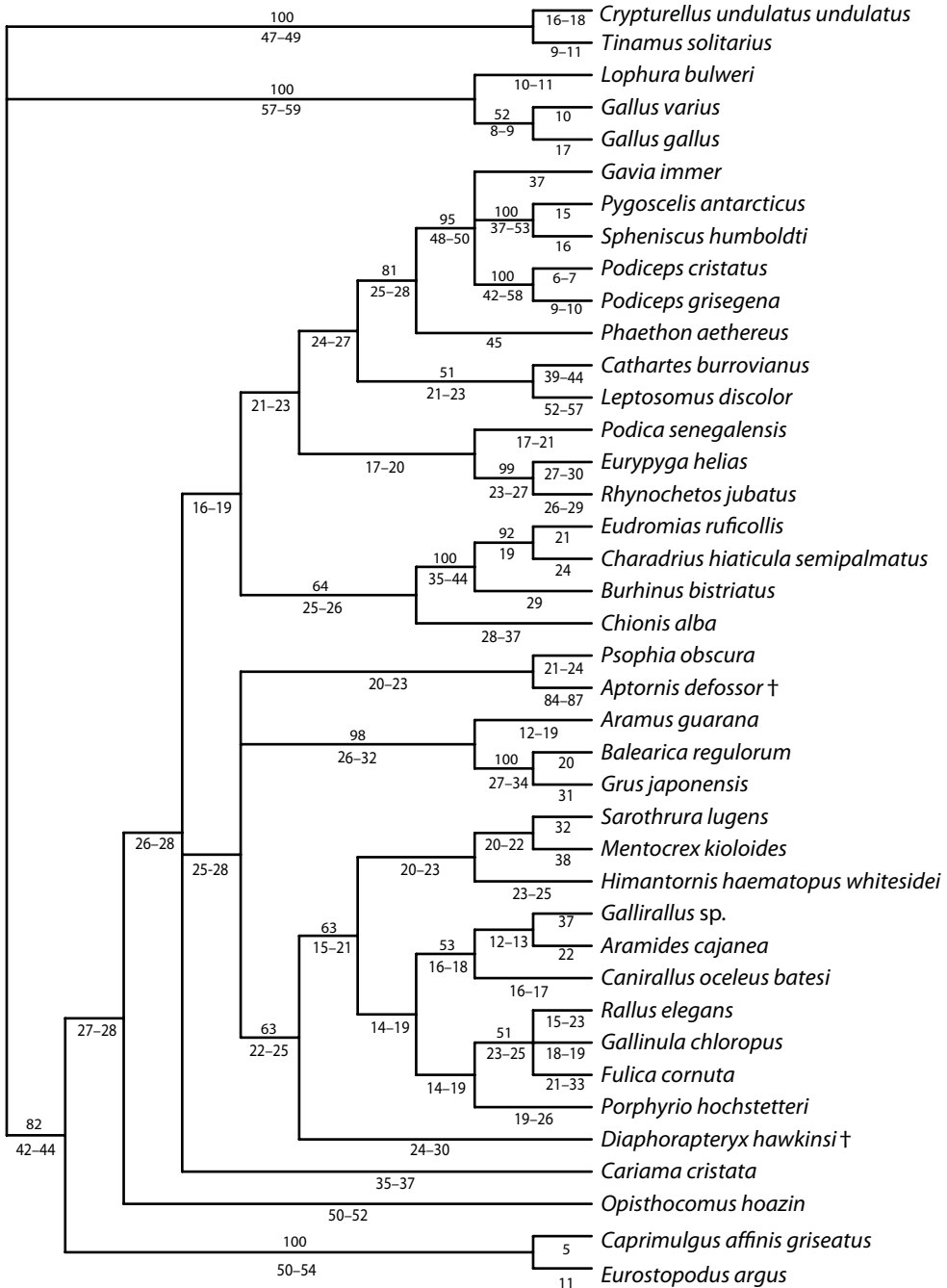


FIGURE 1. Strict consensus cladogram of nine most parsimonious trees (length: 2038, CI: 0.2498, RI: 0.5337, RC: 0.1333, HI: 0.7502) from analysis of our new morphological dataset of 40 taxa and 368 characters in PAUP*. Results support optimization of an *Aptornis defossor* + *Psophia obscura* sister group. Synapomorphies are detailed in table 2. Extinct taxa are denoted with daggers. Bootstrap support values greater than 50% are annotated above branches, with branch length ranges reported below branches.

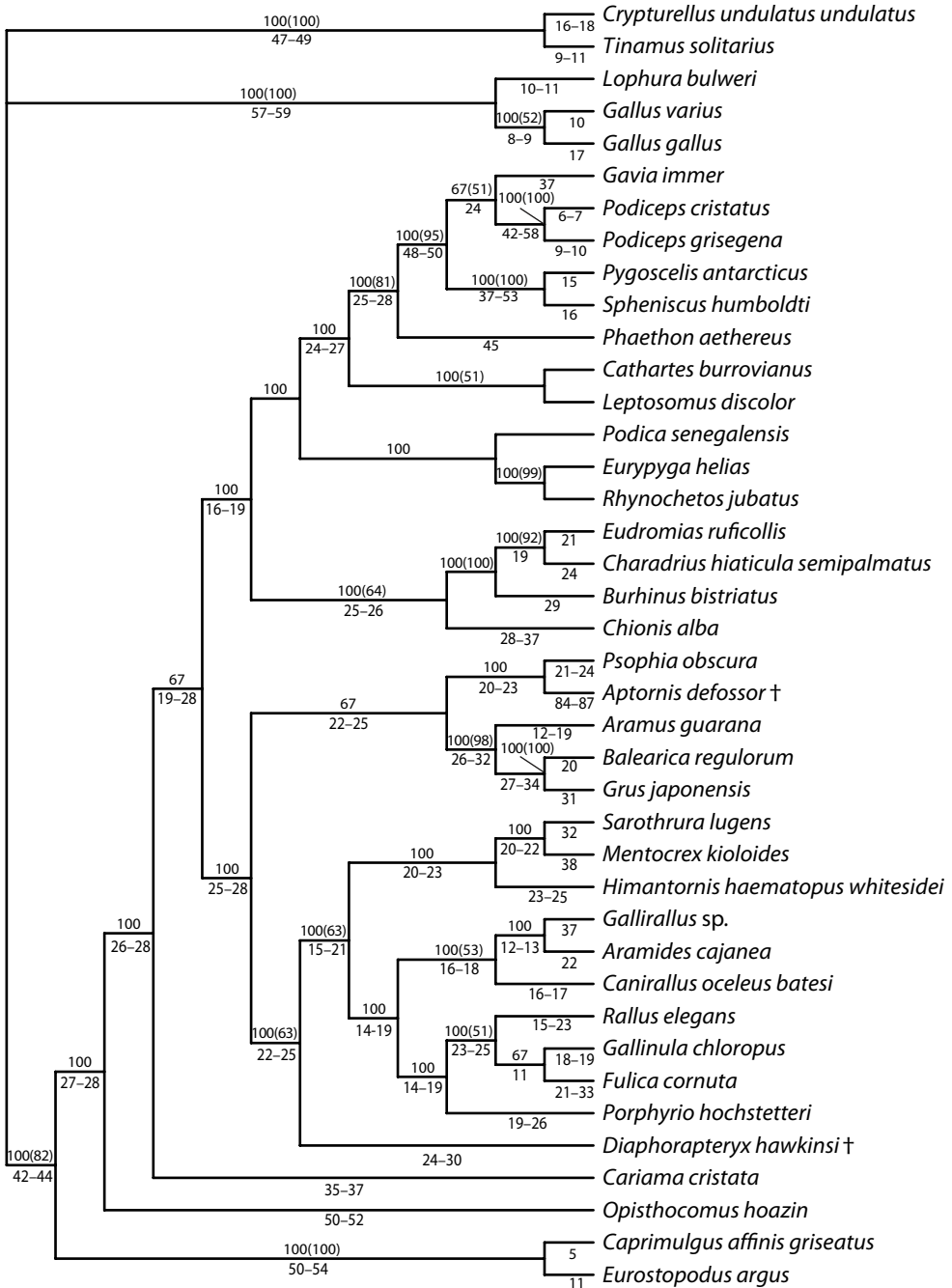


FIGURE 2. Majority-rule cladogram of nine most parsimonious trees (length: 2038, CI: 0.2498, RI: 0.5337, RC: 0.1333, HI: 0.7502) from analysis of our new dataset of 40 taxa and 368 osteological characters. All trees show optimization of an *Aptornis defossor*+*Psophia obscura* sister group. Synapomorphies are detailed in table 2. Extinct taxa are denoted with daggers. Majority-rule percentages are annotated above branches, followed by bootstrap support values greater than 50% in parentheses. Branch length ranges are below branches.

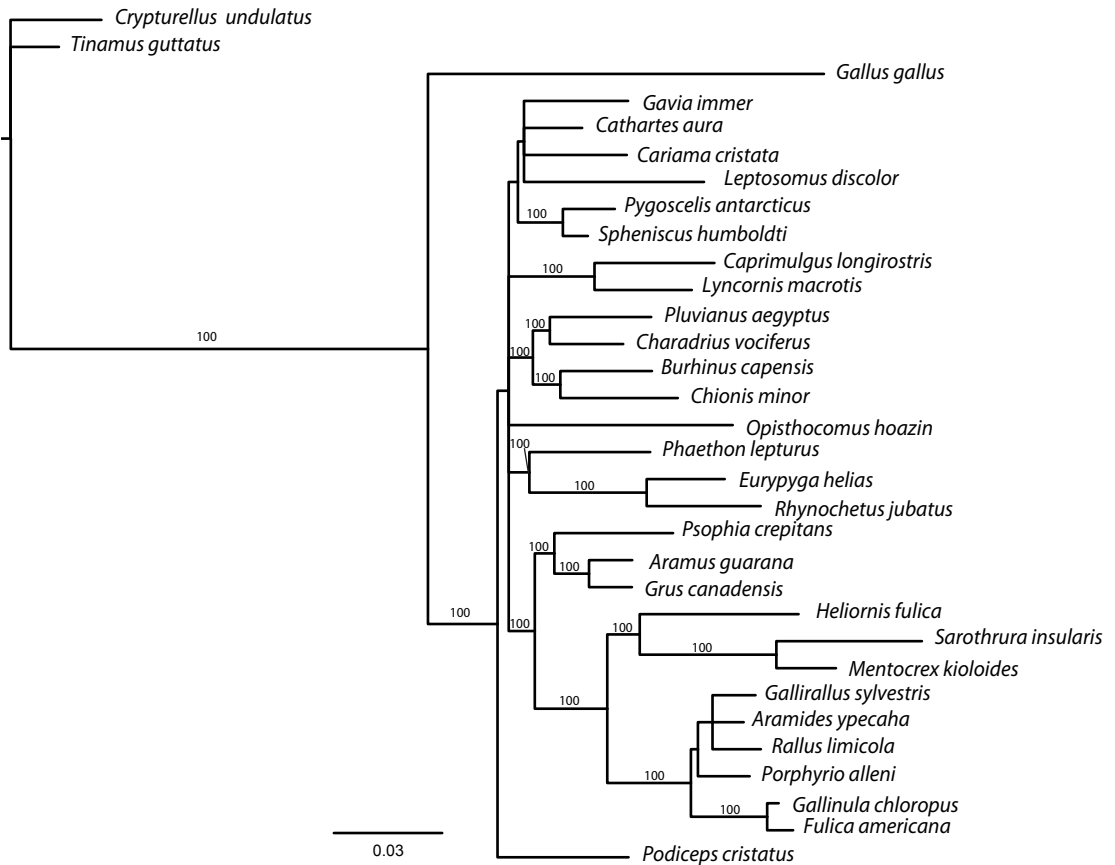


FIGURE 3. A. Resulting tree from Bayesian analysis of 32 RAG1 and RAG2 sequences. Clade credibility values greater than 90% are annotated above branches. Core Gruiformes, Ralloidea, and Gruoidea are well supported with 100% clade credibility values. The scale bar at the bottom of the tree denotes branch length. The data were run in MrBayes for 2,000,000 generations.

A monophyletic core Gruiformes clade was recovered and included well-supported gruoid and ralloid subclades. Within Gruoidea, *Psophia crepitans* was placed with 100% clade credibility as the sister taxon to an *Aramus guarana*+*Grus canadensis* sister group, a result widely recovered in large-scale molecular studies. The stem of Ralloidea was also well supported, with a *Sarothrura insularis*+*Mentocrex kioloides* clade (100%) forming the sister group of *Heliornis fulica* (100%). The stem of Rallidae also received 100% clade credibility support, with a *Gallinula chloropus*+*Fulica americana* lineage (100%) being well supported relative to the nodes of the remaining rails.

RESULTS OF COMBINED DATA ANALYSIS

The combination of morphological and molecular data resulted in increased resolution of phylogenetic relationships and high support values for most groups (fig. 3B). The combined data

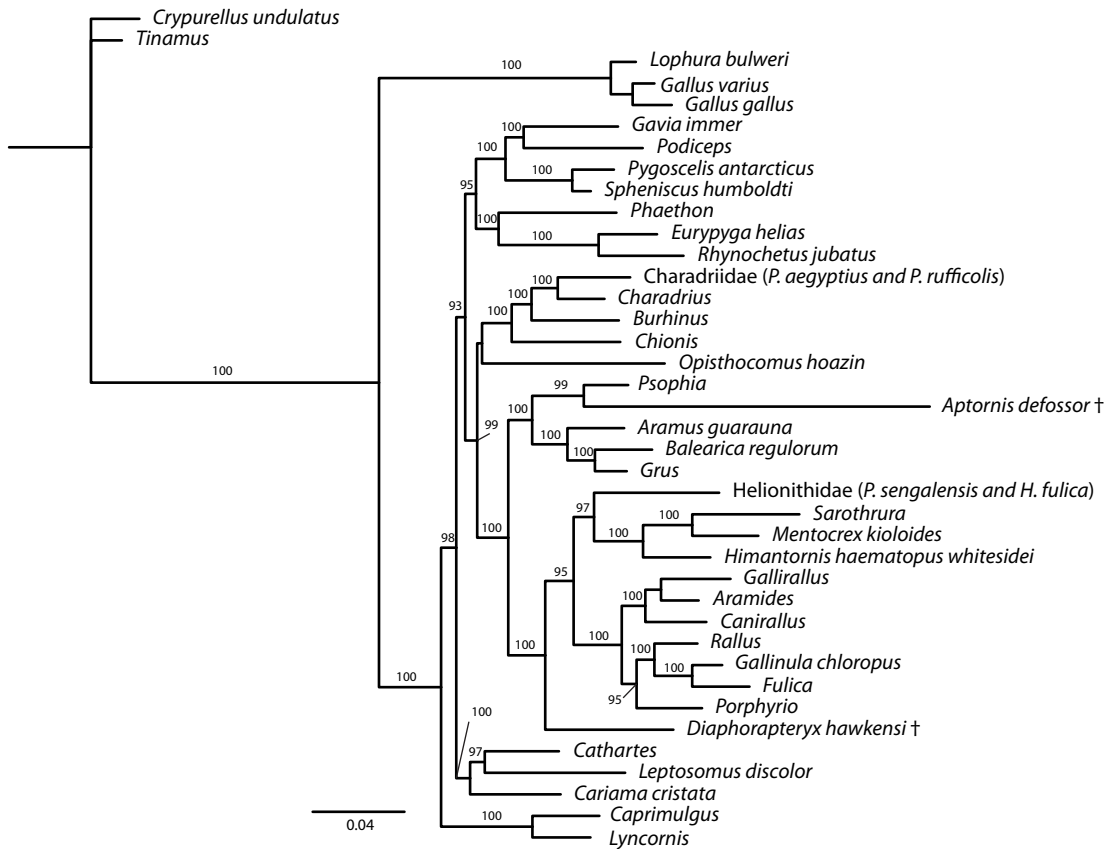


FIGURE 3 (continued). **B.** Resulting tree from Bayesian analysis of our new dataset of 40 taxa and 368 osteological characters combined with 32 sequences of RAG1 and RAG2 nuclear genes. Clade credibility values greater than 90% are annotated above branches. Extinct taxa are denoted with daggers. The scale bar at the bottom of the tree denotes branch length. The data were run in MrBayes for 1,100,000 generations.

analysis resulted in a similar solution to that of the morphological data alone. Clade credibility values for all neoavian nodes other than those of *O. hoazin* and a *Gallirallus*+*Aramides* sister group were 93% or higher and were often 100%. Caprimulgiformes were again placed as the sister group of all other included neoavian taxa (100%). A higher landbird group was recovered (100%), although it was aligned at the base of the neoavian tree following Caprimulgiformes, with *Cariama cristata* found as the sister taxon to a *Leptosomus discolor*+*Cathartes* sister group (97%). The higher land birds were then sister to all remaining taxa (93% at the stem of all other remaining taxa), including core Gruiformes+(Charadriiformes+*O. hoazin*) (99%) and Aequornithes+*Phaethon*, *E. helias*, and *R. jubatus* (95%).

The addition of morphological data resulted in Caprimulgiformes as the first divergence among Neoaves, but branch support is low for a few nodes. The *Burhinus*+*Chionis* sister group recovered in the molecular results was dissolved and their positions instead matched those of the morphological results. Similarly, the Rallidae were better resolved, with results again identi-

cal to those of the morphological data. *Sarothrura*+*Mentocrex kiolooides* remained as sister taxa, as did the spheniscid, caprimulgiform, gruoid, and *E. helias*+*R. jubatus* groups. Again, the combined data results were extremely similar to those of the morphological data, with discrepancies including the placement of *O. hoazin* (placed as the sister taxon to Charadriiformes in the combined results and aligned as the sister taxon to all other neoavian taxa besides Caprimulgiformes in the morphological results), *Phaethon* (moved from a place as the sister taxon of Aequornithes in the morphological results to sister to *E. helias*+*R. jubatus* in the combined results), the higher land birds, and the stems of Gruiformes and Charadriiformes (these are sister groups in the combined results whereas Gruiformes is more basally located in the morphological results), and Heliornithidae (placed as the sister taxon of (*Sarothrura*+*Mentocrex kiolooides*)+*Himantornis haematopus whitesidei* within the combined data results). Finally, the stems of Aequornithes, *Phaethon*, *E. helias*, and *R. jubatus* changed positions slightly, with *Phaethon* and *E. helias*+*R. jubatus* forming the sister group of Aequornithes in the combined results, whereas they were more basally located within the morphological results.

MORPHOLOGICAL EVIDENCE FOR THE PHYLOGENETIC PLACEMENT OF *APTORNIS*

Combined data results and the most parsimonious trees from analysis of morphological data suggest that *Aptornis* is a gruiform, within Gruoidea, and is the sister taxon of *Psophia* (trumpeters).

MOST PARSIMONIOUS TREES: Unweighted parsimony heuristic searches of our morphological data resulted in nine most parsimonious trees (2038 steps) that all grouped *Aptornis defossor* and *Psophia obscura* (the Black-winged Trumpeter) as sister taxa (figs. 1, 2), but with poor bootstrap support (<50%). The *Aptornis*+*Psophia* sister group was placed in an unresolved polytomy with Gruoidea and Ralloidea in the strict consensus (fig. 1). In all but three of the most parsimonious trees, *Aptornis*+*Psophia* was recovered as the sister group to the Gruoidea (see majority-rule consensus tree, fig. 2). *Aptornis* and *Psophia* were grouped together on the basis of 15 optimized derived characters (six additional characters were optimized at that node but were missing in *Aptornis*), none of which was unique to this node (table 2; synapomorphies were largely those of the pelvis).

CHARACTER EVIDENCE FOR THE GRUOID PLACEMENT OF *APTORNIS*: Character support for the placement of *Aptornis* as a gruoid is present throughout the skeleton in 12 synapomorphies (13 additional synapomorphies contained missing data) and largely consists of characters of the skull and mandible (3/12), vertebrae (3/12), and sternum (3/12). Synapomorphies located within other elements are present in the pelvis (1/12), femur (1/12), and tibiotarsus (1/12). The external nares are schizorhinal (character 6(character state 1)), unlike the holorhinal nares of many members of Ralloidea (6(2)). The zygomatic process is divided by a prominent superiolateral crest along its length that terminates near the caudal margin of the temporal fossa (69(1)). This process is absent in most of Ralloidea (69(0)). The ventral mandibular angle is

absent or indistinct in *A. defossor* and Gruoidea (120(0)), but is present and distinct in *R. jubatus* and Ralloidea (120(1)).

The foramina transversaria of the axis vertebra are present (135(1)) in this group but lost in most Ralloidea (135(0)). Pneumatic foramina are present on the lateral laminae of the axis vertebra (136(1)), but absent in those of *R. jubatus* and Ralloidea (136(0)). Pneumatic foramina are also present on the lateral portions of the body of the thoracic vertebrae in *Aptornis* and Gruoidea (143(1)), but are absent in *R. jubatus* and most Ralloidea (143(0)). Within the sternum, the ventral lip reaches ventrally (162(1)), whereas it is dorsally oriented in *R. jubatus* and most Ralloidea (162(2)). The fenestrae and incisurae caudolateralis are lost in this group (183(2)) but are present in most Ralloidea (183(1)). The caudal terminus of the trabecula mediana is broad, linear, or rounded and sometimes tapered in *A. defossor* and Gruoidea (189(1)), whereas it is rounded or subrectangular within most Ralloidea.

An ovoid groove is present along the medial length of the ilium in *Aptornis* and Gruoidea (287(1)), and is absent in *R. jubatus* (287(0)). The impressio ansae m. iliofibularis of the femur is circular in *Aptornis* and Gruoidea (310(2)), but is ovoid in *R. jubatus* and most Rallidae (310(1)). The depression of the epicondylaris lateralis of the tibiotarsus in *Aptornis* and all Gruoidea except *A. guarana* (341(3)) is deeply pitted and the condylus lateralis has a prominently protruding rim (341(2)), whereas it is shallow in *R. jubatus* (341(1)) and largely depressed more caudally in Ralloidea (341(3)).

CHARACTER EVIDENCE FOR AN *APTORNIS+PSOPHIA* SISTER GROUP: The clade uniting *Aptornis+Psophia* is largely supported by characters of the pelvis (6/15; eight additional synapomorphies contained missing data); thus, although the pelvis of *Aptornis* may appear to share several affinities with Rallidae, our results suggest that this element ultimately shares the most derived similarities with *Psophia* (fig. 4 and 5). Both taxa share a cranially oriented semicircular prominence on the cranial margin of the antitrochanter that is unique within core Gruiformes (264(1)). The craniocaudal extent of the foramen ilioischadicum in both taxa is relatively short and makes up only about one third or less of the craniocaudal length of the concavitas infracristalis (266(3)). This contrasts with that of *R. jubatus*, which is limited to one half of the craniocaudal length of the concavitas infracristalis but greater than one third (266(1)). The postacetabular ilia and ischii of *Aptornis* and *Psophia* are subequal in caudal extension (278(3)), whereas most rallids have craniocaudally shorter ilia (278(1)). The postacetabular ilia of *Aptornis* and *Psophia* are extremely lateromedially compressed, which delimits a narrow medial fenestra (288(3)), in contrast to the more laterally splayed ilia of the rails (288(1)) and the extreme lateral positioning of the ilia of *R. jubatus* (288(2)). The caudal margins of the ilia and the caudal extreme of the synsacrum in *Aptornis* and *Psophia* are detached from one another and the synsacrum is elongate and continues well beyond the processus marginis caudalis of the ilium (289(3)), whereas the synsacrum in rails is markedly shortened posteriorly and remains in line with, and fused to, the caudal margin of the ilium (289(2)). The foramina of the caudalmost portion of the synsacrum are small and circular in both taxa (290(2)), unlike the large, ovoid foramina of *R. jubatus* (290(1)).

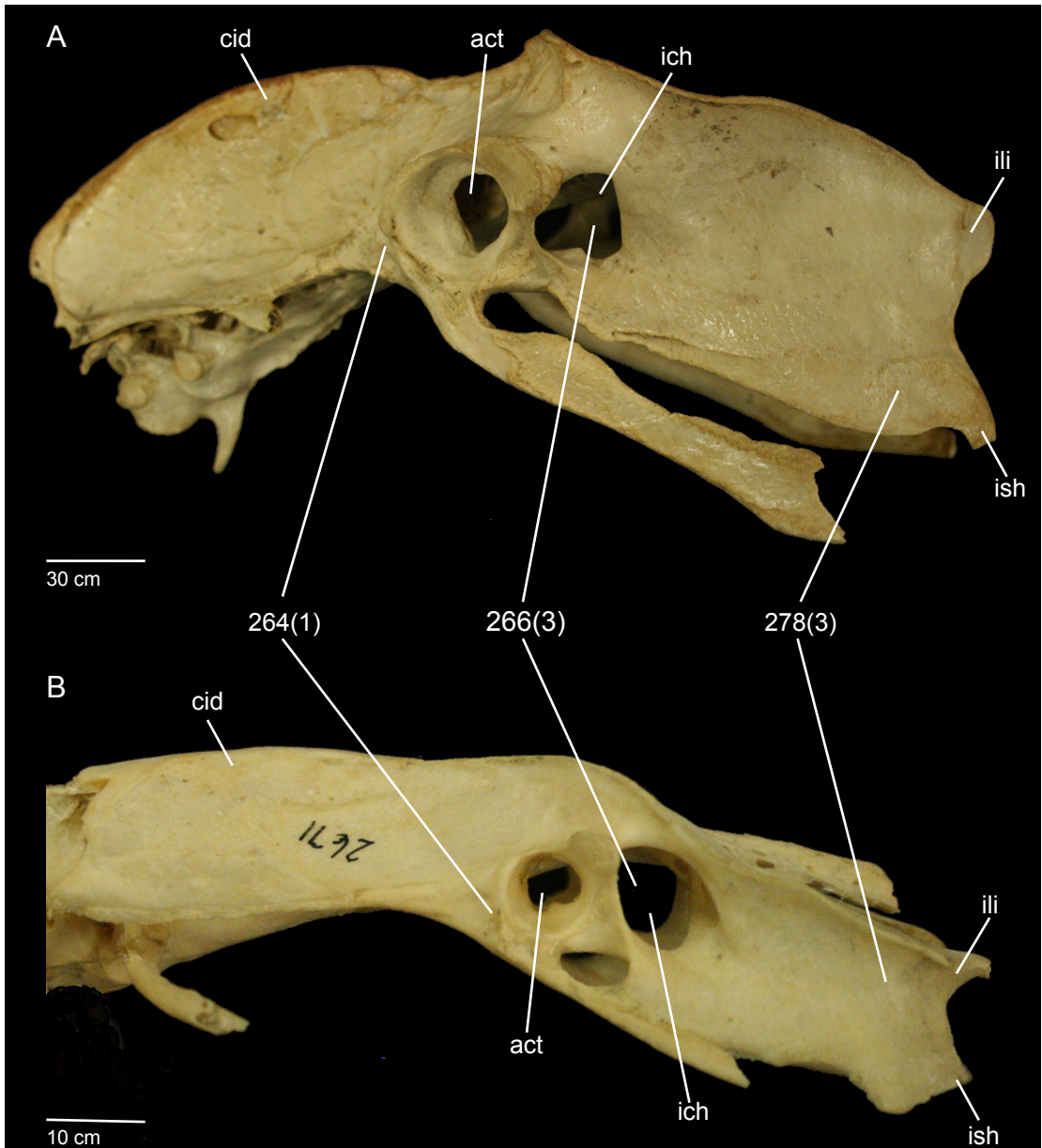


FIGURE 4. Synapomorphies for the pelvis of *Aptornis defossor* (AMNH 7300, A) and *Psophia obscura* (AMNH 2671, B). The pelvises are shown in lateral view. Scale bars vary for each specimen and are shown below each specimen. Labels correspond to synapomorphies, with character numbers followed by character states in parentheses. Abbreviations: **act**, acetabulum; **cid**, crista iliaca dorsalis; **ich**, foramen ilioischadicum; **ili**, post-acetabular ilium; **ish**, postacetabular ischium.

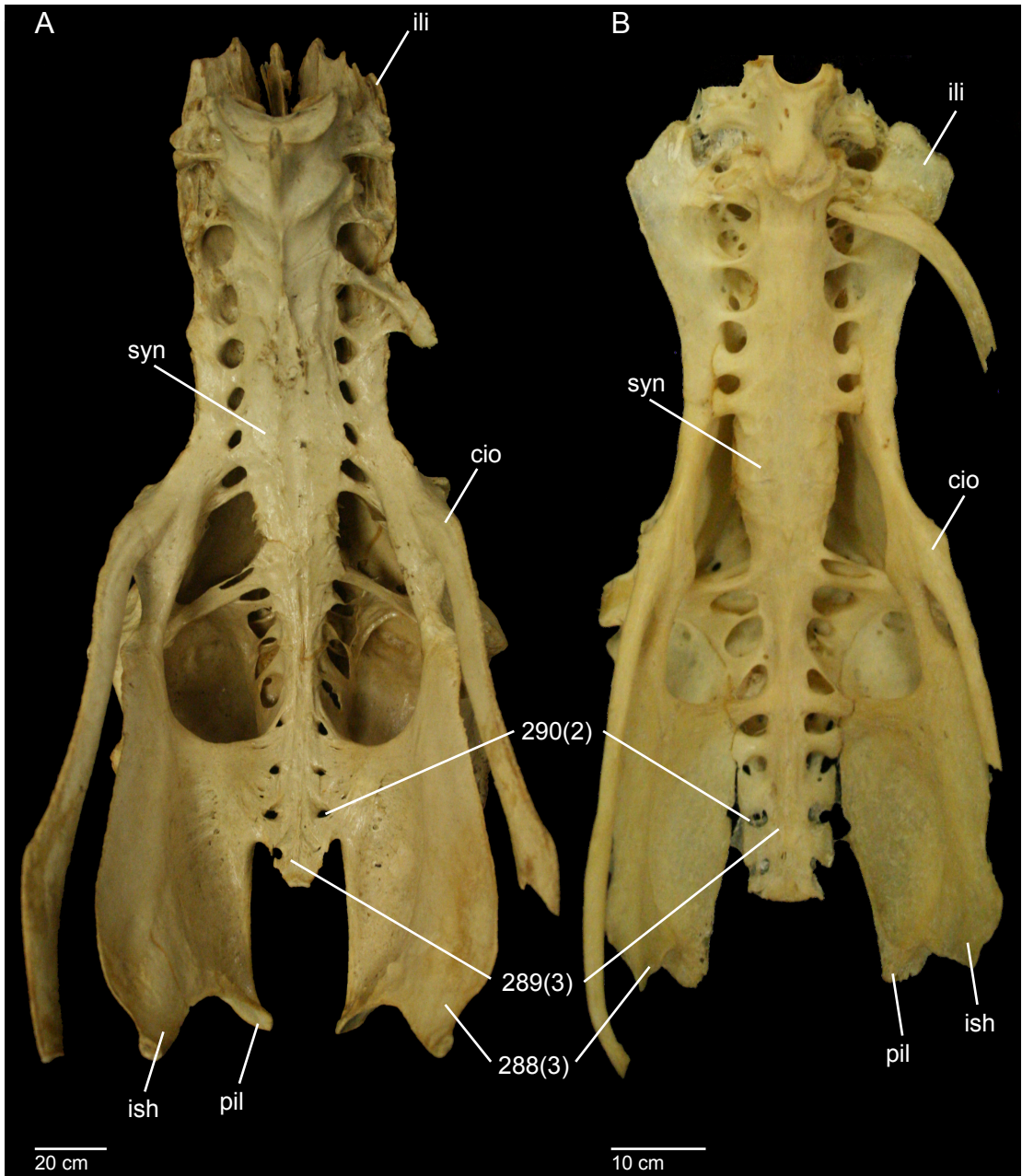


FIGURE 5. Synapomorphies for the pelvis of *Aptornis defossor* (AMNH 7300, A) and *Psophia obscura* (AMNH 2671, B). The pelvises are shown in ventral view. Scale bars are different for each specimen and are shown below each specimen. Labels correspond to synapomorphies, with character numbers followed by character states in parentheses. Abbreviations: **cio**, crista iliaca obliqua; **ili**, preacetabular ilium; **ish**, postacetabular ischium; **pil**, postacetabular ilium; **syn**, symsacrum

Other skeletal elements that exhibit synapomorphies for *Aptornis*+*Psophia* include those of the skull (1/15), the sternum (1/15), the scapula (2/15), the humerus (1/15), the femur (2/15), and the tarsometatarsus (2/15). Within the skull, the caudomedial angle of the palatines in both taxa is rostral to the caudal margin of the lateral portion of the palatines (54(2)). The position of the caudomedial angle tends to be coincident within Rallidae (54(1)). The height of the sternal carina within *Psophia* and *Aptornis* is less than the width of the body (182(2)). No indication of a hooklike tubercle on the costal surface of the scapulae is present (206(0)), unlike the condition in many members of Ralloidea (206(1)). A craniolaterally located tubercle is present on the scapula within the *Aptornis*+*Psophia* sister group (209(1)). This tubercle is often accompanied by a crest that trails distally from the location of the tubercle, and has been lost in *R. jubatus* and most Rallidae (209(2)). The tuberculum dorsale of the humerus in *Aptornis*+*Psophia* is smooth and rounded (214(1)), as opposed to the more acuminate tubercles of many members of Ralloidea (214(2)). The femoral impressiones obturatoriae of the novel sister group are large and often lateromedially elongate (302(3)), unlike the small and circular impressiones of most members of Ralloidea and *R. jubatus* (302(4)). Similarly, *Psophia* and *Aptornis* exhibit deep fossae popliteae (306(2)), which tend to be shallow within many Ralloidea (306(1)). Within the tarsometatarsi, the prominence of the dorsoplantar lamina in *Aptornis*+*Psophia* is greater than or equal to the plantar prominence of the lamina lateralis hypotarsi (349(1)), and the plantar foramina vascularia proximalia are subequal in height (356(2)). This differs from the lesser plantar prominence of the dorsoplantar lamina (349(2)) and relatively distal position of the lateral foramina vascularia proximalia in *R. jubatus* and Ralloidea (356(1)).

MONOPHYLY-CONSTRAINT ANALYSES: Unconstrained analysis recovered the best tree score of 2038 steps (fig. 1 and 2). Monophyly-constraint analysis results are detailed in table 3. The tree with the score closest to the most parsimonious trees (MPTs) was that of *Aptornis*+Gruiformes, which resulted in a tree score of 2041 (3 steps away from the MPT). Monophyly analysis of *Aptornis*+*Diaphorapteryx hawkinsi* resulted in a tree with a score of 2043, five steps from the MPTs. The least parsimonious trees were found when monophyly was constrained for *Aptornis*+Galloanseres and *Aptornis*+Sarothruridae+Heliornithidae, which both resulted in tree scores of 2062. These were 24 steps more than that of the most parsimonious trees (MPTs). The next least parsimonious trees were those of *Aptornis*+*M. kioloides* (2060, 22 steps away from the MPT) and *Aptornis*+Sarothruridae (2056, 18 steps away from the MPT). The tree of *Aptornis*+Rallidae had a score of 2053, 15 more steps than the MPT. Similarly, a score of 2052 resulted from a constrained search for *Aptornis*+*R. jubatus*, 14 more steps from the MPT. Searches constrained to *Aptornis*+Ralloidea and *Aptornis*+Rallinae received scores of 2048 and 2051, respectively (10 and 13 more steps than the MPTs). All past hypotheses regarding the sister relationships of *Aptornis* were thus found to be less parsimonious than the unconstrained MPT. Additionally, *R. jubatus* and *E. helias* were found to be sister taxa and this group was well supported by 26 synapomorphies (three contained missing data, CI<1.0, 99% bootstrap support, table 2). *D. hawkinsi* was recovered as a sister taxon to Ralloidea (63% bootstrap support).

TABLE 3. Synapomorphies for sister groups of monophyly constraint analyses.

Sister groups are arranged from most parsimonious tree score to the least parsimonious, with *Aptornis*+Gruiformes resulting in the tree closest to the most parsimonious tree. Synapomorphies presented are those from tree 1 of each analysis. Synapomorphies are denoted by character number, followed by the character state in parentheses. Character descriptions are detailed in appendix 1. Synapomorphies that contain missing data for *Aptornis* or differing scorings of terminal taxa are annotated with an asterisk. Terminal sister taxa of *Aptornis* resulting from constraint analyses of larger groups are reported and denoted with two asterisks.

Group constraint	Tree score	Unique synapomorphies (CI=1.0)	Other synapomorphies, tree 1 (CI<1.0)
<i>Aptornis</i> +Gruiformes	2041	none	38(1), 69(1), 84(2), 93(1)*, 195(1), 209(1), 255(1), 260(2), 264(1), 266(3), 275(2)*, 284(2), 287(1), 300(1), 337(1)
<i>Aptornis</i> + <i>D. hawkinsi</i>	2043	none	28(2), 131(1), 257(2), 311(1), 314(3), 317(1), 322(1), 348(1)*
<i>Aptornis</i> +Ralloidea	2048	none	3(1), 80(1), 173(1), 232(1), 266(3), 275(2), 321(2)
<i>Aptornis</i> +Rallinae	2051	none	1(1), 76(2), 79(2), 104(0), 290(2), 306(2), 309(2), 321(2), 350(1), 357(2), 359(2)
<i>Aptornis</i> + <i>R. jubatus</i>	2052	none	8(1), 23(1), 68(4), 73(2), 81(1), 116(2), 141(1), 183(2), 256(3), 257(2), 293(1), 317(1), 330(2), 348(1), 351(2), 357(2)
<i>Aptornis</i> +Rallidae	2053	none	290(2), 359(2)
<i>Aptornis</i> + <i>H. h. whitesidei</i> **	2053	none	23(1), 69(1), 107(1), 166(1), 174(1), 200(2), 214(1), 226(1), 227(1), 258(2), 259(3), 274(1), 278(3), 287(1), 296(1), 310(2), 330(2)
<i>Aptornis</i> +Sarthruridae	2056	40(1)*	6(1), 8(1), 62(1)*, 68(2)*, 70(2), 137(2)*, 150(1)*, 162(1), 194(3), 202(1), 236(1)*, 240(1), 264(1), 265(2), 281(2), 298(1)*, 306(2), 311(1), 339(1), 348(1), 350(1), 353(1)
<i>Aptornis</i> + <i>M. kioloides</i>	2060	40(1)*, 168(0)*	6(1), 8(1), 15(1)*, 62(1)*, 68(2)*, 70(2)*, 137(2)*, 150(1)*, 169(0)*, 181(2)*, 186(2)*, 236(1)*, 240(1), 245(1)*, 250(1)*, 265(2), 269(1)*, 298(1)*, 306(2), 311(1), 350(1)
<i>Aptornis</i> +Sarthruridae+Heliornithidae	2062	40(1)*	62(1)*, 68(2)*, 70(2), 137(2)*, 150(1)*, 194(3), 197(2)*, 236(1)*, 240(1), 256(2)*, 258(3)*, 264(1), 285(4)*, 339(1), 348(1), 350(1), 353(1)
<i>Aptornis</i> +Galloanseres	2062	none	85(2), 112(2), 209(1), 279(1), 301(2), 321(2), 322(1)

COMBINED DATA EVIDENCE FOR THE PHYLOGENETIC PLACEMENT OF *APTORNIS*

Bayesian analysis of combined data produced almost identical results to those of the morphological data, but exhibited higher support values for each relationship (fig. 3B). The *Aptornis*+*Psophia* sister group was recovered again but exhibited a clade credibility value of 99%. The *Kagu*+*Sunbittern* sister group was resolved with a 100% clade credibility value. *Diaphorapteryx hawkinsi* was placed as the sister taxon to Ralloidea with a 100% clade credibility value.

TABLE 4. Accession numbers and provenance for 32 included RAG1 and RAG2 sequences.

All sequences can be found within the associated nexus file available online via Morphobank (O'Leary and Kaufman, 2012; Project 3419, <http://morphobank.org/permalink/?P3419>). Sequences are identified by their accession numbers in GenBank, otherwise they are identified by the museum catalog numbers, for the following institutions: AM, Auckland Museum, Auckland, New Zealand; DOT, Department of Ornithology Tissue, American Museum of Natural History; FMNH, Field Museum of Natural History; LSUMNS, Louisiana State University Museum of Natural Sciences; USNM, Smithsonian Museum of Natural History.

Taxon	RAG1 Gene	RAG2 Gene
<i>Crypturellus undulatus</i>	–	DOT 2312
<i>Tinamus guttatus</i>	AF143726.1	DOT 8857
<i>Gallus gallus</i>	AF143730 G&B	AY443150.1
<i>Gavia immer</i>	KT954386.1	KT954486.1
<i>Pygocelis antarcticus</i>	DQ137242.1	–
<i>Spheniscus humboldti</i>	AF143734.1	DOT 10239
<i>Podiceps cristatus</i>	KT954360.1	KT954445.1
<i>Caprimulgus longirostris</i>	KT954373.1	KT954470.1
<i>Lyncornis macrotis</i>	USNM B03732	USNM B03732
<i>Pluvianus aegyptius</i>	EF373203.1	–
<i>Burhinus capensis</i>	FMNH 4166	FMNH 4166
<i>Charadrius vociferus</i>	KT954380.1	KT954479.1
<i>Chionis minor</i>	AY228782.1	–
<i>Opisthocomus hoatzin</i>	AY233357	DOT 7609
<i>Phaethon lepturus</i>	KT954366.1	KT954452.1
<i>Psophia crepitans</i>	KT954375.1	KT954472.1
<i>Aramus guarauna</i>	DOT10112	DOT10112
<i>Grus canadensis</i>	LSUMNS B10365	LSUMNS B10365
<i>Heliornis fulica</i>	KT954376.1	KT954474.1
<i>Sarothrura insularis</i>	FMNH 384729	FMNH 384729
<i>Mentocrex kioloides</i>	FMNH 345622	–
<i>Gallirallus sylvestris</i>	KC613976	–
<i>Aramides ypecaha</i>	AY756084.1	–
<i>Rallus limicola</i>	KT954378.1	KT954476.1
<i>Gallinula choropus</i>	KC613931.1	–
<i>Fulica americana</i>	KC613923.1	–
<i>Porphyrio alleni</i>	KC613952.1	–
<i>Eurypyga helias</i>	DOT 15474	DOT 15474
<i>Rhynchotus jubatus</i>	AM B8454, B8455	AM B8454, B8455
<i>Cathartes aura</i>	AY461395.1	–
<i>Cariama cristata</i>	KT954424.1	KT954535.1
<i>Leptosomus discolor</i>	FMNH 449184	FMNH 449184

DISCUSSION

IMPLICATIONS FOR BASAL NEOAVIAN PHYLOGENY

Despite small discrepancies between the results of analyses of the three datasets, the morphological results exhibit a strong phylogenetic signal and are similar to those of the molecular and combined data. This morphological dataset is the most congruent to date with molecular data, and conflicts generally involve nodes that have so far been difficult to resolve.

Placement of Caprimulgiformes alone as the first divergence of Neoaves in our morphological (figs. 1, 2) and combined results (fig. 3B) is consistent with the results of Prum et al. (2015). Gruiformes were recovered as the next basalmost group in our morphological results. Gruiformes have been found to be a more basal group than Charadriiformes and other Aequornithes in Mayr and Clarke (2003) and Prum et al. (2015). They were additionally found to be a more basal divergence than Aequornithes in Jarvis et al. (2014). Our combined results additionally posit a Gruiformes+Charadriiformes sister group. A close relationship between these groups has similarly been recovered by several morphological and molecular studies (Cracraft, 1988; Tuinen et al., 2001; Livezey and Zusi, 2007; Bertelli et al., 2011; Jarvis et al., 2014). Further phylogenetic analyses are needed to better assess whether a Gruiformes+Charadriiformes sister group is the most likely phylogenetic hypothesis for these basal groups, but mounting evidence suggests that they have close affinities. *O. hoazin* was placed near the base of Neoaves based on morphological data and as the sister taxon of Charadriiformes in combined analysis. *O. hoazin* was similarly aligned as the sister taxon of a Charadriiformes+Gruiformes sister group by Jarvis et al. (2014). This enigmatic taxon has been associated with several different neoavian groups in past studies, including at the base of Neoaves, closely related to Musophagidae and Cariamidae, as the sister taxon of Cuculidae or of Cuculimorphae, as the sister taxon of Phoenicopteridae or of Trogonidae within a polytomy of many groups including several historic gruiform groups, and as the sister taxon of higher land birds (Mindell et al., 1997; Sibley and Ahlquist, 1990; Mayr and Clarke, 2003; Sorenson et al., 2003; Mayr, 2005; Ericson et al., 2006; Livezey and Zusi, 2007; Prum et al., 2015, respectively). Due to the alignment of this taxon with many different groups in past morphological and molecular studies, it is difficult to confirm the placement of this taxon more specifically given this dataset.

Although our morphological analyses generally recovered relationships that were consistent with those of recent molecular studies, our morphological dataset also found a small number of anomalous relationships that are likely the result of missing data, taxon sampling and/or a lack of identified synapomorphies for that taxon. This applies to the resulting relationships of *Phaethon aethereus* and *Podica senegalensis*, the latter for which a skull was unavailable. *Phaethon* was recovered as the sister taxon of the *R. jubatus*+*E. helias* group within our combined results, which is consistent with recent molecular studies (Jarvis et al., 2014; Prum et al., 2015). A sister relationship between *Gavia immer* (Common Loon) and *Podiceps* (Grebes) recovered in six out of the nine MPTs and the combined data result is undoubtedly due to morphological convergence related to foot-propelled diving, as grebes are now well corroborated to be the sister taxon of flamingos (Tuinen and Hedges, 2001; Chubb, 2004; Mayr, 2004;

Morgan-Richards et al., 2007; Hackett et al., 2008; Jarvis et al., 2014; Prum et al., 2015). The Grebe+Loon sister group has often been recovered by past morphological studies based on several skeletal similarities, especially within the pelvis and hindlimb (Cracraft, 1982b; Hedges and Sibley, 1994; Mayr and Clarke, 2003; Bourdon et al., 2005; Livezey and Zusi, 2007).

NOVEL PHYLOGENETIC PLACEMENT OF *APTORNIS*

The *Aptornis*+*Psophia* sister group was found to be the most parsimonious hypothesis for the placement of *Aptornis* in our morphological and monophyly-constraint analyses and was recovered in combined analysis results with high support. This sister group hypothesis has not been found in any previous phylogenetic study, and it suggests that *Aptornis* is a gruiform and more closely related to Gruoidea than to Ralloidea. *Psophia* is now firmly established as the sister taxon of other Gruoidea (Aramidae and Gruidae), although some past morphological studies have suggested an association between *Psophia* and *Aptornis* (Cracraft, 1982a; Livezey, 1998; Livezey and Zusi, 2007). Additionally, our results strongly support a *R. jubatus*+*E. helias* sister group, which is consistent with recent molecular hypotheses (Fain and Houde, 2004; Ericson et al., 2006; Hackett et al., 2008; Jarvis et al., 2014; Prum et al., 2015). All these results refute the hypothesis of a close relationship between *Aptornis* and *R. jubatus*. Alternative phylogenies recovered from our constraint analyses of *Aptornis*+Ralloidea, *Aptornis*+Rallidae, and *Aptornis*+Rallinae are similarly unparsimonious; thus, our results strongly indicate that *Aptornis* is not a galloanserine or ralloid.

BIOGEOGRAPHIC IMPLICATIONS

The proposed relationship between *Psophia* and *Aptornis* raises a perplexing biogeographic problem given their respective distributions in South America and Zealandia and their lack of strong flight capability. *Aptornis* was likely flightless and although *Psophia* can fly weakly, these birds are predominantly terrestrial and often fly only short distances to roost in trees at night (Hoyo et al., 2019; Worthy and Holdaway, 2002). This strongly disjunct distribution pattern and sister group relationship between a flightless and a weakly flighted bird is paralleled in the *Rhynochetos*+*Eurypyga* sister group, in which the weakly flighted *Eurypyga* occurs in South America and the flightless *Rhynochetos* is endemic to New Caledonia (within Zealandia). Each of these confounding biogeographic patterns entails around 8000–10,000 km of spatial separation that apparently occurred tens of millions of years ago.

A common approach to explaining such patterns might include invoking parallel events of long-distance dispersal and loss of flight. This argument is often framed in terms of assumptions about the ages of taxa and land connections. If it is determined that the loss of land connections is older than the age of the taxon split, it is concluded that the distributional pattern must be a consequence of long-distance dispersal. If the respective ages are similar, then vicariance may be invoked. Debates about these two scenarios are often clear cut, but they most frequently arise when the paleogeography is complex and the evidence for potential land con-

nections and their timing are nuanced, and when the ages of taxon splits are seemingly too young. Zealandia is one of those regions, and *Aptornis*+*Psophia* is one of those taxa.

With respect to the two disjunct patterns discussed here, it is first appropriate to ask whether a potential common temporal history exists between them. Three recent avian time trees (Jarvis et al., 2014; Prum et al., 2015; Claramunt and Cracraft, 2015) suggest some temporal bounds on the history of these two southern groups, although the data sets and methods, including calibrations, are not entirely equivalent. Claramunt and Cracraft (2015) hypothesized that *Psophia* separated from the other gruoids around 42 mya. If *Aptornis* is sister to *Psophia*, then 42 mya is an upper bound on their divergence. Claramunt and Cracraft (2015) also recovered a 56 mya estimated age for the separation of Ralloidea and Gruoidea. The Prum et al. (2015) analyses resulted in slightly younger age estimates than those of Claramunt and Cracraft (2015), with the divergence date of *Psophia*+Gruoidea estimated at approximately 31 mya and the ralloid-versus-gruoid divergence date estimated to have occurred around 40 mya. Only the Claramunt and Cracraft (2015) study provided an estimated divergence date for the split between *R. jubatus* and *E. helias*, which was hypothesized to be approximately 33–32 mya. All three studies put forth a similar estimate of around 58–61 mya for the divergence between the stem of the *Rhynochetos*+*Eurypyga* sister group and Phaethontiformes.

Divergences estimated using whole mtDNA genomes for core Gruiformes (Boast et al., 2019) recovered deeper age estimates than those based on nuclear and genomic-level data genes. Thus, Boast et al. (2019), which recovered *Aptornis* as diverging from Sarothruridae at approximately 39 mya, also found the base of Ralloidea to be around 54 mya and the gruoid-ralloid divergence to be around 64 mya. These estimates imply pushing the radiation of Neoaves well back into the Late Cretaceous. It should also be noted that divergence dates based on the whole mtDNA study of Boast et al. (2019) appear to have large error bars. The study of García-R et al. (2014), which included both mtDNA and nuclear sequences for members of all ralloid subgroups and core Gruiformes, resulted in divergence estimates for *Psophia* that are closer to that of Prum et al. (2015) at about 35 mya.

Discrepancies among these results suggest that different data types—the slow nuclear, constant-rate genes used in Jarvis et al. (2014) and Claramunt and Cracraft (2015) versus the mostly exonic anchored-probe dataset of Prum et al. (2015) and the mitochondrial sequences of Boast et al. (2019)—may play a role in the inconsistent divergence date estimates across several of these studies (see Reddy et al., 2017). This supposition is consistent with the overall similarities in ages for shared nodes found across the trees of Jarvis et al. (2014) and Claramunt and Cracraft (2015).

The interpretations outlined above imply that the biogeographic patterns exhibited by the *Aptornis*+*Psophia* and *Rhynochetos*+*Eurypyga* sister groups may be roughly contemporaneous sometime in the late Eocene, between 40–30 mya, especially given substantial error rates surrounding divergence age estimates. Considering probable outgroup phenotypes, parsimony suggests that the common ancestor of both pairs was volant, and that *Rhynochetos* and *Aptornis* became flightless subsequent to their respective separations. The stem of *Rhynochetos* and *Eurypyga* is likely sufficiently old enough to have had a broad Gondwanan distribution encompass-

ing South America, Antarctica, Australia, and perhaps emergent portions of Zealandia, much of which would have been linked via direct land connections at various times. Core Gruiformes appear to have originated in West Gondwana (South America, adjacent portions of Antarctica), thus their early biogeographic history may well have involved the same lands as the *Rhynchotos+Eurypyga* clade (Claramunt and Cracraft, 2015). Assuming *Aptornis* is the sister taxon of *Psophia* and given the ages just cited for the divergence between *Psophia* and other gruoids, an overwater dispersal event may be implicated. If, however, *Aptornis* is sister to core Gruiformes, Gruoidea, or Ralloidea, then a deeper history for *Aptornis* may imply that a fragmentation hypothesis would be more likely.

The paleogeographic history of Zealandia-Australia has been more complex than depicted in many biogeographic interpretations. The 84 mya separation of Zealandia from West Antarctica and southeastern Australia/Tasmania has frequently been used to assess whether a taxon on part of Zealandia is sufficiently old to have been isolated via vicariance or young enough to have been established by long-distance dispersal; however, the Tasman Basin arose by propagation (“unzipping”) to the north, so that the age of the transform fault separating northern Australia and Zealandia today is considerably younger, around 50 mya (Schellart et al., 2006). In addition, a series of now-submerged microcontinents lie between the northern part of the Lord Howe Rise and northeastern Australia (Gaina et al., 1998; Exon et al., 2006), including the Marion Plateau of northeastern Australia. Thus, continental fragments from the east and west of Australia and Zealandia, respectively, are now separated by the extremely narrow Cato Trough. Hotspot activity in the region has also created numerous seamounts, some emergent at various times, in the region throughout much of the Tertiary. The region has been characterized by widespread shallow marine shelves and Paleogene subaerial volcanics, and portions of the Lord Howe Rise itself were subaerial at times (Exon et al., 2006; Sutherland et al., 2010). Sea levels were also lower at various times in the Oligocene and Miocene than they are today, which is potentially important for land connections or subaerial adjacency (Miller et al., 2005).

All these observations suggest that intermittent land connections over millions of years would have facilitated biotic interchange at times of land emergence. Realistically, however, the conundrum regarding the biogeographic history of these pairs of taxa as well as many others is not likely to be resolved until older *Aptornis* and core-gruiform fossils are found on these, or other, Gondwanan landmasses.

ALTERNATIVE HYPOTHESES FOR THE POSITION OF ADZEBILLS

Three most parsimonious trees resulting from our morphological data place the *Aptornis+Psophia* sister group as the sister group of core Gruiformes. This may be due to the highly autapomorphic and/or plesiomorphic character states of *Aptornis*. If *Aptornis* is not the sister taxon of *Psophia*, our results logically suggest that *Aptornis* represents an old, deep lineage within core Gruiformes. *Aptornis* could be a sister taxon to core Gruiformes or the sister taxon of Gruoidea or Ralloidea, as monophyly analysis recovered the *Aptornis+Gruiformes* tree as the closest in branch length to the MPTs, followed by that of *Aptornis+D. hawkinsi* (table 3).

At the same time, an affinity with Ralloidea may be due to locomotor convergence. This is especially supported by forced monophyly analysis of *Aptornis*+Rallidae, which yielded an *Aptornis*+*H. haematopus whitesidei* sister group in which much of the shared synapomorphies were those of the pelvis and pectoral girdle.

Our results do not suggest a close affinity between *Aptornis* and Sarothruridae as recovered by Boast et al. (2019). Monophyly-constraint analysis placed the *Aptornis*+*M. kioloides*, *Aptornis*+Sarothruridae and *Aptornis*+Sarothruridae+Heliornithidae groups as the least parsimonious along with *Aptornis*+Galloanseres (table 3). These groups additionally were 18–24 steps away from the MPT. Two unambiguous synapomorphies were recovered for the *Aptornis*+*M. kioloides* sister group (40(1), 168(0)) and one each (40(1)) was recovered for *Aptornis*+Sarothruridae and *Aptornis*+Sarothruridae+Heliornithidae; however, *Aptornis* contained missing data for all of these synapomorphies; thus, whether these synapomorphies would remain unambiguous if *Aptornis* was able to be scored is currently unknown. Although we also agree that *Aptornis* is gruiform, we caution against the “resolution” of the position of *Aptornis* within core Gruiformes as being within crown Ralloidea (Boast et al., 2019). The morphology of this taxon makes it difficult to place, and the conflicting placement of *Aptornis* across these two most recent studies indicates that further investigations incorporating different data types are needed to confidently assess the placement of *Aptornis* within core Gruiformes. This is especially true as Boast et al. (2019) did not incorporate morphological data or nuclear gene data into their mtDNA dataset. Morphological data of Livezey and Zusi (2007) and Livezey (1998) additionally needs to be treated carefully during reanalysis as performed in Boast et al. (2019), as these datasets were created with the preconception that historic “Gruiformes” were monophyletic and that *Aptornis* was the sister taxon of *R. jubatus*. Several characters scored for *Aptornis* in these datasets assumed homology and cooccurrence of several highly apomorphic states that were combined into one character under the assumption that these states were related to flight loss and/or gigantism. We reject that these assumptions should be made about any taxon, especially *Aptornis*, and within our dataset took care to logically separate characters so that such assumptions would be minimized. This should be taken into consideration for future morphological studies creating novel characters that include *Aptornis*, especially when studying highly apomorphic elements such as the humerus. We agree that both morphological and molecular data for this taxon are valuable and should be further explored, especially within the context of combined data, to better elucidate the position of this taxon.

Our results may reflect missing data for *Aptornis*, a prevalence of shared nongruoid and/or gruiform traits between *Psophia* and *Aptornis*, and/or a lack of unique synapomorphies for core Gruiformes found within our dataset in general. Synapomorphies for core Gruiformes within our dataset were ambiguous (CI <1.00). Moreover, past morphological studies have not uncovered many unique traits for core Gruiformes. Livezey and Zusi (2007), for example, found only one unambiguous synapomorphy for this group (a coracoidal character), as did Livezey (1998) for core Gruiformes exclusive of Turnices and Otidides (a tibiotarsal character). Taxon sampling, character representation, and character coding bias and/or error remain as possible influences of our morphological results.

NOVEL PLACEMENT OF *DIAPHORAPTERYX*, *HIMANTORNIS*, AND *MENTOCREX*

Three taxa previously considered to be members of Rallidae, the extinct *Diaphorapteryx hawkinsi* and the extant *Himantornis haematopus* (Nkulengu rail) and *Mentocrex kiolooides* (Madagascan wood rail, synonym of the older name *Canirallus kiolooides* of Pucheran, 1845), exhibit novel phylogenetic placement within our dataset. *H. haematopus* and *M. kiolooides* were found to be more closely related to Sarothruridae than to Rallinae within both our morphological and combined data results, and a *Sarothrura*+*Mentocrex kiolooides* sister group was recovered by the molecular results (less than 50% bootstrap value for both placements within the morphological results, 100% clade credibility value for both novel placements in the combined results, and 73% clade credibility value for *Sarothrura*+*Mentocrex* in the molecular results). Past phylogenetic and anatomical studies that include *H. haematopus* have largely placed this taxon as the sister of Rallinae, and tend to place *M. kiolooides* within Rallidae (Olson, 1973; Livezey, 1998; Clarke et al., 2005; Hackett et al., 2008). Olson (1973) placed *H. haematopus* and *M. kiolooides* as members of the “most basal Rallinae” based on anatomical similarities. Livezey (1998) recovered *M. kiolooides* as the sister taxon of *Canirallus* within Rallinae and *H. haematopus* as the sister taxon to Rallinae with high support (98% bootstrap value). Clarke et al. (2005) also recovered *H. haematopus* as the sister taxon to Rallinae with robust support based on morphology (100% bootstrap value). Hackett et al. (2008) similarly recovered *Himantornis* as the sister taxon of *Rallus*, based on nuclear DNA sequences from 19 nuclear loci (including introns, exons and untranslated regions) with 100% bootstrap values. Although García-R et al. (2014) recovered *H. haematopus* as the sister taxon of Ralloidea within a maximum likelihood phenogram (100% bootstrap support) based on characters compiled by Livezey (1998), their maximum likelihood analyses of mitochondrial (*cytb*, COI, 16S) and nuclear DNA (RAG1, FGB-7) resulted in an *H. haematopus*+*M. inepta* sister group within Rallidae with moderate support (<70% bootstrap support, 0.99 posterior probability). Differences in placement of *H. haematopus* between our study and that of García-R et al. (2014) may be due to exclusion of RAG2 sequences and/or inclusion of mitochondrial genes in the latter. García-R et al. (2014) placed *Sarothrura rufa* within Rallidae as the sister taxon of a *M. kiolooides*+*Rallina* sister group within the phenogram (less than 70% bootstrap support), but found *M. kiolooides* to be the sister taxon of *S. rufa* with high support in the 5-gene concatenated analysis (100% bootstrap value, 1.0 posterior probability). Most recently, Boast et al. (2019) recovered *H. haematopus* within Rallidae (*H. haematopus*+*Megacrex inepta*, 83% clade credibility) but similarly found *M. kiolooides* to be within Sarothruridae as the sister taxon of a *S. rufa*+*S. ayresi* sister group (100% clade credibility value) using mtDNAs. Our results corroborate this latter placement of *M. kiolooides* using morphological and molecular data, and suggest that the taxonomic position of this species within Rallidae is questionable.

Diaphorapteryx hawkinsi is an extinct, flightless taxon of New Zealand that has long been thought to have been raillike and most closely related to *Gallirallus*, although it remains phylogenetically underanalyzed (Worthy et al., 2017). Livezey (1998) recovered

D. hawkinsi as the sister group of *Cabalus modestus* (Chatham Rail) within Rallidae. MtDNA studies place *D. hawkinsi* within Rallidae. García-R et al. (2014) recovered *D. hawkinsi* as the sister taxon of *Habroptila wallacii* (<90% clade credibility) in a 5-gene concatenated analysis and identified *D. hawkinsi* as the sister taxon of *Gallirallus modestus* within a phenogram. Boast et al. (2019) also found *D. hawkinsi* to be located within Rallidae as the sister taxon of a large group containing the genera *Habroptila*, *Gallirallus*, *Hypotaenidia*, and *Eulabeornis* (100% clade credibility). Our novel placement of *D. hawkinsi* as the apparent sister group of Ralloidea suggests that further study is needed to clarify its position.

MORPHOLOGICAL TRANSITIONS OF CORE GRUIFORMES

In addition to robust placement of *Aptornis*, our results present an opportunity to probe the morphological transitions of each major group within core Gruiformes. Parsimony analysis of morphological data optimized 11 synapomorphies (11 additional with missing data/differing scorings) for *D. hawkinsi*+Ralloidea of the skull (3/11), humerus (2/11), pelvis (3/11), femur (1/11) and tibiotarsus (2/11). This suggests that the plesiomorphic condition for Ralloidea within the skull and mandible comprised rostrocaudal alignment of the zona flexoria craniofacialis (14(1)), the presence of a pair of acuminate projections located on the rostral margin of the parasphenoid (93(1)), and the presence of a dorsally oriented projection located on the caudal portion of the mandible (129(1)). Postcranial synapomorphies for Ralloidea consist of proximal elevation of the tuberculum ventrale of the humerus, so that it is immediately above the tuberculum dorsale and projects cranially or cranioproximally (213(3)); possession of a dorsoventrally narrow crus dorsale fossae (219(1)); a markedly prominent dorsal iliac crest of the pelvis that exceeds the height of the dorsal postacetabular synsacrum (257(2)); a prominent, flange-shaped and ventrally oriented caudolateral angle of the pelvis that is undercut by a deep concavitas infracristalis (272(2)); virtual absence of pelvic incisurae (277(0)), a cranially projected trochanteric crest of the femur (299(1)), and a medially compressed (338(2)) and craniocaudally elongate trochlea cartilaginis tibialis within the tibiotarsus (339(2)).

Apart from the pelvic characters, many of these synapomorphies suggest a very small additional tuberculum or slight change in feature shape. These results may indicate that the morphological correlates of flighted and flightless taxa are subtler and more variable within Ralloidea than previously assumed. This has been echoed in past morphological and molecular phylogenetic studies of Rallidae in which flightless taxa have been found to be more closely related to flighted group members than to other flightless rallids. Trewick (1997) created a phylogeny focused on endemic New Zealand rails using 12S rRNA, cytochrome *b*, and ancient DNA. Results recovered the flightless *Gallirallus australis*, *Rallus sylvestris*, and *Rallus p. dieffenbachia* as being more closely related to volant rallids than to each other. Livezey (1998) similarly found that many flightless rallids were aligned with volant taxa and exhibited a diversity of morphological characters.

CONCLUSIONS

Our analyses present a novel, robust result for the position of *Aptornis* within core Gruiformes and suggest a gruoid affiliation for this taxon. If our results suggesting that *Aptornis* is related to *Psophia* are incorrect, the data do indicate that *Aptornis* represents a deep lineage that is more likely sister to core Gruiformes, Gruoidea, or Ralloidea than to rallids per se. Our results indicate a Gondwanan origin for core Gruiformes. Further morphological and total evidence phylogenetic analyses will be required to clarify the position of *Aptornis* in relation to core Gruiformes, especially in the context of other extinct gruiformlike taxa. More comprehensive study will better resolve both the placement of *Aptornis* and the relationships and phenotypic transitions of core and historic Gruiformes and basal Neoaves. Our dataset represents an initial foundation for these goals. The continued development of this dataset holds potential for providing a more robust solution to the complex problem of basal neoavian stem lineage phylogeny, phenotypic evolution, and biogeographic history.

ACKNOWLEDGMENTS

We are most appreciative of the collections staff of the Division of Paleontology of the American Museum of Natural History, Mark Norell, Ruth O'Leary, and Carl Mehling, for facilitating the study of fossil material in their care. We thank the Field Museum of Natural History, especially Shannon Hackett, John Bates, and Ben Marks, for loaning the specimen of *Mentocrex kiolooides*. We are also indebted to Daniel Ksepka and Don Melnick for reading several early drafts of this manuscript and providing invaluable feedback. We thank Daniel Field, Rob DeSalle, and Julia Clarke for their valuable insight and advice. We would like to acknowledge an NSF Graduate Research Fellowship Program award (to G.M.M., grant number DGE-16-4486), NSF Award 1241066 (to J.C.), and the AMNH Department of Ornithology, as well as the Ecology, Evolution and Environmental Biology Department at Columbia University for additional funding for this research.

REFERENCES

- Andrews, C.W. 1896. On the extinct birds of the Chatham Islands. *Novitates Zoologicae* 3: 260–271.
- Beddard, F.E. 1890. On the anatomy of *Podica senegalensis*. *Zoological Society of London 1889/1890*: 425–443.
- Beddard, F.E. 1898. *The structure and classification of birds*. London: Longmans, Green.
- Bertelli, S., L.M. Chiappe, and G. Mayr. 2011. A new Messel rail from the early Eocene Fur Formation of Denmark (Aves, Messelornithidae). *Journal of Systematic Paleontology* 9: 551–562.
- Bertelli, S., L.M. Chiappe, and G. Mayr. 2014. Phylogenetic interrelationships of living and extinct Tinamidae, volant paleognathous birds from the New World. *Zoological Journal of the Linnean Society* 172: 145–184.
- Boast, A.P., et al. 2019. Mitochondrial genomes from New Zealand's extinct Adzebills (Aves: Aptornithidae: *Aptornis*) support a sister-taxon relationship with the Afro-Madagascan Sarothruridae. *Diversity* 11: 24 (<https://doi.org/10.3390/d11020024>).

- Bourdon, E., B. Bouya, and M. Iarochène. 2005. Earliest African neornithine bird: a new species of Prophaethontidae (Aves) from the Paleocene of Morocco. *Journal of Vertebrate Paleontology* 25: 157–170.
- Buller, W.L. 1878. Article XXIV—On the species forming the genus *Ocydromus*, a peculiar group of brevi-pennate Rails [read before the Wellington Philosophical Society, 12 January]. Published in 2016. *In* The pamphlet collection of Sir Robert Stout, vol. 22. Wellington, New Zealand: Victoria University of Wellington.
- Chubb, A.L. 2004. New nuclear evidence for the oldest divergence among neognath birds: the phylogenetic utility of ZENK (i). *Molecular Phylogenetics and Evolution* 30: 140–151.
- Claramunt, S., and J.L. Cracraft. 2015. A new time tree reveals Earth history's imprint on the evolution of modern birds. *Science Advances* 1: 11.
- Clarke, J.A., M.A. Norell, and D. Dashzeveg. 2005. New avian remains from the Eocene of Mongolia and the phylogenetic position of the Eogruidae (Aves, Gruoidea). *American Museum Novitates* 3494: 1–17.
- Clarke, J.A., D.T. Ksepka, N.A. Smith, and M.A. Norell. 2009. Combined phylogenetic analysis of a new North American fossil species confirms widespread Eocene distribution for stem rollers (Aves, Coraci). *Zoological Journal of the Linnean Society* 157: 586–611.
- Cracraft, J.L. 1982a. Phylogenetic relationships and transantarctic biogeography of some gruiform birds. *Geobios* 6: 393–402.
- Cracraft, J. 1982b. Phylogenetic relationships and monophyly of loons, grebes, and hesperornithiform birds, with comments on the early history of birds. *Systematic Zoology* 31: 35–56.
- Cracraft, J. 1988. The major clades of birds. *In* M.J. Benton (editor), *The phylogeny and classification of the tetrapods*, vol. 1. Amphibians, reptiles, birds: 339–361. Oxford: Systematics Association.
- Cracraft, J.L., and J.A. Clarke. 2001. The basal clades of modern birds. *In* J. Gauthier and L.F. Gall (editors), *New perspectives on the origin and early evolution of birds*: 143–156. New Haven: Peabody Museum of Natural History, Yale University.
- Ericson, P.G.P., et al. 2006. Diversification of Neoaves: integration of molecular sequence data and fossils. *Biology Letters* 2: 543–547.
- Exon, N.F., P.J. Hill, Y. Lafoy, C. Heine, and G. Bernardel. 2006. Kenn Plateau off northeast Australia: a continental fragment in the southwest Pacific jigsaw. *Australian Journal of Earth Sciences* 53: 541–564.
- Fain, M.G., and P. Houde. 2004. Parallel radiations in the primary clades of birds. *Evolution* 58: 2558–2573.
- Fain, M.G., C. Krajewski, and P. Houde. 2007. Phylogeny of “core Gruiformes” (Aves: Grues) and resolution of the Limpkin-Sungrebe problem. *Molecular Phylogenetics and Evolution* 43: 515–529.
- Fleming, C.A. 1969. Rats and moa extinction. *Notornis* 16: 210–211.
- Fürbringer, M. 1888. *Untersuchungen zur Morphologie und Systematik der Vögel*. Amsterdam: van Halkema.
- Gaina, C., et al. 1998. The tectonic history of the Tasman Sea: a puzzle with 13 pieces. *Journal of Geophysical Research* 103: 12413–12433.
- García-R, J.C., G.C. Gibb, and S.A. Trewick. 2014. Deep global evolutionary radiation in birds: diversification and trait evolution in the cosmopolitan bird family Rallidae. *Molecular Phylogenetics and Evolution* 81: 96–108.
- Hackett, S.J., et al. 2008. A phylogenomic study of birds reveals their evolutionary history. *Science* 320: 1763.

- Hamilton, A. 1891. On the genus *Aptornis*, with more especial reference to *Aptornis defossor*, Owen. Transactions of the Royal Society of New Zealand 24: 175–184.
- Hedges, B.S., and C.G. Sibley. 1994. Molecules vs. morphology in avian evolution: The case of the “pelecaniform” birds. Proceedings of the National Academy of Sciences of the United States of America 91: 9861–9865.
- Hesse, A. 1990. Die Beschreibung der Messelornithidae (Aves: Gruiformes: Rhynocheti) aus dem alttertiär Europas und Nordamerikas. Courier Forschungsinstitut Senckenberg 128: 1–176.
- Houde, P., A. Cooper, E. Leslie, A.E. Shand, and G.A. Montano. 1997. Phylogeny and evolution of 12S rDNA in Gruiformes (Aves). In D.P. Mindell (editor), Avian molecular evolution and systematics: 117–154. San Diego: Academic Press.
- Hoyo, J. del, A. Elliott, J. Sargatal, D.A. Christie, and E. de Juana (editors). 2019. Handbook of the birds of the world alive. Barcelona: Lynx Edicions.
- Huelsenbeck, J.P., and F. Ronquist. 2001. MrBayes: Bayesian inference of phylogeny. Bioinformatics 17: 754–755.
- Jarvis, E.D., et al. 2014. Whole-genome analyses resolve early branches in the tree of life of modern birds. Science 346: 1320–1331.
- Kearse, M., et al. 2012. Geneious Basic: an integrated and extendable desktop software platform for the organization and analysis of sequence data. Bioinformatics 28: 1647–1649.
- Ksepka, D.T., and J.A. Clarke. 2012. A new stem parrot from the Green River Formation and the complex evolution of the grasping foot in Pan-Psittaciformes. Journal of Vertebrate Paleontology 32: 395–406.
- Lanave, C., G. Preparata, C. Saccone, and G. Serio. 1984. A new method for calculating evolutionary substitution rates. Journal of Molecular Evolution 20: 86–93.
- Lewis, P.O. 2001. A likelihood approach to estimating phylogeny from discrete morphological character data. Systematic Biology 50: 913–925.
- Livezey, B.C. 1986. A phylogenetic analysis of recent anseriform genera using morphological characters. *The Auk* 103: 737–754.
- Livezey, B.C. 1998. A phylogenetic analysis of the Gruiformes (Aves) based on morphological characters, with an emphasis on the rails (Rallidae). Philosophical Transactions of the Royal Society of London B, Biological Sciences 353: 2077–2151.
- Livezey, B.C., and R.L. Zusi. 2006. Higher-order phylogeny of modern birds (Theropoda, Aves: Neornithes) based on comparative anatomy (I. Methods and characters). Bulletin of Carnegie Museum of Natural History 37: 1–544.
- Livezey, B.C., and R.L. Zusi. 2007. Higher-order phylogeny of modern birds (Theropoda, Aves: Neornithes) based on comparative anatomy (II. Analysis and discussion). Zoological Journal of the Linnaean Society 149: 1–95.
- Lowe, P.R. 1926. More notes on the quadrate as a factor in avian classification. Ibis 68: 152–188.
- Mantell, G.A. 1848. On the fossil remains of birds collected in various parts of New Zealand by Mr. Walter Mantell, of Wellington. Quarterly Journal of the Geological Society of London 4: 225–238.
- Mayr, G. 2004. Morphological evidence for sister group relationship between flamingos (Aves: Phoenicopteridae) and grebes (Podicipedidae). Zoological Journal of the Linnaean Society 2: 157–169.
- Mayr, G. 2005. The Paleogene Old World Potoo *Paraprefica* Mayr, 1999 (Aves, Nyctibiidae): its osteology and affinities to the New World *Preficinae* Olson, 1987. Journal of Systematic Palaeontology 3: 359–370.
- Mayr, G. 2006. A rail (Aves, Rallidae) from the early Oligocene of Germany. Ardea 94: 23–31.

- Mayr, G., and J.A. Clarke. 2003. The deep divergences of neornithine birds: a phylogenetic analysis of morphological characters. *Cladistics* 19: 527–553.
- Miller, K.G., et al. 2005. The Phanerozoic record of global sea-level change. *Science* 310: 1293–1298.
- Mindell, D.P., et al. 1997. Phylogenetic relationships among and within select avian orders based on mitochondrial DNA. In D.P. Mindell (editor), *Avian molecular evolution and systematics*: 213–247. San Diego: Academic Press.
- Morgan-Richards, M., et al. 2007. Bird evolution: testing the Metaves clade with six new mitochondrial genomes. *BioMed Central Evolutionary Biology* 8:1–12.
- O’Leary, M.A., and S.G. Kaufman. 2012. MorphoBank 3.0: Web application for morphological phylogenetics and taxonomy.
- Oliver, W.R.B. 1945. Avian evolution in New Zealand and Australia. *Emu* 45: 119–152.
- Oliver, W.R.B. 1955. *New Zealand birds*, 2nd ed. Wellington, New Zealand: A.H. and A.W. Reed.
- Olson, S.L. 1973. A classification of the Rallidae. *Wilson Bulletin* 85: 381–416.
- Olson, S.L. 1985. The fossil record of birds. In D.S. Farner, J.R. King, and K.C. Parkes (editors), *Avian biology*, vol. 8: 79–256. New York: Academic Press.
- Olson, S.L. 1987. More on the name *Rallus hodgenorum*. *Notornis* 34: 167–168.
- Olson, S.L., and D.W. Steadman. 1981. The relationships of the Pedionomidae (Aves: Charadriiformes). *Smithsonian Contributions to Zoology* 337: 1–25.
- Owen, R. 1843. On *Dinornis Novae-Zelandiae*. [proceedings of a meeting of January 24, 1843: part 1 of Owen’s first memoir on *Dinornis*, containing original proposal of *Dinornis novaezealandiae*]. *Proceedings of the Zoological Society of London*, part 11: 8–10.
- Owen, R. 1849. On *Dinornis*, an extinct genus of tridactyle struthious birds, with descriptions of portions of the skeleton of five species which formerly existed in New Zealand (part III). *Transactions of the Zoological Society of London* 3: 235–275, pls. 28–30.
- Owen, R. 1849. On *Dinornis*: Containing a description of the skull and beak of that genus, and of the same characteristic parts of *Palapteryx*, and two other genera of those birds, *Notornis* and *Nestor*; forming part of an extensive collection of ornithic remains discovered by Mr. Walter Mantell at Waingongoro, North Island of New Zealand (part V). *Transactions of the Zoological Society of London* 3: 345–378.
- Owen, R. 1871. Preliminary notice of 17th memoir on *Dinornis*. *Proceedings of the Zoological Society of London* 8: 119–126.
- Owen, R. 1879. *Memoirs on the Extinct wingless birds of New Zealand, with an appendix on those of England, Australia, Newfoundland, Mauritius and Rodriguez*. London: John van Voorst.
- Parker, W.K. 1866. VIII. On the structure and development of the skull in the ostrich tribe. *Philosophical Transactions of the Royal Society of London Series B, Biological Sciences* 156: 113–183.
- Prum, R.O., et al. 2015. A comprehensive phylogeny of birds (Aves) using targeted next-generation DNA sequencing. *Nature* 526: 569–573.
- Pucheran, J. 1845. Notes sur quelques espèces Madécasses de l’ordre des Échassiers. *Revue Zoologique* 8: 277–280.
- Reddy, S., et al. 2017. Why do phylogenomic data sets yield conflicting trees? Data type influences the avian tree of life more than taxon sampling. *Systematic Biology* 66: 857–879.
- Ronquist, F., and J.P. Huelsenbeck. 2003. MrBayes 3: Bayesian phylogenetic inference under mixed models. *Bioinformatics* 19:1572–1574.
- Salisbury, B.A. 1999. Misinformative characters and phylogeny shape. *Systematic Biology* 48: 153–169.

- Schellart, W.P., G.S. Lister, and V.G. Toy. 2006. A Late Cretaceous and Cenozoic reconstruction of the southwest Pacific region: tectonics controlled by subduction and slab rollback processes. *Earth-Science Reviews* 76: 191–233.
- Sélys Longchamps, E. de. 1848. Résumé concernant les oiseaux brevipedes mentionnés dans l'ouvrage de M. Strickland sur le Dodo. *Revue Zoologique* 11: 292–295.
- Sibley, C.G., and J.E. Ahlquist. 1990. Phylogeny and classification of birds: a study in molecular evolution. *Journal of Field Ornithology* 63: 380–384.
- Sorenson, M.D., E. Oneal, J. García-Moreno, and D.P. Mindell. 2003. More taxa, more characters: the hoatzin problem is still unresolved. *Molecular Biology and Evolution* 20: 1484–1498.
- Sutherland, R., et al. 2010. Lithosphere delamination with foundering of lower crust and mantle caused permanent subsidence of New Caledonia Trough and transient uplift of Lord Howe Rise during Eocene and Oligocene initiation of Tonga-Kermadec subduction, western Pacific. *Tectonics* 29: TC2004.
- Swofford, D.L. 2002. PAUP* phylogenetic analysis using parsimony (*and other methods), version 4. Sunderland, MA: Sinauer Associates.
- Trewick, S.A. 1997. Flightlessness and phylogeny amongst endemic rails (Aves: Rallidae) of the New Zealand region. *Philosophical Transactions of the Royal Society of London B, Biological Sciences* 352: 429–446.
- Tuinen, M. van, and S.B. Hedges. 2001. Calibration of avian molecular clocks. *Molecular Biology and Evolution* 18: 206–213.
- Tuinen, M. van, D.B. Butvill, J.A.W. Kirsch, and S.B. Hedges. 2001. Convergence and divergence in the evolution of aquatic birds. *Proceedings of the Royal Society of London Series B, Biological Sciences* 268: 1345–1350.
- Weber, E., and A. Hesse. 1995. The systematic position of *Aptornis*, a flightless bird from New Zealand. *Courier Forschungsinstitut Senckenberg* 181: 293–301.
- Weber, E., and F.T. Krell. 1995. Case 2879: *Aptornis* Owen, [1848] (Aves): proposed conservation of as the correct original spelling. *Bulletin of Zoological Nomenclature* 52: 170–174.
- Wilmhurst, J.M., A.J. Anderson, T.F.G. Higham, and T.H. Worthy. 2008. Dating the late prehistoric dispersal of Polynesians to New Zealand using the commensal Pacific rat. *Proceedings of the National Academy of Sciences of the United States of America* 105: 7676–7680.
- Wood, J.R., R.P. Scofield, J. Hamel, and J.M. Wilmhurst. 2017. Bone stable isotopes indicate a high trophic position for New Zealand's extinct South Island Adzebill (*Aptornis defossor*) (Gruiformes: Aptornithidae). *New Zealand Journal of Ecology* 41: 240–244.
- Worthy, T.H., and R.N. Holdaway. 1993. Quaternary fossil faunas from caves in the Punakaiki area, West Coast, South Island, New Zealand. *Journal of the Royal Society of New Zealand* 23: 147–254.
- Worthy, T.H., and R.N. Holdaway. 1994. Quaternary fossil faunas from caves in Takaka Valley and on Takaka Hill, northwest Nelson, South Island, New Zealand. *Journal of the Royal Society of New Zealand* 24: 297–391.
- Worthy, T.H., and R.N. Holdaway. 2002. *The lost world of the Moa: prehistoric life of New Zealand*. Bloomington: Indiana University Press.
- Worthy, T.H., and D.C. Mildenhall. 1989. A late Otiran-Holocene palaeoenvironment reconstruction based on cave excavations in northwest Nelson, New Zealand. *New Zealand Journal of Geology and Geophysics* 32: 243–253.
- Worthy, T.H., A.J.D. Tennyson, and R.P. Scofield. 2011. Fossils reveal an early Miocene presence of the aberrant gruiform Aves: Aptornithidae in New Zealand. *Journal of Ornithology* 152: 669–680.

- Worthy, T.H., and R.P. Scofield. 2012. Twenty-first century advances in knowledge of the biology of the moa (Aves: Dinornithiformes): a new morphological analysis and moa diagnoses revised. *New Zealand Journal of Zoology* 39: 87-153.
- Worthy, T.H., V.L. De Pietri, and R.P. Scofield. 2017. Recent advances in avian palaeobiology in New Zealand with implications for understanding New Zealand's geological, climatic and evolutionary histories. *New Zealand Journal of Zoology* 44: 177-211.
- Yang, Z. 1994. Maximum likelihood phylogenetic estimation from DNA sequences with variable rates over sites: approximate methods. *Journal of Molecular Evolution* 39: 306-314.
- Yang, Z., and B. Rannala. 1997. Bayesian phylogenetic inference using DNA sequences: a Markov chain Monte Carlo method. *Molecular Biology and Evolution* 14: 717-724.

APPENDIX 1

CHARACTER DESCRIPTIONS

Description of 368 discrete osteological characters. State (0) is reserved for absence only. Citations are provided where overlap with a previously created character has occurred and/or where the character has been modified based on assessment of previously created characters. Citations of previously created characters are not meant to represent a comprehensive list of character overlap, and largely comprise the characters of Livezey and Zusi (2006) due to our focus on reevaluation of this dataset. Characters are anglicized as much as possible, but Latin anatomical terms are used for standardization across previously published studies.

SKULL: ROSTRUM

1. Rostrum, dorsal aspect, a pair of distinct foramina near anterior rostral terminus (exclusive of pori pneumatici), status: absent (0); present (1). *Aptornis defossor* was coded as 1 based on AMNH 7300. *Diaphorapteryx hawkinsi* was coded as 1 based on AMNH 7424.
2. Rostrum, dorsal aspect, midline length from the apex of the premaxilla to the zona flexoria craniofacialis relative to that of the cranium: 0.40-2.00 (1); 2.01-3.00 (2). *A. defossor* was coded as 1 based on AMNH 7300. *D. hawkinsi* was coded as 1 based on AMNH 7424. Livezey and Zusi (2006), character 260.
3. Rostrum, dorsal aspect, mediolateral extension of the anterior maxillonasal portion of the rostrum: intermediate, between states 2 and 3 (1); medially compressed (2); extremely laterally splayed (3). *A. defossor* was coded as 1 based on AMNH 7300. *D. hawkinsi* was coded as 2 based on AMNH 7424.
4. Rostrum, lateral aspect, general profile: curved inferiorly (1); lacking inferior curvature so that rostrum appears to be flat along ventral margin or recurved superiorly (2). *A. defossor* was coded as 1 based on AMNH 7300. *D. hawkinsi* was coded as 1 based on AMNH 7424. *Podica senegalensis* was coded as 1 using Beddard (1890: fig. 2).
5. Rostrum, external nares, lateromedially and craniocaudally extensive, approach terminal end of rostrum of maxilla, status: absent (0); present (1). *A. defossor* was coded as 0 based on AMNH 7300 and AMNH 60. *D. hawkinsi* was coded as 0 based on AMNH 7424. Livezey and Zusi (2006), character 346.
6. Rostrum, external nares, form: schizorhinal, caudal margin acuminate (1); holorhinal, caudal margin rounded (2). *A. defossor* was coded as 1 based on AMNH 7300. *D. hawkinsi* was coded as 2 based

- on AMNH 7424. *P. senegalensis* was coded as 2 using Beddard (1890: fig. 2). Livezey (1998), character 1; Mayr and Clarke (2003), character 6.
7. Rostrum, lateral aspect, external bony nostrils: absent (0); present (1). *A. defossor* was coded as 1 based on AMNH 7300. *D. hawkinsi* was coded as 0 based on Andrews (1896: pl. III). Character based on description accompanying Owen (1879: pl. LXXXIII).
 8. Rostrum, internal bony septum that is dorsoventrally expansive and unaccompanied by additional intranasal ossification, ankylosed to ventral midline of intranasal area: absent (0); present (1). *A. defossor* was coded as 1 based on AMNH 7300. *D. hawkinsi* was coded as 0 based on AMNH 7424. *P. senegalensis* was coded as 0 using Beddard (1890: fig. 2).
 9. Rostrum, lateral aspect, nasal sulcus, status: present, complete to terminal end of rostrum (1); lost or truncated (2). *A. defossor* was coded as 2 based on AMNH 7300. *D. hawkinsi* was coded as 2 based on AMNH 7424. Livezey and Zusi (2006), character 272.
 10. Rostrum, shape is triangular and dorsoventrally compressed, status: absent (0); present (1). *A. defossor* was coded as 0 based on AMNH 7300. *D. hawkinsi* was coded as 0 based on AMNH 7424. Livezey and Zusi (2006), character 280.
 11. Rostrum, ventral aspect, ventromedial fenestra, status and form: present and confluent with fenestra choanalis, occurs in approximately one half or less of rostrum (1); present and prominent, like state 1 but extends through entire or almost entire rostrum (2); lost, typically due to occlusion by spongy bone (3). *A. defossor* was coded as 1 based on AMNH 7300. *D. hawkinsi* was coded as 2 based on AMNH 7424. Livezey and Zusi (2006), character 289.
 12. Rostrum, ventral aspect, ventrolateral fenestra, status: absent, lacking caudal lamina (0); present, closed caudally by maxillojugal pons (1). Livezey and Zusi (2006), character 290.
 13. Rostrum, external nares, site of caudal terminal end relative to zona flexoria craniofacialis: rostral or subequal (1); caudal (2). *A. defossor* was coded as 1 based on AMNH 7300. *D. hawkinsi* was coded as 1 based on AMNH 7424. *P. senegalensis* was coded as 1 using Beddard (1890: fig. 2). Livezey and Zusi (2006), character 341.
 14. Zona flexoria craniofacialis, lateral and medial portions of zona flexoria, rostrocaudal alignment, status: absent, medial region rostral to lateral region (0); present, forms a continuous, lateromedial transverse axis (1). *D. hawkinsi* was coded as 1 based on AMNH 7424. Livezey and Zusi (2006), character 603.
 15. Zona flexoria craniofacialis, conformation as variably distinct transverse lines, often buttressed by frontal bone, status and form: absent or indistinct (0); present, a distinct lamina or groove (1); present, a deep fissure with bordering frontal eminentia (2). *D. hawkinsi* was coded as 0 based on AMNH 7424. Mayr and Clarke (2003), character 5; Livezey and Zusi (2006), character 604.

SKULL: CRANIUM

16. Postorbital cranium, general form: craniocaudally elongate (1); craniocaudally compressed (2). *A. defossor* was coded as 2 based on AMNH 60. *D. hawkinsi* was coded as 1 based on AMNH 7424. *P. senegalensis* was coded as 1 using Beddard (1890: fig. 2). Livezey and Zusi (2006), character 7.
17. Frontal bone, dorsal aspect, nasal gland sulcus, status: absent or poorly defined (0); present, may be accompanied by a pair of distinct, large foramina located between the lacrimals (1). *A. defossor* was coded as 0 based on AMNH 60. *D. hawkinsi* was coded as 0 based on AMNH 7424. Livezey (1998), character 72.
18. Cranium, dorsal aspect, interorbital area, form: convex and not furrowed (1); furrowed, concave medially (2). *A. defossor* was coded as 2 based on AMNH 7300. *D. hawkinsi* was coded as 2 based on AMNH 7424. Livezey (1998), character 70.

19. Cranium, dorsal aspect, pair of prominent, hornlike protruberences, status: absent (0); present (1). *A. defossor* was coded as 0 based on AMNH 7300. *P. senegalensis* was coded as 0 using Beddard (1890: fig. 2).
20. Frontoparietal suture, status in adults: present (1); lost (2). *A. defossor* was coded as 2 based on AMNH 7300. *D. hawkinsi* was coded as 2 based on AMNH 7424. Livezey and Zusi (2006), character 213.
21. Maxilla, tomial crest, tomial angle, extension of caudal terminal end as distinct tubercle or short process caudal to jugomaxillary suture and lateral to arc of jugum, status: absent (0); present, composed entirely of maxilla (1). *A. defossor* was coded as 0 based on AMNH 7300. Livezey and Zusi (2006), character 408.
22. Maxilla, ventral aspect, process of palate, caudal margin, form: simple blade, shell or cone, with variable numbers of exposed trabeculae pneumatica (1); largely enclosed, variably inflated, containing numerous trabeculae pneumatica, producing sponge-like form (2). Livezey and Zusi (2006), character 420.
23. Supraorbital crest, dorsal aspect, pori pneumatici regardless of presence of foramina pneumatica, status: absent (0); present (1). Noncomparable for genera with highly specialized salt glands present (eg. *Gavia*, Spheniscidae, some Charadriiformes). *A. defossor* was coded as 1 based on AMNH 60. *D. hawkinsi* was coded as 0 based on AMNH 7424.
24. Orbital margin, dorsal aspect, general form: essentially not extended or decurved (1); projecting dorsolaterally, creating a sharp and prominent supraorbital crest that extends laterally over orbit (2). *A. defossor* was coded as 1 based on Owen (1879: pl. LXXXIII). *D. hawkinsi* was coded as 1 based on Andrews (1896: pl. III). *P. senegalensis* was coded as 1 using Beddard (1890: fig. 2).
25. Orbital margin, dorsal aspect, distinct foramen pneumaticum exclusive of pori pneumatici, status and form: absent (0); present, large, ovoid, taking up almost entire width of frontal bone (1); present, small and ovoid or round and often laterally located (2). Noncomparable for Charadriiformes. *A. defossor* was coded as 0 based on AMNH 7300. *D. hawkinsi* was coded as 0 based on AMNH 7424.
26. Processus postorbitalis, lateral aspect, status and form: obsolete or absent (0); present and truncate (1); present and extremely elongate, sometimes ankylosing to processus zygomaticus (2). *A. defossor* was coded as 1 based on AMNH 7300. *D. hawkinsi* was coded as 1 based on AMNH 7424. *P. senegalensis* was coded as 1 using Beddard (1890: fig. 2). Claramunt and Rinderknecht (2005), character 31.
27. Processus postorbitalis, dorsolateral aspect, form: convex (1); concave, appears grooved (2). *A. defossor* was coded as 2 based on AMNH 7300. *D. hawkinsi* was coded as 1 based on AMNH 7424.
28. Interorbital septum, mediolateral thickness, form: thin, in some places translucent (1); thick, opaque throughout (2). *A. defossor* was coded as 2 based on AMNH 7300. *D. hawkinsi* was coded as 2 based on AMNH 7424.
29. Foramen nervi facialis, form: essentially circular (1); ovoid, craniocaudally elongate (2); ovoid, like state 2 but craniocaudally compressed (3). *D. hawkinsi* was coded as 1 based on AMNH 7424.
30. Lacrimal, ankylosis to jugal, status: absent (0); present (1). Noncomparable if lacrimal is absent or indiscernible. *D. hawkinsi* was coded as 0 based on AMNH 7424. *P. senegalensis* was coded as 0 using Beddard (1890: fig. 2). Mayr and Clarke (2003), character 12; Livezey and Zusi (2006), character 195.
31. Lacrimal, processus supraorbitalis, form: semicircular (sometimes slightly acuminate at terminal end), projecting laterally (1); slender and terminal end projecting laterocaudally, V-shaped fenestra created between the terminal end of the projection and the cranium (2); in line with cranium, not

- creating fenestra between lacrimal and cranium, lateral margin may be pronounced (3). Noncomparable if lacrimal is absent. *D. hawkinsi* was coded as 3 based on AMNH 7424. Mayr and Clarke (2003), character 13; Livezey and Zusi (2006), character 206.
32. Lacrimal, processus orbitalis, recess and/or foramen pneumaticum/pori pneumatici, status: absent (0); present, pori pneumatici and/or foramen pneumaticum only (1); pori pneumatici present, but deep recess also present (2). Noncomparable if lacrimal is absent. *D. hawkinsi* was coded as 0 based on AMNH 7424. Livezey and Zusi (2006), character 197.
 33. Lacrimal, especially processus orbitalis, form: extremely thin or minimally thickened (1); relatively thick (2). Noncomparable if lacrimal is absent. Clarke et al. (2009), character 11.
 34. Lacrimal, foramen pneumaticum, status and form if present: small, round, barely visible (1); large, ovoid (2); lost (3). Noncomparable if lacrimal and foramen are absent. *D. hawkinsi* was coded as 1 based on AMNH 7424.
 35. Lacrimal, foramen pneumaticum, site if present: anterior (1); lateral (2). Noncomparable if lacrimal and foramen are absent. *D. hawkinsi* was coded as 1 based on AMNH 7424.
 36. Lacrimal, most ventral terminus of processus orbitalis, form: terminal end projecting caudally (1); terminal end projecting cranially (2). Not comparable for *E. helias* or if lacrimal is absent.
 37. Ectethmoid, foramen pneumaticum exclusive of foramen orbitonasale laterale, status and number: absent (0); present, 1 (1); present, 2 or more (2). Noncomparable in absence of or indiscernible ectethmoid.
 38. Ectethmoid, form: extremely thick and well developed (1); moderately developed (2). Noncomparable if ectethmoid is absent or indiscernible. *A. defossor* was coded as 1 based on AMNH 60. *D. hawkinsi* was coded as 1 based on AMNH 7424. Mayr and Clarke (2003), character 14; Livezey and Zusi (2006), character 189.
 39. Ectethmoid, position relative to interorbital septum: ankylosed to interorbital septum (1); not ankylosed to interorbital septum (2). Noncomparable if ectethmoid is absent or indiscernible. *A. defossor* was coded as 1 based on AMNH 60. *D. hawkinsi* was coded as 1 based on AMNH 7424.
 40. Quadrate, lateral aspect, facies articularis quadratojugalis, caudodorsally oriented, prominent, terminally tapered flange, status: absent (0); present (1).
 41. Maxilla, lateral aspect, triangular, caudal projection extending from maxilla, just below jugal, can be made up of both jugal and maxilla: absent (0); present and prominent (1); present but thinned and truncate (2). *A. defossor* was coded as 0 based on AMNH 7300.
 42. Jugal arc, pronounced lateral bowing (convexity) of arc, status: absent, arc essentially straight (0); present and curved (1). *P. senegalensis* was coded as 0 using Beddard (1890: fig. 2). Livezey and Zusi (2006), character 298.
 43. Jugal arc, pronounced ventral bowing (convexity) of arc, status: absent (0); present (1). *P. senegalensis* was coded as 0 using Beddard (1890: fig. 2). Livezey and Zusi (2006), character 299.
 44. Ectethmoid, braced by inferior process of lacrimal, status: present (1); lost (2). Noncomparable for Caprimulgiformes.
 45. Palatines, form: palatines contact maxillae only (1); palatines contact premaxillae (2). *A. defossor* was coded as 2 based on AMNH 60, 7300 and Owen (1879: pl. LXXXIII). *P. senegalensis* was coded as 2 using Beddard (1890: fig. 2). Cracraft and Clarke (2001), character 8.
 46. Palatines, height of ventral and lateral crests relative to each other: height of lateral crest greater than that of medial crest (1); heights subequal or crests barely visible (2); height of medial crest greater than that of lateral crest (3).

47. Palatines, lateral portion, status: well developed (1); rudimentary or vestigial (2). *A. defossor* was coded as 1 based on AMNH 60, 7300 and Owen (1879: pl. LXXXIII). Livezey and Zusi (2006), character 447.
48. Palatines, lateral portion, marked caudolateral orientation, status: absent (0); present (1). *A. defossor* was coded as 0 based on AMNH 60, 7300 and Owen (1879: pl. LXXXIII). Livezey and Zusi (2006), character 451.
49. Palatines, lateral portion, lateral margin broad, flattened and rounded, status: absent (0); present (1). *A. defossor* was coded as 0 based on AMNH 60 and Owen (1879: pl. LXXXIII). Livezey and Zusi (2006), character 452.
50. Palatines, lateral portion, ventral fossa, oblique crest, a rostral, sharply defined, sloping crest that defines a smaller, rostral fossa in the lateral portion of the palatines, status: absent (0); present (1). Livezey and Zusi (2006), character 457.
51. Palatines, caudomedial angle, foramen pneumaticum, status: absent (0); present (1).
52. Cranium, ventral aspect, palatines, choanalis, ventral lamella, status: rudimentary or vestigial (1); prominent (2). Livezey and Zusi (2006), character 441.
53. Palatines, choanalis, ventral lamella, medial separation of bilateral lamellae, form: moderate (1); great (2). Livezey and Zusi (2006), character 444.
54. Palatines, choanalis, ventral lamella, position of caudomedial angle relative to that of the lateral portion, caudal margin, rostrocaudal site, form: coincident (1); rostral (2); caudal (3). *A. defossor* was coded as 2 based on AMNH 60 and Owen (1879: pl. LXXXIII). Livezey and Zusi (2006), character 443.
55. Palatines, caudolateral angle, position relative to area of ankyloses with pterygoids: rostral (1); subequal (2); caudal (3). Not comparable for Tinamiformes. *A. defossor* was coded as 1 based on AMNH 60 and Owen (1879: pl. LXXXIII). *P. senegalensis* was coded as 1 using Beddard (1890: fig. 2).
56. Palatines, pterygoid portion, processus pterygoideus, status: present (1); lost (2). *A. defossor* was coded as 1 based on AMNH 60 and Owen (1879: pl. LXXXIII). *P. senegalensis* was coded as 1 using Beddard (1890: fig. 2). Livezey and Zusi (2006), character 458.
57. Palatines, processus pterygoideus, foramen pneumaticum, status and number: present, 2 or more (1); present, 1 foramen (2); lost (3). Not comparable in absence of the processus pterygoideus.
58. Pterygopalatine juncture, form: syndesmosis and pterygopalatine propria rostrocaudally extensive with the caudal terminus approaching the processus quadraticus pterygoidei (1); articulation of mesipterygopalatina with rudimentary gomphosis intrapterygoidea (2); articulation of pterygopalatina simplex (3). *A. defossor* was coded as 3 based on AMNH 60 and Owen (1879: pl. LXXXIII). Livezey and Zusi (2006), character 601.
59. Palatines and pterygoids, form: sutured (1); articulated (2). Cracraft and Clarke (2001), character 6.
60. Pterygoids (pes pterygoidei), anterior portion, form: linear, often with a lateral projection along the body of the pterygoid that is semicircular in shape, or has variable projections (1); distinctly laterally splayed (2). Bertelli et al. (2011), character 9.
61. Pterygoids, dorsoventral site of pterygopalatine juncture relative to parasphenoidal rostrum: slightly ventral, articulation pterygorostroparasphenoidalis absent (1); on rostrum, pterygorostroparasphenoidalis articulation present (2). Livezey and Zusi (2006), character 480.
62. Pterygoids, body of pterygoid, pes pterygoidei, facies articularis with palatines, lateromedial separation of bilaterally paired caudal extremes (ventral aspect), and corresponding interpterygoid juncture (articulation), form: moderately or slightly separated, juncture only slightly lateral to rostrum

- or barely reaching planum of parasphenoid rostrum (1); not separated, interpterygoid articulation or suture present (2). Livezey and Zusi (2006), character 477.
63. Pterygoids, quadratic margin of pterygoid, facies articularis quadratica, form: only moderately enlarged relative to body of pterygoid, subcondylar (1); markedly broadened and dorsally elongate (2). Livezey and Zusi (2006), character 483.
 64. Processus basiptyergoideus, status: absent (0), present (1). *A. defossor* was coded as 2 based on AMNH 60. *D. hawkinsi* was coded as 2 based on AMNH 7424. Cracraft and Clarke (2001), character 33.
 65. Quadratoptyergoid juncture, form: articulatio duplex, moderate dorsal extension on medial face of processus orbitalis combined with condylus ptyergoideus (1); articulatio simplex, limited to condylus ptyergoideus (2). *A. defossor* was coded as 2 based on AMNH 60 and Owen (1879: pl. LXXXIII). *P. senegalensis* was coded as 2 using Beddard (1890: fig. 2). Livezey and Zusi (2006), character 600.
 66. Temporal fossa, form: mostly only visible from lateral view, terminal end located ventrocranially to nuchal crest (1); edges of temporal fossae almost meeting or meeting above nuchal crest (2). *A. defossor* was coded as 1 based on AMNH 60. *D. hawkinsi* was coded as 1 based on AMNH 7424. *P. senegalensis* was coded as 1 using Beddard (1890: fig. 2). Bertelli et al. (2011), character 19.
 67. Temporal fossa crest, form: shallow, at same level as top of skull (1); prominently raised, distinctive crest (2). *A. defossor* was coded as 2 based on AMNH 60. *D. hawkinsi* was coded as 2 based on AMNH 7424.
 68. Processus zygomaticus, status and form: present, short, typically longer than processus suprameaticus, blunt or acuminate (1); obsolete or absent, although often associated with ossified aponeurosis zygomatica (2); present, short and pointed, nearly identical in size and shape to processus suprameaticus (3); present, long and robust, in some taxa associated with ventral lamina (4). *A. defossor* was coded as 4 based on AMNH 60. *D. hawkinsi* was coded as 1 based on AMNH 7424. Livezey and Zusi (2006), character 146.
 69. Processus zygomaticus, divided by prominent superiolateral crest running the length of the process and terminates caudally on or near caudal margin of temporal fossa, status: absent (0); present (1). Noncomparable in the absence of processus zygomaticus. *A. defossor* was coded as 1 based on AMNH 60. *D. hawkinsi* was coded as 0 based on AMNH 7424.
 70. Processus zygomaticus, articular notch of process of squamous that articulates with quadrate, form: notch facing cranially (1); notch angled ventrally (2). *A. defossor* was coded as 2 based on AMNH 60. Noncomparable in absence of the processus zygomaticus. *D. hawkinsi* was coded as 1 based on AMNH 7424.
 71. Processus suprameaticus, status: absent as distinct process, in most or all cases homologous bone is continuous as rostral margin of meatus acusticus externus (0); present as variably prominent processus postorbitalis (1). *A. defossor* was coded as 1 based on AMNH 60. *D. hawkinsi* was coded as 1 based on AMNH 7424. Livezey and Zusi (2006), character 143.
 72. Foramen dorsomediana, supraoccipital aspect, cf. foramen (ostium), status and site: absent, formaina bilaterally symmetrical within occipital region (0); present, distinctly dorsal, often proximate to transverse nuchal crest (1). *A. defossor* was coded as 0 based on AMNH 60. Livezey and Zusi (2006), character 77.
 73. Transverse nuchal crest, form: shallow or barely visible (1), distinct and prominent (2). *A. defossor* was coded as 2 based on AMNH 60. *D. hawkinsi* was coded as 1 based on AMNH 7424.
 74. Occipital bone, fonticuli occipitalis, pair of perforate, large ovoid foramina superior to foramen magnum within margin of occipital bone, status: absent (0); present (1). *A. defossor* was coded as

- 0 based on AMNH 60. *D. hawkinsi* was coded as 0 based on AMNH 7424. Livezey (1986), character 9.
75. Occipital bone, pair of small nuchal area foramina located near lateral margins, status: absent (0); present (1). *A. defossor* was coded as 0 based on AMNH 60.
76. Occipital bone, foramen v. occipitalis externa, status: present or very distinctly visible (1); lost or smoothed to the point of being hardly or not visible (2). *A. defossor* was coded as 2 based on AMNH 60.
77. Occipital bone, prominentia cerebellaris, form: right and left portions of occipital complex indistinguishable or have very faint, smoothed division (1); occipital complex distinctly separated by median nuchal crest, appearance of a line or extremely bulbous process dividing the complex (2). *A. defossor* was coded as 1 based on AMNH 60.
78. Occipital bone, foramen magnum, form: round or craniocaudally ovoid (1); lateromedially elongate (2). *A. defossor* was coded as 1 based on AMNH 60. *D. hawkinsi* was coded as 1 based on AMNH 7424. Livezey and Zusi (2006), character 27.
79. Foramen n. abducentis, form: round (1); craniocaudally elongate (2). *A. defossor* was coded as 2 based on AMNH 60. *D. hawkinsi* was coded as 1 based on AMNH 7424.
80. Occipital bone, occipital condyle, form: essentially circular (1); distinctly bilobate or reniform, lobes partitioned by medial condylar notch, lateromedially elongate (2); essentially round but flattened along ventral margin of foramen magnum (3). *A. defossor* was coded as 1 based on AMNH 60. *D. hawkinsi* was coded as 3 based on AMNH 7424. Livezey and Zusi (2006), character 21.
81. Occipital bone, occipital condyle, rostrocaudal position relative to exoccipital, processus paroccipitalis: rostral (1); approximately equal or caudal (2). *A. defossor* was coded as 1 based on AMNH 60. Livezey and Zusi (2006), character 24.
82. Occipital bone, subcondylar fossa, form: deep (1); shallow (2); lost (3). *A. defossor* was coded as 2 based on AMNH 60. *D. hawkinsi* was coded as 2 based on AMNH 7424.
83. Occipital bone, canalis nervi hypoglossi, form: circular (1); elongate (2). *A. defossor* was coded as 1 based on AMNH 60. *D. hawkinsi* was coded as 2 based on AMNH 7424.
84. Occipital bone, processus paroccipitalis, lateral crest, form: not very distinct, flattened (1); extremely prominent, oriented relatively caudally (2); extremely prominent, oriented relatively cranially (3). *A. defossor* was coded as 2 based on AMNH 60. *D. hawkinsi* was coded as 2 based on AMNH 7424.
85. Laterosphenoid, orbital face, processus postorbitalis, ventral extent (lateral aspect) relative to cotyla quadratica otici and squamosi, form: dorsal (1); approximately equal (2). *A. defossor* was coded as 2 based on AMNH 60. *D. hawkinsi* was coded as 1 based on AMNH 7424. Livezey and Zusi (2006), character 94.
86. Sphenoid, form: medially compressed (1); laterally splayed (2). *A. defossor* was coded as 1 based on AMNH 60. *D. hawkinsi* was coded as 1 based on AMNH 7424.
87. Parasphenoid, crista fossa parabasalis, status and form: present, prominent, lateromedially compressed crista (1); present, pons comparatively robust but not cristate or lateromedially compressed (2); present, pons incomplete or fibriform (3); lost (4). *A. defossor* was coded as 1 based on AMNH 60. *D. hawkinsi* was coded as 1 based on AMNH 7424. Livezey and Zusi (2006), character 120.
88. Parasphenoid, processus lateralis of parasphenoid, anulus tympanicus, status: absent (0); present (1). *A. defossor* was coded as 0 based on AMNH 60. *D. hawkinsi* was coded as 0 based on AMNH 7424. Livezey and Zusi (2006), character 121.
89. Parasphenoid, lamina, processus lateralis of parasphenoid, status and form: obsolete (1); moderately developed (2); prominent (3). Noncomparable for Caprimulgiformes and *A. defossor*. *D. hawkinsi* was coded as 2 based on AMNH 7424. Livezey and Zusi (2006), character 122.

90. Parasphenoid, lamina, tuberculum basilare, processus medialis parasphenoidalis, status: absent or obsolete (0); present, distinct (1). *D. hawkinsi* was coded as 1 based on AMNH 7424. Livezey and Zusi (2006), character 123.
91. Sphenoid (lamina), form: sphenoid is coplanar with ventral face of skull and oriented craniocaudally (1); sphenoid is coplanar with occipital and is oriented superioinferiorly (2). *A. defossor* was coded as 2 based on AMNH 60. *D. hawkinsi* was coded as 1 based on AMNH 7424.
92. Sphenoid, foramen pneumaticum in center of sphenoid, status: absent (0); present (1). *A. defossor* was coded as 1 based on AMNH 60. *D. hawkinsi* was coded as 0 based on AMNH 7424.
93. Parasphenoid, pair of acuminate and rostrally oriented projections, status: absent (0); present (1). *A. defossor* was coded as 1 based on AMNH 60. *D. hawkinsi* was coded as 1 based on AMNH 7424.
94. Parasphenoid rostrum, eustacian tubes fossa, status and form: absent or indiscernible because cranial portion of sphenoid ankylosed to parasphenoid rostrum (0); deep (1); shallow (2). *A. defossor* was coded as 1 based on AMNH 60. *D. hawkinsi* was coded as 1 based on AMNH 7424.

SKULL: QUADRATE

95. Quadrate, fossa articularis quadratica, cotylae fossae articularis, extreme rostrocaudal compaction (especially cotyla lateralis and processus medialis), status: absent (0); present (1). *A. defossor* was coded as 0 based on AMNH 60. *D. hawkinsi* was coded as 0 based on AMNH 7424. Livezey and Zusi (2006), character 695.
96. Quadrate, lateral aspect of body and base of processus orbitalis, form: convex (1); concave (2). *A. defossor* was coded as 1 based on AMNH 60.
97. Quadrate, processus oticus, capitulum (condylus) squamosum and capitulum (condylus) oticus, marked separation at least as great as that between condyli medialis and lateralis of processus mandibularis quadrati, status: absent (0); present (1). *A. defossor* was coded as 0 based on AMNH 60. Livezey and Zusi (2006), character 551.
98. Quadrate, processus oticus, cotylae, number and form: two cotylae apparent, adjacent or juxtaposed, distance between centers of cotylae less than one fourth of the maximal distance between the outer margins of the cotylae (1); two cotylae apparent, moderately separated, distance between centers of cotylae between one fourth and one half of maximal distance between the outer margins of the cotylae (2). *A. defossor* was coded as 2 based on AMNH 60. Livezey and Zusi (2006), character 150.
99. Quadrate, processus oticus, foramen pneumaticum (medial face), status: present (1); lost (2). *A. defossor* was coded as 2 based on AMNH 60. Livezey and Zusi (2006), character 508.
100. Quadrate, processus oticus, foramen pneumaticum (caudal face), status: present (1); lost (2). Mayr and Clarke (2003), character 36; Livezey and Zusi (2006), character 554.
101. Quadrate, processus oticus, pronounced lateromedial compression, resulting in narrowing of incisura intercapitularis and reduction in size and comparative juxtaposition of capitulum (condylus) oticum and capitulum (condylus) squamosum, status: absent (0); present, facies articularis a single tuberculum (1). *A. defossor* was coded as 0 based on AMNH 60. Livezey and Zusi (2006), character 542.
102. Quadrate, processus orbitalis, status and form relative to processus oticus: present, of comparable length to the processus oticus (1); lost (2). *A. defossor* was coded as 1 based on AMNH 60. Livezey and Zusi (2006), character 532.
103. Quadrate, processus orbitalis, marked elongation of process, status and form: present, process markedly robust (1); lost (2); present, process markedly slender, subacuminate (3). *A. defossor* was coded as 2 based on AMNH 60. Livezey and Zusi (2006), character 534.

104. Quadrate, processus orbitalis, elongation (exceeding processus oticus in length) and rostral expansion into spatulate terminus (latter at least as broad as any other part of the processus orbitalis) in which rostral margin is rounded, status and form: absent (0); present, terminus spatulate with rostral margin rounded (1); present, terminus subrectangular with rostral margin flattened (2). Non-comparable for Caprimulgiformes. *A. defossor* was coded as 0 based on AMNH 60. Livezey and Zusi (2006), character 535.
105. Quadrate, processus orbitalis, terminal process, apical margin markedly slender, subspinous, status: absent (0); present (1). Noncomparable for Caprimulgiformes. *A. defossor* was coded as 0 based on AMNH 60. Livezey and Zusi (2006), character 538.
106. Quadrate, condylus pterygoideus, form: flattened laterally, relatively large, wide, craniocaudally and lateromedially elongate (1); small, ball shaped, extremely small compared to other condyles (2). *A. defossor* was coded as 1 based on AMNH 60. Livezey and Zusi (2006), character 522.
107. Quadrate, condylus medialis, form: aligned craniocaudally (1); aligned mediolaterally (2). *A. defossor* was coded as 1 based on AMNH 60.
108. Quadrate, condylus medialis, form: convex and bulbous, undivided (1); bilobate, two lobes approximately equal in size (2); bilobate, lateral lobe distinctly smaller than medial lobe (3). Livezey and Zusi (2006), character 518.
109. Quadrate, processus mandibularis, facies articularis pterygoidea (ventral face in those taxa having two), form: facies articularis, with slight anteromedial eminentia on basis (1); condylar, tubercular, or jugosublinear (2). *A. defossor* was coded as 2 based on AMNH 60. *D. hawkinsi* was coded as 2 based on AMNH 7424. Livezey and Zusi (2006), character 523.
110. Quadrate, processus mandibularis, condylus medialis, conformation as elongate, lateromedially compressed discus, distinctly larger than condylus lateralis and with distinctly oblique orientation in which rostral terminus is medial to the caudal terminus, paralleling the pterygoid, status: absent (0); present (1). *A. defossor* was coded as 0 based on AMNH 60. Livezey and Zusi (2006), character 516.
111. Quadrate, processus mandibularis of condylus lateralis cotyla quadratojugalis, caudolateral site relative to processus mandibularis: lateral (1); caudal (2). *A. defossor* was coded as 1 based on AMNH 60. Livezey and Zusi (2006), character 513.
112. Quadrate, condylus mandibularis lateralis, terminal: facing cranially (1); facing caudally (2). *A. defossor* was coded as 2 based on AMNH 60.
113. Quadrate, processus mandibularis, condylus caudalis (typically associated with an opposing fossa articularis quadratica, sulcus intercotylaris of mandibula), status: present, distinct (1); obsolete or lost (2). *A. defossor* was coded as 1 based on AMNH 60. Livezey and Zusi (2006), character 510.
114. Quadrate, processus mandibularis, facies articularis quadratojugalis, form: fovea and cotyla, comparatively shallow and with variably deep rostral incisura and processus subcotylaris to accommodate os quadratojugale (1); incisura—concave, troughlike, raised margin lacking entirely or at least in two, geometrically opposing points (2); fovea and cotyla—concave, orbiculate, with a variably raised rim (3). *A. defossor* was coded as 3 based on AMNH 60. Livezey and Zusi (2006), character 511.

SKULL: MANDIBLE

115. Mandible, symphysis, foramina neurovascularia, caudodorsal site: on dorsal face of symphysis (1); on caudal margin of symphysis (2). *A. defossor* was coded as 2 based on AMNH 61. *D. hawkinsi* was coded as 1 based on AMNH 7425. Livezey and Zusi (2006), character 654.
116. Mandible, symphysis, length as a proportion of the total length of the mandible, with the symphysis included in the total length: short, less than one fifth (1); medium, between one fifth and one

- third (2); long, between one third and one half (3). *A. defossor* was coded as 2 based on AMNH 61. *D. hawkinsi* was coded as 3 based on AMNH 7425. Livezey and Zusi (2006), character 676.
117. Mandible, ramus, general form: medially compressed (1); laterally splayed (2). *A. defossor* was coded as 1 based on AMNH 61. *D. hawkinsi* was coded as 1 based on AMNH 7425. Livezey and Zusi (2006), character 280.
118. Mandible, ramus, symphysis, extreme dorsoventral attenuation, status: absent (0); present (1). *A. defossor* was coded as 0 based on AMNH 61. *D. hawkinsi* was coded as 0 based on AMNH 7425. Livezey and Zusi (2006), character 678.
119. Mandible, lateral perspective, ramus, pars intermedia and segment of pars audalis rostral to fossa articularis quadratica, ventral margin, curvature in lateral perspective, status and form: present, variably but distinctly decurved (1); obsolete, i.e., virtually straight (2). *A. defossor* was coded as 1 based on AMNH 61. *D. hawkinsi* was coded as 1 based on AMNH 7425. Livezey and Zusi (2006), character 673.
120. Mandible, ramus, ventral mandibular angle, status: absent or indistinct (0); distinct (1). *A. defossor* was coded as 0 based on AMNH 61. *D. hawkinsi* was coded as 1 based on AMNH 7425. Livezey and Zusi (2006), character 681.
121. Mandible, ramus, fenestra rostralis mandibulae, status: essentially absent (0); substantial and transverse, completely or largely perforate (1). *A. defossor* was coded as 1 based on AMNH 61. *D. hawkinsi* was coded as 1 based on AMNH 7425. Livezey and Zusi (2006), character 684.
122. Mandible, angular, processus retroarticularis, dorsal recurvature, produced by caudal elongation and dorsal drawing of the dorsocaudal vertex of the ramus, status and form: absent, region typically undistinguished or at most tubercular (0); present, a small but distinct hamulus (1); present, typically very large, lateromedially compressed, with ventral margin monotonically curved, and length at least as great as that of rostrocaudal dimension of fossa articularis quadratica mandibulae (2); present, moderately large, lateromedially compressed, with ventral margin angular, and length less than that of rostrocaudal dimension of fossa articularis quadratica mandibulae (3). *A. defossor* was coded as 0 based on AMNH 61. *D. hawkinsi* was coded as 0 based on AMNH 7425. Livezey and Zusi (2006), character 620.
123. Mandible, cranial surface, dentary, caudal development, form: strongly forked (1); weakly forked posteriorly into dorsal and ventral rami (2). *A. defossor* was coded as 2 based on AMNH 61. *D. hawkinsi* was coded as 2 based on AMNH 7425. Cracraft and Clarke (2001), character 4.
124. Mandible, caudal aspect, fossa articularis quadratica, cotyla lateralis, form: oriented laterocaudally, thin and craniocaudally elongate, raised dorsally above lateral crista, convex (1); broad, cranial portion typically acuminate (2); large, broad, confluent with cotyla medialis to form larger, semicircular cotyla, convex (3); craniocaudally oriented, elongate and sometimes bilobate, typically convex caudally and concave cranially, variable prominence (4); small and almost circular, concave (5). *A. defossor* was coded as 3 based on AMNH 61. *D. hawkinsi* was coded as 2 based on AMNH 7425.
125. Mandible, caudal aspect, dorsal perspective, fossa articularis quadratica, foramen pneumaticum, status and site: absent (0); ovoid or circular, located caudomedially on processus medialis (1). *A. defossor* was coded as 1 based on AMNH 61. *D. hawkinsi* was coded as 2 based on AMNH 7425.
126. Mandible, fossa articularis quadratica, sulcus intercotylaris, foramina pneumatica, status: absent (0); present (1). *A. defossor* was coded as 0 based on AMNH 61. *D. hawkinsi* was coded as 0 based on AMNH 7425. Livezey and Zusi (2006), character 696.
127. Mandible, caudal portion, fossa articularis quadratica, cotylae fossae articularis, tuberculum intercotylare, form: variably tuberculate with intervening depressions (1); single, centrally positioned,

- rostromedially oriented jugum (2). *A. defossor* was coded as 1 based on AMNH 61. *D. hawkinsi* was coded as 1 based on AMNH 7425. Livezey and Zusi (2006), character 696.
128. Mandible, caudal portion, processus medialis, form: relatively shorter, more robust, and triangular (1); long and thin fingerlike projection, often equal in length to processus retroarticularis (2). *A. defossor* was coded as 1 based on AMNH 61. *D. hawkinsi* was coded as 1 based on AMNH 7425. Mayr and Clarke (2003), character 45.
129. Mandible, caudal aspect, processus retroarticularis, dorsally oriented accessory projection, status and form: absent or indistinguishable from processus retroarticularis (0); present (1); present but very elongate (2). *A. defossor* was coded as 0 based on AMNH 61. *D. hawkinsi* was coded as 1 based on AMNH 7425. Mayr and Clarke (2003), character 44.
130. Mandible, zona flexoria intramandibularis rostralis, effected by variably distinct, localized thinning and flattening of rami mandibulae immediately proximal to symphysis, status: absent, flexibility variable but generalized throughout ramus (0); present, localized (1). *A. defossor* was coded as 0 based on AMNH 61. *D. hawkinsi* was coded as 0 based on AMNH 7425. Livezey and Zusi (2006), character 711.
131. Mandible, surface of articulation with quadrate, caudal portion, foramen pneumaticum, status: absent (0); present, large and ovoid, located on caudal portion of articular surface (1). *A. defossor* was coded as 1 based on AMNH 61. *D. hawkinsi* was coded as 1 based on AMNH 7425.

VERTEBRAE: CERVICAL VERTEBRAE

132. Atlas, corpus atlantis, processus ventralis corporis, modalis, form: variably prominent, represented as shallow shelf, bifurcate or tripartate flange, or single medial processus (1); represented by prominent, caudally extensive (craniocaudal depth significantly exceeding that of arcus atlantis), dorsoventrally compressed, bilaterally convex, typically carinate lamina (2). *A. defossor* was coded as 2 based on AMNH 7300. Mayr and Clarke (2003), character 46; Livezey and Zusi (2006), character 772.
133. Axis, corpus, processus ventralis corporis, status and form: essentially absent (0); present, represented by variably thick, rounded or subangular crista (1); present, represented by a ventrally elongated, caudally deflected, rounded spina (2); present, represented by a ventrally elongated, bilaterally compressed, craniocaudally restricted lamina (3). *A. defossor* was coded as 3 based on AMNH 7300. Livezey and Zusi (2006), character 783.
134. Axis, arcus, processus costalis axis, status: present, typically vestigial, i.e., represented only by head (1); lost (2). *A. defossor* was coded as 2 based on AMNH 7300. Mayr and Clarke (2003), character 50; Livezey and Zusi (2006), character 787.
135. Axis, arcus, ansa costotransversaria, foramen transversarium, status: absent (0); present (1). *A. defossor* was coded as 1 based on AMNH 7300. Livezey (1998), character 104; Mayr and Clarke (2003), character 49.
136. Axis, arcus, lamina lateralis arcus, foramen pneumaticum, status: absent (0); present (1). *A. defossor* was coded as 1 based on AMNH 7300. Livezey (1998), character 107; Mayr and Clarke (2003), character 48.
137. Marked heterogeneity of form involving relative elongation of intermediate elements, status: present (1); lost (2). Livezey (1998), character 111.
138. Section I, arcus vertebrae, dorsal lamina, arcus interzygopophysialis lateralis, status: absent on all elements (0); present (1). *A. defossor* was coded as 1 based on AMNH 7300. Livezey (1998), character 806.

139. Section II, corpus vertebrae, lateral aspect, processus costalis, status: present throughout section II (1); present in cranial elements but absent in caudal elements of section II (2); absent throughout section II (3). *A. defossor* was coded as 2 based on AMNH 7300. Livezey (1998), character 820.
140. Section II, corpus and arcus vertebrae, ansa costotransversaria, processus costalis, lamina corporo-costalis, status: absent or poorly developed (0); moderately or well developed (1). *A. defossor* was coded as 1 based on AMNH 7300. Livezey (1998), character 826.
141. Section II, arcus vertebrae, lamina arcocostalis, foramen transversarium caudalis, delimited medially by corpus and arcus vertebrae, dorsolaterally by the lamina arcocostalis, and ventrally by the solum arcocostalis of variable craniocaudal breadth, status: absent (0); present (1). *A. defossor* was coded as 1 based on AMNH 7300. Livezey and Zusi (2006), character 829.
142. Section II, arcus vertebrae, ansa costotransversaria, processus costalis, lamina supracostalis, status: absent or poorly developed (0); moderately or well developed, and, in those taxa possessing both structures, fused with the vertebral margin of the lamina arcocostalis (1). *A. defossor* was coded as 0 based on AMNH 7300. Livezey and Zusi (2006), character 830.

VERTEBRAE: THORACIC AND CAUDAL VERTEBRAE

143. Corpus vertebrae, lateral aspect, foramen pneumaticum, status and form: absent (0); present, medium to large, positioned rostrally on centrum (1); large and located caudally on centrum (2). *A. defossor* was coded as 1 based on AMNH 7300. Livezey and Zusi (2006), character 850.
144. Corpus vertebrae, lateral faces, bilateral compression, often accompanied by reduced or virtual absence of pneumaticity of elements, status and form: absent, corpus cylindrical (1); present, manifested by concavitas lateralis, oval depressions (2); present, manifested by virtually laminar structure of corpus between cranial and caudal facies articulares (3). *A. defossor* was coded as 1 based on AMNH 7300. Livezey and Zusi (2006), character 858.
145. Arcus vertebrae, lamina dorsalis arcus, recessus dorsocranialis pneumatici, status: absent (0); present (1). *A. defossor* was coded as 0 based on AMNH 7300. Livezey and Zusi (2006), character 866.
146. Arcus vertebrae, lamina dorsalis arcus, fovea interzygopophysialis, foramina pneumatica, status: absent (0); present (1). *A. defossor* was coded as 0 based on AMNH 7300. Livezey and Zusi (2006), character 867.
147. Arcus vertebrae, processus transversus vertebrae, craniocaudal gradual but distinct elongation of processes in seratium among presynsacral elements, status: absent, processes transverses essentially of uniform width throughout presynsacral elements or moderately reversed (0); present, processes transverses distinctly increasing in width throughout presynsacral elements (1). *A. defossor* was coded as 0 based on AMNH 7300. Livezey and Zusi (2006), character 875.
148. Caudalmost elements of thoracic and caudal vertebrae (cranial to synsacral vertebrae), corpus vertebrae, facies articularis caudalis of penultimate element and facies articularis cranialis of ultimate element, type: heterocoelous, surfaces saddle shaped, comprising articulationes sellares (1); amphicoelous, both surfaces variably, often slightly concave, with rounded margins (2); opisthocoelous, cranial element with facies articularis caudalis concave and rounded, caudal element with facies articularis cranialis convex and rounded (3); *A. defossor* was coded as 1 based on AMNH 7300. Mayr and Clarke (2003), character 57; Livezey and Zusi (2006), character 888.
149. Vertebra 15, width as compared to craniocaudal length: processus spinosus lateromedially compressed, width much less than craniocaudal length (1); processus spinosus width equal to craniocaudal length (2). *D. hawkinsi* was coded as 1 based on AMNH 7427. Based on description from Worthy (2011).

150. Vertebra 16, craniocaudal extent of processus spinosus as compared to that of vertebra 15, form: subequal (1); that of 16 is shorter than that of 15 (2). Based on description from Worthy et al. (2011).
151. Notarium, status and magnitude: present, 4 vertebrae (1); lost (2); present, 3 vertebrae (3); present, 5 vertebrae (4). *A. defossor* was coded as 2 based on AMNH 7300. Mayr and Clarke (2003), character 56; Livezey and Zusi (2006), character 892.
152. Notarium, corpus, ventral crest, fenestrae intercrustales, status: typically present, ligamenta intercrustales of adjacent vertebrae notarii (often robustly) ossified (1); typically lost, cristae ventrales demarcated ventrally by incisurae cristae, ligamenta intercrustales of adjacent vertebrae notarii not ossified (2). Not comparable for taxa without a notarium. Livezey and Zusi (2006), character 895.
153. Notarium, arcus notarii, foramina (intervertebralia) interarcuales, status and form: present, small, diameter approximately equal to that of fovea costalis (1); present, obsolete, reduced to minute perforations or evidently absent (2). Not comparable for taxa without a notarium. Livezey and Zusi (2006), character 896.

VERTEBRAE: SYNSACRUM

154. Synsacral vertebrae, number: 14–18 (1); 10–13 (2). *A. defossor* was coded as 1 based on AMNH 7300. *D. hawkinsi* was coded as 1 based on AMNH 7428. Livezey and Zusi (2006), character 897.
155. Preacetabular synsacral vertebrae, processes transverses relative to adjacent foramina (fenestrae) intertransversaria, transverse form, magnitude: former less than or equal to the latter (1); former much greater than latter, reducing diameter of foramina intertransversaria to prominent pori (2). *A. defossor* was coded as 1 based on AMNH 7300. *D. hawkinsi* was coded as 1 based on AMNH 7427. Livezey and Zusi (2006), character 904.
156. Preacetabular synsacral vertebrae, cranialmost incorporated element (i.e., caudalmost thoracic vertebrae), processes transverses, termini laterales, longitudinal junctura via crista lateralis, synostosis with facies ventralis of preacetabular ilium, status: absent (0); present (1). *A. defossor* was coded as 0 based on AMNH 7300. *D. hawkinsi* was coded as 0 based on AMNH 7428. Livezey and Zusi (2006), character 906.
157. Cranial synsacrum, caudalmost vertebrae thoracicae synsacri, dorsal exposure of lateral faces such that single foramen intervertebrale and part of vertebrae synsacrales ventral to processes costales are exposed dorsocranially to acetabulum, status: absent (0); present (1). *A. defossor* was coded as 0 based on AMNH 7300. *D. hawkinsi* was coded as 0 based on AMNH 7427. Livezey and Zusi (2006), character 910.
158. Synsacral vertebrae, cranialmost vertebrae caudales synsacri, lateral faces of vertebrae, penetration and visibility through foramen ilioischadicum (lateral perspective), status: absent (0); present (1). *A. defossor* was coded as 0 based on AMNH 7300. *D. hawkinsi* was coded as 0 based on AMNH 7427. Livezey and Zusi (2006), character 933.

STERNUM

159. Body of sternum, rostrum sterni, spina externa rostri, status and form: absent or obsolete (0); present, small tuberculum and cunneatus (1); present, variably elongate, laminar spina (2). Noncomparable by presence of spina communis or synostosis. Noncomparable by presence of spina communis or synostosis. *A. defossor* was coded as 0 based on AMNH 7300. *D. hawkinsi* was coded as 0 based on Andrews (1896: pl. III). Mayr and Clarke (2003), character 70; Livezey and Zusi (2006), character 1157.

160. Body of sternum, cranial margin, depressiones (sulcus) artiuales coracoidei, dorsal lip, form: reaches dorsally (1); reaches ventrally (2). Not comparable for *A. defossor* due to absence of dorsal lip extension.
161. Body of sternum, cranial margin, depressiones (sulcus) artiuales coracoidei, dorsal lip, cranial margin of dorsal lip region, pair of cranially extending flanges, status: absent (0); present (1). *A. defossor* was coded as 0 based on AMNH 7300.
162. Body of sternum, cranial margin, depressiones (sulcus) artiuales coracoidei, ventral lip, form: reaches ventrally (1); reaches dorsally (2). *A. defossor* was coded as 1 based on AMNH 7300.
163. Body of sternum, cranial margin, site of depressiones (sulcus) artiuales coracoidei: centrally located above ventral lip (1); splayed laterally so that sternum becomes “y-shaped”, ventral lip lost (2). *A. defossor* was coded as 2 based on AMNH 7300. *D. hawkinsi* was coded as 1 based on Andrews (1896: pl. III). Livezey and Zusi (2006), character 1132.
164. Body of sternum, cranial margin, processus craniolateralis, form: long, creating fenestra (1); robust extension but not creating fenestra (2); barely projecting or not at all (3). *A. defossor* was coded as 3 based on AMNH 7300. *D. hawkinsi* was coded as 2 based on Andrews (1896: pl. III). Livezey and Zusi (2006), character 1141.
165. Body of sternum, cranial margin, processus craniolateralis with respect to axis majoris carinae, angle: extending laterally (1); extending rostrally (2). *A. defossor* was coded as 2 based on AMNH 7300. Livezey and Zusi (2006), character 1142.
166. Body of sternum, visceral face, base of processus craniolateralis and/or processus craniolateralis proprius, impressio origii m. sternocoracoidei, status: present (1); lost (2). *A. defossor* was coded as 1 based on AMNH 7300. Livezey and Zusi (2006), character 1149.
167. Body of sternum, visceral face, sulcus medianus sterni immediately caudal to cranial margin, foramen pneumaticum exclusive of pori pneumatici, status and form: absent (0); present, undivided, enclosing pori pneumatici and os spongiosum (1); present, divided medially by osseus lamina or trabecula, enclosing pori pneumatici and os spongiosum (2). *A. defossor* was coded as 0 based on AMNH 7300. Livezey and Zusi (2006), character 1108.
168. Body of sternum, visceral face, site of sulcus medianus sterni and/or foramen pneumaticum: beginning within margin of or immediately caudal to pila coracoidea (1); significantly caudal to pila coracoidea, approximately caudal to basis carinae (2). Livezey and Zusi (2006), character 1109.
169. Body of sternum, visceral face, pori pneumatici, exclusive of those included within foramen pneumaticum, status and site: absent (0); present, cranial margin (1); present, medial sulcus (2); present, cranial margin and medial sulcus (3). *A. defossor* was coded as 3 based on AMNH 7300. Livezey and Zusi (2006), character 1110.
170. Body of sternum, visceral face, sulcus medianus sterni, status: present (1); lost (2). *A. defossor* was coded as 2 based on AMNH 7300. Livezey and Zusi (2006), character 1111.
171. Body of sternum, ventral face, facies muscularis, sulcus ventrolateralis (longitudinal trough on ventral surface of element immediately medial to processus costales), form: absent or so shallow as to be indistinct (1); distinct, typically for length of costal margin (2). *A. defossor* was coded as 2 based on AMNH 7300. Livezey (1998), character 153.
172. Body of sternum, costal margin, craniocaudal length relative to that of entire corpus sterni on axis mediana: less than one fourth (1); between one fourth and three fourths (2); greater than three fourths (3). *A. defossor* was coded as 2 based on AMNH 7300. *D. hawkinsi* was coded as 2 based on Andrews (1896: pl. III). Livezey (1998), character 1114.

173. Body of sternum, costal margin, articular surfaces for sternal ribs, number: 4 (1); 3 (2); 5 (3); 6 (4); 7 (5); 8 (6). *A. defossor* was coded as 1 based on AMNH 7300. *D. hawkinsi* was coded as 4 based on Andrews (1896: pl. III). Mayr and Clarke (2003), character 71.
174. Body of sternum, costal margin, incisurae intercostales, perforatitas and pneumaticas, status: present (1); lost (2). *A. defossor* was coded as 1 based on AMNH 7300. Livezey and Zusi (2006), character 1115.
175. Carina sterni, status and form: distal portion extremely medially compressed so that dorsal portion delineated by lineae intermusculares is extremely small (1); distal portion less medially compressed or not compressed so that dorsal portion delineated by lineae intermusculares is large (2); lost (3). *A. defossor* was coded as 3 based on AMNH 7300. *D. hawkinsi* was coded as 2 based on Andrews (1896: pl. III). Livezey and Zusi (2006), character 1194.
176. Carina sterni, cranial margin, lateral cristae of carina, status: present (1); lost (2). Noncomparable for taxa without a carina. *D. hawkinsi* was coded as 1 based on Andrews (1896: pl. III). Livezey and Zusi (2006), character 1207.
177. Carina sterni, cranial margin, sulcus carinae, status: absent (0); present (1). Not comparable for taxa without a carina. *D. hawkinsi* was coded as 1 based on Andrews (1896: pl. III). Livezey and Zusi (2006), character 1213.
178. Carina sterni, cranial margin of carina, sulcus carinae or homologous site, foramen pneumaticum, status and form: absent (0); present, variable size and shape (1). Not comparable for taxa without a carina. Livezey and Zusi (2006), character 1218.
179. Carina sterni, apex, site relative to spina externae or most proximal point of sternum, form: cranial to spina externae or most proximal point of sternum (1); located somewhat caudally (2); located extremely cranially (3). *D. hawkinsi* was coded as 2 based on Andrews (1896: pl. III). Livezey and Zusi (2006), character 1198.
180. Carina sterni, apex carina, facies articularis clavicularis, status and form: absent (0); present, incisura or concavity (1); carina fused to furcula (2). Noncomparable for taxa without a carina. Livezey and Zusi (2006), character 1200.
181. Carina sterni, cranial margin, site and degree of thickening: dorsally thickened (1); ventrally thickened (2); width of both portions subequal (3). Noncomparable for taxa without a carina.
182. Carina sterni, maximal depth ventral and normal to body of sternum, facies muscularis, relative to minimal width of body of sternum (exclusive of processes laterales, if present) across points on costal margin directly lateral to that of maximal depth of carina, form: height equal to or greater than width of body, not including processus craniolateralis (1); height less than width of body (2). *A. defossor* was coded as 2 based on AMNH 7300. Livezey and Zusi (2006), character 1199.
183. Caudal sternum, fenestra and incisura caudolateralis, status: present as incisura or fenestra (1); lost (2). *A. defossor* was coded as 2 based on AMNH 7300. *D. hawkinsi* was coded as 1 based on Andrews (1896: pl. III). Livezey and Zusi (2006), character 1182.
184. Caudal sternum, incisura and fenestra caudolateralis (if present), cranial extent, form: elongate—length of incisura and fenestra greater than two thirds craniocaudal length of corpus sterni, approaching terminis caudalis of processus costales sterni (1); intermediate—length of incisura and fenestra between one third and two thirds of craniocaudal length of corpus sterni (2); abbreviate—length of incisura and fenestra less than one third craniocaudal length of corpus sterni (3); absent despite discernable pila (4). Noncomparable where incisura (fenestra) and/or trabecula absent. *D. hawkinsi* was coded as 3 based on Andrews (1896: pl. III). Livezey and Zusi (2006), character 1183.

185. Caudal sternum, costal margin, processus caudolateralis (if present), orientation relative to body of sternum as reflected (in part) by angle defined by incisura caudolateralis, vertex cranialis angulae, form: angle undefined, processus is unparallel to costal margin and “vertex” is ellipsoidal (1); between 15° and 45°, parabolic (2); approximately 45° (3); parallel, angle undefined, “vertex” is pointed and triangular (4). Noncomparable by absence of processus or incisura, or indeterminate orientation. *D. hawkinsi* was coded as 1 based on Andrews (1896: pl. III). Livezey and Zusi (2006), character 1184.
186. Caudal sternum, trabecula caudolateralis (if present), caudal terminal margin, form: rounded or (sub)rectangular, often obliquely aligned (1); cruciate, with terminal, transverse pila (2); (sub)acuminate, variably oriented (3). Noncomparable where presence of trabecula uncertain or known to be absent. *D. hawkinsi* was coded as 3 based on Andrews (1896: pl. III). Livezey and Zusi (2006), character 1185.
187. Cranial sternum, ventral lip, lateral margin, craniocaudally limited, rounded flangelike processus protruding dorsocraniolaterally or dorsolaterally, status and form: absent (0); present but truncated, reduced to small, rounded eminentia (1); prominent, elongate and thin (2). Noncomparable for *A. defossor*.
188. Caudal sternum, incisura and fenestra intermediana, relative cranial extent, form: rudimentary, incisura is a minor concavity (1); abbreviated, length of incisura and fenestra less than one third craniocaudal length of corpus sterni (2). Noncomparable for taxa without trabecula intermediana. Livezey and Zusi (2006), character 1188.
189. Caudal sternum, trabecula mediana, margin and caudal terminus, definitive form: not tapered or weakly tapered, transversely broad, linear or rounded (1); distinctly tapered, rounded or subrectangular (2); distinctly tapered, cruciate (3); distinctly tapered, irregularly invaginated or concave (4). *A. defossor* was coded as 1 based on AMNH 7300. *D. hawkinsi* was coded as 3 based on Andrews (1896: pl. III). Livezey and Zusi (2006), character 1191.
190. Caudal sternum, trabeculae caudolateralis, intermediana, and mediana, relative caudal extents as compared to caudal margin: mediana \geq intermedia \geq caudolateralis (1); caudolateralis \geq intermedia \geq mediana (2); intermedia \geq caudolateralis \geq mediana (3); mediana \geq caudolateralis \geq intermedia (4). Noncomparable for taxa missing one or more of these trabeculae. Livezey and Zusi (2006), character 1192.

RIBS

191. Head of sternal rib, medial face, foramen pneumaticum, status: typical (1); lost (2). *A. defossor* was coded as 2 based on AMNH 7300. Livezey (1998), character 132.

CORACOID

192. Omalis of coracoid, processus acrocoracoideus, form: present, typical (1); present but truncated processus essentially limited to width accommodating facies articularis clavicularis (2). *A. defossor* was coded as 2 based on AMNH 7300. Livezey and Zusi (2006), character 1266.
193. Omalis of coracoid, processus acrocoracoideus, principal dorsoventral orientation relative to major craniocaudal axis of coracoid, form: distinctly ventral (1); essentially coplanar (2). *A. defossor* was coded as 2 based on AMNH 7300. Livezey and Zusi (2006), character 1267.
194. Omalis of coracoid, processus acrocoracoideus (tuberculum brachiale), dorsomedial curvature with respect to major axis of coracoid, status and form: present, moderate medioventral inflection or angling (1); present, pronounced ventral angling, distinctly hamulate (2); lost, angling or curvature

- obsolete, processus aligned cranially (3). Not comparable for *Cariama*. *A. defossor* was coded as 3 based on AMNH 7300. Mayr and Clarke (2003), character 64; Livezey and Zusi (2006), character 1268.
195. Omalis of coracoid, processus acrocoracoideus, impressio ligamenti acrocoracohumeralis, status and form: present, well developed (1); present, rudimentary or vestigial, represented by variously vague indications of limita (2); lost (3). *A. defossor* was coded as 1 based on AMNH 7300. Livezey and Zusi (2006), character 1276.
196. Omalis of coracoid, dorsal aspect, glenoid process, facies (sulcus) articularis humeralis and labrum glenoidale, primary dorsoventral and lateromedial position relative to processus acrocoracoideus, form: laterodorsal (1); dorsolateral (2). *A. defossor* was coded as 2 based on AMNH 7300. Livezey and Zusi (2006), character 1280.
197. Omalis of coracoid, dorsal aspect, processus procoracoideus, status and comparative prominence: present but rudimentary, an angle, shallow cotyla, or cristula (1); present, moderately prominent, a typically curved tuberculum, terminus proprius (exclusive of ancillary tuberculae) approximating medial body margin (2); an elongate processus verae, terminus proprius distinctly extending medially and/or dorsal to corpus, some manifesting former condition curving mediodorsally around medial body margin (3); markedly curved, creating a circular connection with processus acrocoracoideus (4); curving crista lost, juts out at a 90° angle to axis of coracoid, extremely elongate (5). *A. defossor* was coded as 5 based on AMNH 7300. Livezey and Zusi (2006), character 1283.
198. Shaft of coracoid, foramen nervi supracoracoidei, status and form: absent (0); present, circular (1); present, craniocaudally elongate (2). *A. defossor* was coded as 2 based on AMNH 7300. Mayr and Clarke (2003), character 65; Livezey and Zusi (2006), character 1286.
199. Shaft of coracoid, general form sensu length relative to width of facies articularis sternalis: moderately elongate, length between three and four times the width (1); typically proportioned, length between two and three times the width (2); truncate (less than two times the width) (3). *A. defossor* was coded as 1 based on AMNH 7300. Livezey and Zusi (2006), character 1292.
200. Sternal coracoid, impressio musculi sternocoracoidei on dorsal surface of extremitas sternalis, depth and general form: smooth, shallow or difficult to discern (1); ridged and typically deep (2). *A. defossor* was coded as 2 based on AMNH 7300. Mayr and Clarke (2003), character 67. Livezey and Zusi (2006), character 1294.
201. Sternal coracoid, dorsal surface, impressio musculi sternocoracoidei, foramen pneumaticum, size. Small or not visible (1); large, ovoid (2); extremely large so that almost entire impression is pneumatic (3). *A. defossor* was coded as 1 based on AMNH 7300.
202. Sternal coracoid, medial margin, form: crista only partially existent or lacking crista medialis (1); with medial, variably prominent crista medialis, continued cranially by crista procoracoidei (2). *A. defossor* was coded as 1 based on AMNH 7300. Livezey (1998), character 194.
203. Sternal coracoid, processus lateralis, form relative to facies articularies sternalis, form: protrudes laterocaudally, not in line with facies articularis sternalis (1); raised cranially (2); projects laterally, in line with facies articularis sternalis (3). *A. defossor* was coded as 3 based on AMNH 7300. Livezey and Zusi (2006), character 1303.
204. Sternal coracoid, facies articularis sternalis, large and distinct foramen, status: absent (0); present (1). *A. defossor* was coded as 1 based on AMNH 7300. Livezey and Zusi (2006), character 1074.
205. Sternal coracoid, facies articularis sternalis, labrum externa, cranial extent of cranial margin (and correlated cranial expanse) relative to those of labrum interna, form: former approximately equal to latter, producing facies articularis of dorsoventrally equal expanse (1); former distinctly caudal

to latter, producing internally (dorsally) angled facies articularis (2); former significantly cranial to the latter, producing externally (ventrally) angled facies articularis (3). *A. defossor* was coded as 2 based on AMNH 7300. Livezey and Zusi (2006), character 1314.

SCAPULA

206. Collum scapulae, medial aspect, acuminate, ventrally oriented projection, status and form: absent (0); present (1); vestigial scar present as a raised tubercle that is sometimes acuminate (2). *A. defossor* was coded as 0 based on AMNH 7300. Based on description from Mayr (2006).
207. Scapus scapulae, monotonic ventral curvature general to scapus, form: moderate, body and distal margin of scapula is slightly to moderately convex (1); pronounced, body and distal margin of scapula conspicuously convex (2). *A. defossor* was coded as 1 based on AMNH 7300. Livezey and Zusi (2006), character 1260.
208. Scapus scapulae, lateral aspect, concavitas longitudinalis, status: present, distinctly concave throughout, accented by lateral displacement of dorsal margin of scapus (1); lost, essentially planar throughout or shallow concavitas limited to cranial and medial portions (2). *A. defossor* was coded as 2 based on AMNH 7300. Livezey and Zusi (2006), character 1257.
209. Scapus scapulae, ventrolateral aspect, tubercle of variable size located cranially, often accompanied by pitted crest trailing distally, status: present (1); lost (2). *A. defossor* was coded as 1 based on AMNH 7300.
210. Scapus scapulae, especially distal portion, form: widened dorsocaudally, spatulate (1); long, blade-like, compressed dorsocaudally (2). *A. defossor* was coded as 2 based on AMNH 7300. Livezey and Zusi (2006), character 1264.

HUMERUS

211. Proximal humerus, tuberculum ventrale, general form and caudal prominence: smooth and often rounded, not very prominent (1); extremely prominent and laterally flattened, projecting well beyond rest of bone caudally (2). *A. defossor* was coded as 2 based on AMNH 7300. *D. hawkinsi* was coded as 2 based on AMNH 7426. Livezey and Zusi (2006), character 1364.
212. Proximal humerus, tuberculum ventrale, proximodistal position relative to fossa pneumotricipitalis or homologous site, form: comparatively cranioproximal, completely exposing fossa pneumotricipitalis (1); comparatively caudodistal, largely or completely concealing fossa pneumotricipitalis (2). *A. defossor* was coded as 1 based on AMNH 7300. *D. hawkinsi* was coded as 2 based on AMNH 7426. Livezey and Zusi (2006), character 1366.
213. Proximal humerus, tuberculum ventrale, proximal elevation regardless of fossa pneumotricipitalis exposure: inferior to tuberculum dorsale, projects cranially (1); subequal in elevation to that of tuberculum dorsale, projects cranially (2); elevated immediately proximally to tuberculum dorsale, projects cranially or cranioproximally (3); elevated well proximal to tuberculum dorsale, proximal to head of humerus and projects proximally (4). Noncomparable for Spheniscidae. *A. defossor* was coded as 4 based on AMNH 7300. *D. hawkinsi* was coded as 3 based on AMNH 7426.
214. Proximal humerus, tuberculum dorsale, form: smooth and rounded (1); acuminate (2). *A. defossor* was coded as 1 based on AMNH 7300. *D. hawkinsi* was coded as 2 based on AMNH 7426. Livezey and Zusi (2006), character 1370.
215. Proximal humerus, caudal aspect, incisura capitis, form: extremely deep and prominent (1); shallow (2). *A. defossor* was coded as 2 based on AMNH 7300. *D. hawkinsi* was coded as 1 based on AMNH 7426. Livezey and Zusi (2006), character 1358.

216. Proximal humerus, fossa pneumotricipitalis, foramen pneumaticum, status: present, deep and pneumatic (1); present and apneumatic (2); lost (3). *A. defossor* was coded as 3 based on AMNH 7300. *D. hawkinsi* was coded as 2 based on AMNH 7426. Livezey and Zusi (2006), characters 1414 and 1415.
217. Proximal humerus, caudal aspect, fossa pneumotricipitalis, distinct circularity of densely rimmed atrium situated at approximate normality with respect to major axis of corpus of humerus, status: absent (0); present (1). *A. defossor* was coded as 0 based on AMNH 7300. *D. hawkinsi* was coded as 0 based on AMNH 7426. Livezey and Zusi (2006), character 1422.
218. Proximal humerus, fossa pneumotricipitalis, apparent torsion of element about major proximodistal axis such that entire fossa is ventral to corpus humeri, status: absent, no torsion apparent nor position altered (0); present, torsion apparent and position altered (1). *A. defossor* was coded as 0 based on AMNH 7300. *D. hawkinsi* was coded as 0 based on AMNH 7426. Livezey and Zusi (2006), character 1424.
219. Proximal humerus, fossa pneumotricipitalis, crus dorsale fossae, form: dorsoventrally narrow (1); dorsoventrally broad (2). *A. defossor* was coded as 2 based on AMNH 7300. *D. hawkinsi* was coded as 1 based on AMNH 7426. Livezey (1998), character 202.
220. Proximal humerus, head, form: bulbous, robust, elevated and oriented proximally (1); mediolaterally compressed, somewhat reduced, oriented diagonally, depressed and in line with incisura capitis (2); extremely reduced, ventromedially compressed and located below ventral tubercle (3). Not comparable for Spheniscidae. *A. defossor* was coded as 3 based on AMNH 7300. *D. hawkinsi* was coded as 2 based on AMNH 7426.
221. Proximal humerus, head, triangular and distal-reaching tuberosity ankylosed to tuberculum ventrale, status: absent (0); present (1). *A. defossor* was coded as 0 based on AMNH 7300. *D. hawkinsi* was coded as 0 based on AMNH 7426. Bertelli et al. (2014), character 79.
222. Proximal humerus, cranial aspect, planum intertuberculare, sulcus (canalis) nervi coracobrachialis, status: absent or indistinguishable (0); present, represented by sulcus and/or canalis (1). *A. defossor* was coded as 0 based on AMNH 7300. *D. hawkinsi* was coded as 0 based on AMNH 7426. Livezey and Zusi (2006), character 1428.
223. Proximal humerus, cranial aspect, sulcus ligamentosus transversus, status and form in terms of dorsoventral extent: extremely abbreviated, almost obsolete, at most suggested by shallow, abbreviated depression or dorsally restricted fovea (1); present, shallow, and often abbreviated, typically limited to roughly entire proximal margin of bicipital face and reaching midpoint of the proximal portion of the humerus, cranial surface (2); present, deep and long, extends dorsoventrally across proximal portion of humerus to intersect bases tuberculum dorsale and ventrale humeri (3). *A. defossor* was coded as 3 based on AMNH 7300. *D. hawkinsi* was coded as 1 based on AMNH 7426. Livezey and Zusi (2006), character 1431.
224. Proximal humerus, cranial aspect, sulcus ligamentosus transversus, ventral section, marked triangular raised subplanar region delimited by pronounced cristae marginales and enclosing deep ventral fovea, status: absent (0); present (1). *A. defossor* was coded as 0 based on AMNH 60. *D. hawkinsi* was coded as 0 based on AMNH 7426. Livezey and Zusi (2006), character 1432.
225. Proximal humerus, crista bicipitalis, form: extremely prominent, with rounded margin (1); not very prominent, typically rounded (2); prominent but “squared off” i.e., distal portion located much more proximally (3); extremely reduced, essentially lost (4). *A. defossor* was coded as 4 based on AMNH 7300. *D. hawkinsi* was coded as 3 based on AMNH 7426. Bertelli et al. (2011), character 52.

226. Proximal humerus, crista bicipitalis, form of cranial face sensu planarity or slight concavity, status: absent, facies cranialis variably convex (0); present (1). *A. defossor* was coded as 1 based on AMNH 7300. *D. hawkinsi* was coded as 0 based on AMNH 7426. Livezey and Zusi (2006), character 1405.
227. Proximal humerus, crista bicipitalis, terminus on shaft, ventral margin, form: abruptly discontinued proximally on corpus humeri, ventral margin (1); gradually continued by shallow, low but distinct jugum along corpus humeri, ventral margin (2). *A. defossor* was coded as 1 based on AMNH 7300. *D. hawkinsi* was coded as 1 based on AMNH 7426. Livezey and Zusi (2006), character 1413.
228. Proximal humerus, head, separation from crista deltopectoralis and tuberculum dorsale, status: pronounced, offset and well distinguished from tuberculum dorsale (1); diminished, low and poorly distinguished adjacent features (2). *A. defossor* was coded as 2 based on AMNH 7300. *D. hawkinsi* was coded as 1 based on AMNH 7426. Livezey and Zusi (2006), character 1354.
229. Proximal humerus, crista deltopectoralis, lateral extension and general form: variable prominence, rounded, oriented cranially (1); extremely prominent, rounded, flares ventrally (2); atypical such that proximal portion of crest is markedly reduced and distal portion of crest appears as a triangular, cranially oriented process (3); variable prominence, trapezoidal, oriented cranially (4). *A. defossor* was coded as 3 based on AMNH 7300. *D. hawkinsi* was coded as 1 based on AMNH 7426. Livezey and Zusi (2006), character 1374.
230. Proximal humerus, crista deltopectoralis, comparative proximodistal length relative to that of corpus of humerus, magnitude: great, well developed, and extending at least one third length of corpus humeri (1); small, diminutive, triangular emittentia, extending less than one third length of corpus humeri (2). *A. defossor* was coded as 2 based on AMNH 7300. *D. hawkinsi* was coded as 2 based on AMNH 7426. Livezey and Zusi (2006), character 1382.
231. Proximal humerus, crista deltopectoralis, oblique caudal aspect, proximodistal extent relative to that of crista bicipitalis, magnitude: terminus of crista deltopectoralis distal to that of crista bicipitalis (1); termini approximately subequal (2). *A. defossor* was coded as 1 based on AMNH 7300. *D. hawkinsi* was coded as 1 based on AMNH 7426. Livezey and Zusi (2006), character 1383.
232. Shaft of humerus, proximal section of shaft with triangular cross section, status: absent (0); present (1). *A. defossor* was coded as 1 based on AMNH 7300. *D. hawkinsi* was coded as 0 based on AMNH 7426. Bertelli et al. (2011), character 56.
233. Shaft of humerus, bilateral compression or departure from essentially elliptical form (planum transversus), status: absent, elliptical, lacking notable flattening or bifacial compression throughout (0); present, strongly craniocaudally compressed, virtually laminate throughout (1). *A. defossor* was coded as 0 based on AMNH 7300. *D. hawkinsi* was coded as 0 based on AMNH 7426. Livezey and Zusi (2006), character 1439.
234. Shaft of humerus, virtual linearity independent of relative elongation, status and form: absent, curved (0); present, linear (1). *A. defossor* was coded as 0 based on AMNH 7300. *D. hawkinsi* was coded as 0 based on AMNH 7426. Livezey and Zusi (2006), character 1347.
235. Distal humerus, pronounced and generalized craniocaudal compression, producing sublaminar form, status: absent (0); present (1). *A. defossor* was coded as 0 based on AMNH 7300. *D. hawkinsi* was coded as 0 based on AMNH 7426. Livezey and Zusi (2006), character 1443.
236. Distal humerus, caudal aspect, fossa olecrani, form: limited depth and proximodistal width (1); present, markedly deep, proximodistally broad, and typically sharply delimited (2); present, markedly deep cavity (3). *D. hawkinsi* was coded as 1 based on AMNH 7426. Livezey and Zusi (2006), character 1482.

237. Distal humerus, caudal aspect, sulcus tendinis m. scapulotricipitalis, status and form. Absent (0); present, weakly defined, typically broad, shallow and truncate (1); present, conspicuously defined, usually narrow, deep and elongate (2). Not comparable for Spheniscidae. *D. hawkinsi* was coded as 1 based on AMNH 7426. Mayr and Clark (2003), character 81; Livezey and Zusi (2006), character 1488.
238. Distal humerus, caudal aspect, epicondylus ventralis (entepicondylus), proximodistal site relative to those of epicondylus dorsalis (ectepicondylus) and condylus ventralis, form: former proximal to latter (1); former approximately equal or distal to latter (2). *A. defossor* was coded as 2 based on AMNH 7300. *D. hawkinsi* was coded as 2 based on AMNH 7426. Livezey and Zusi (2006), character 1475.
239. Distal humerus, cranial aspect, fossa m. brachialis, dorsoventral position relative to axis medianus of humerus: ventral (1); medial (2). *A. defossor* was coded as 2 based on AMNH 7300. *D. hawkinsi* was coded as 1 based on AMNH 7426. Livezey and Zusi (2006), character 1460.
240. Distal humerus, cranial aspect, impression of brachialis anticus (brachial depression), form: shallow and small, ovoid, or brachial depression nonexistent (1); deep and part of brachial depression, distal portion of humerus tends to be especially depressed (2). *A. defossor* was coded as 1 based on AMNH 7300. *D. hawkinsi* was coded as 1 based on AMNH 7426. Mayr and Clarke (2003), character 80. Livezey and Zusi (2006), character 1456.
241. Distal humerus, cranial aspect, tuberculum (processus) supracondylaris dorsalis (distinct epicondylus dorsalis), status and form: present, moderately large tuberculum (1); extremely small, almost absent (2); lost (3); present, prominent, subtriangular process oriented dorsoproximally (4). *D. hawkinsi* was coded as 1 based on AMNH 7426. Livezey and Zusi (2006), character 1467.
242. Distal humerus, cranial aspect, epicondylus dorsalis (ectepicondylus), status and form sensu dorsal prominence, status and form: absent or virtually coplanar with dorsal face of humerus, vertically intersecting terminal curves of condyles at dorsodistal vertex of element (0); present, of varying prominence (1). *A. defossor* was coded as 0 based on AMNH 7300. *D. hawkinsi* was coded as 0 based on AMNH 7426. Livezey and Zusi (2006), character 1461.
243. Distal humerus, cranial aspect, condyli dorsalis and ventralis humeri, general form: craniocaudally compressed (1); thick, rounded (2). *A. defossor* was coded as 1 based on AMNH 7300. *D. hawkinsi* was coded as 1 based on AMNH 7426. Livezey and Zusi (2006), character 1451.
244. Distal humerus, cranial aspect, condylus dorsalis humeri, proximal extent relative to distal margin of fossa m. brachialis, form: condylus distal to distal terminus of fossa and typically separated from distal margin fossa m. brachialis by smooth area of bone from latter (1); condylus (proximal margin) typically extending at least proximal to distal margin of fossa m. brachialis (2); condylus markedly proximal to fossa, including extreme proximal condylorum dorsalis and ventralis (3). Not comparable for Spheniscidae or *A. defossor*. *D. hawkinsi* was coded as 2 based on AMNH 7426. Livezey and Zusi (2006), character 1447.

ULNA

245. Proximal ulna, processus cotylaris dorsalis, pronounced ventral orientation such that apex process is approximately coplanar with facies dorsalis corporis, status: absent, apex of process variably elevated dorsally compared to corpus of ulna (0); present (1). Not comparable for Spheniscidae. Livezey and Zusi (2006), character 1492.
246. Proximal ulna, processus cotylaris dorsalis, cotyla dorsalis, facies articularis relative to cotyla ventralis, form: less expansive (1); subequal (2). Not comparable for Spheniscidae or *A. defossor*. Livezey and Zusi (2006), character 1496.

247. Proximal ulna, processus cotylaris dorsalis, crista intercotylaris, form: crista rudimentary but evident despite more typically conformed cotylae (1); variably prominent, cotylae dorsalis and ventralis distinct (2). Livezey and Zusi (2006), character 1497.
248. Proximal ulna, interosseus margin (cranial margin), impressio insertii m. brachialis, form: impressio planum and facies ancorae, proximocaudal margin only slightly elevated (1); modestly concave, deep with proximocaudal margin or brachial crest elevated only proximally, and typically not undercutting cotylae proximales (2). Livezey and Zusi (2006), character 1502.
249. Proximal ulna, dorsal aspect, incisura radialis, status and form: absent or indistinct, sulcus narrow, cotyla closely juxtaposed, and process rounded to triangular with distinct apex (0); present and variably pronounced (1). Livezey and Zusi (2006), character 1505.
250. Distal ulna, tuberculum carpale, jugum tuberculae cranialis, status: present, distinctly curving, proximal margin is concave, jugum extending across dorsal face from caudal tuberculum carpale to caudal margin of ulna (1); lost or incompletely developed or indistinct (2). Not comparable for Spheniscidae. Livezey and Zusi (2006), character 1534.

CARPOMETACARPUS

251. Proximal carpometacarpi, trochlea carpalis, sulcus trochlearis, form: shallow, rounded in cranial or caudal view, or is somewhat deep laterally but not cranially (1); deep, subangular in cranial or caudal view (2). Not comparable for *A. defossor*. Livezey (1998), character 236.
252. Proximal carpometacarpi, dorsal aspect, trochlea carpalis, dorsal labrum, proximal terminus of dorsal rim of trochlea, form: weakly angular (1); rounded (2); strongly angular, almost pointed, elongated proximally (3). Not comparable for *A. defossor*. Livezey (1998), character 238.
253. Proximal carpometacarpi, ventral aspect, os metacarpale minus, small tuberculum on os metacarpale minus immediately distal to synostosis metacarpalis proximalis, status and form: elongate (1); distinct and rounded (2); obsolete (3). Not comparable for *A. defossor*. Livezey (1998), character 244.
254. Distal carpometacarpi, dorsal aspect, synostosis metacarpalis distalis, sulcus interosseus ventralis, status and form: present, shallow (1); lost (2); present, deep (3). Not comparable for *A. defossor*. Livezey (1998), character 253.

PELVIS

255. Preacetabular and postacetabular ilium, dorsal face, relative craniocaudal lengths, indexed by ratio of length of former divided by length of latter, form: preacetabular ilium greater in craniocaudal length than postacetabular ilium, ratio significantly greater than unity (1); subequal (2); postacetabular ilium greater in craniocaudal length than preacetabular ilium, ratio less than unity (3). *A. defossor* was coded as 1 based on AMNH 7300. *D. hawkinsi* was coded as 1 based on AMNH 7427. Livezey and Zusi (2006), character 1890.
256. Preacetabular ilium, dorsal aspect, dorsomedial margin, dorsal iliac crest, dorsomedial synostosis forming carina iliaca dorsalis, status and form: present, carina is rudimentary or vestigial, cristae are dorsally prominent and approach medially, but are clearly separated from crista spinosa synsacri by variably narrow but distinct sulci iliosynsacrales (1); lost, cristae limited to ventral lamina not approaching medially, typically exposing fenestrae intertransversae (2); present, carina is distinct and synostotic (3). *A. defossor* was coded as 3 based on AMNH 7300. *D. hawkinsi* was coded as 3 based on AMNH 7427. Livezey and Zusi (2006), character 1814.

257. Preacetabular ilium and synsacrum, dorsal aspect, dorsal iliac crest, height: shallow or flat, arc of crest (or highest portion of separated crests) does not exceed height of postacetabular dorsal portion of the synsacrum (1); extremely prominent, arc of crest (or highest portion of separated crests) exceeds height of postacetabular dorsal portion of the synsacrum (2). *A. defossor* was coded as 2 based on AMNH 7300. *D. hawkinsi* was coded as 2 based on AMNH 7427. Livezey and Zusi (2006), character 1819.
258. Preacetabular ilium, lateral aspect, angle respective to transverse plane of synsacrum: oblique (1); subvertical (2); subhorizontal (3). *A. defossor* was coded as 2 based on AMNH 7300. *D. hawkinsi* was coded as 1 based on AMNH 7427. Livezey and Zusi (2006), character 1823.
259. Acetabular and preacetabular ilium, lateral aspect, preacetabular tubercles, status and form: jut out craniolaterally, distinctly lengthened (1); relatively small, close to corpus of pelvis, but blunted cranio-lateral projections still evident (2); lost or barely discernable (3). *A. defossor* was coded as 3 based on AMNH 7300. *D. hawkinsi* was coded as 3 based on AMNH 7427. Livezey and Zusi (2006), character 1810.
260. Acetabular ilium, dorsal aspect, interacetabular width relative to synsacral length, magnitude: great, exceeding one half postacetabular synsacral length (1); moderate, one half to one third synsacral length (2); small, approximately one fourth synsacral length (3); extremely small, approximately one sixth synsacral length (4). *A. defossor* was coded as 2 based on AMNH 7300. *D. hawkinsi* was coded as 2 based on AMNH 7427. Livezey and Zusi (2006), character 1845.
261. Acetabular ilium, dorsal aspect, dorsomedial margin of ilium, orbiculate fenestrae paired with adjacent, medial fenestrae intertransversae synsacrales, status: present (1); lost (2). *A. defossor* was coded as 2 based on AMNH 7300. *D. hawkinsi* was coded as 1 based on AMNH 7427. Livezey and Zusi (2006), character 1851.
262. Acetabulum, located immediately lateral or lateroventral to synsacrum due to extreme bilateral compression of pelvis, status: absent (0); present (1). *A. defossor* was coded as 0 based on AMNH 7300. *D. hawkinsi* was coded as 0 based on AMNH 7427. Livezey and Zusi (2006), character 1766.
263. Acetabular ilium, lateral aspect, antitrochanter, form: raised dorsally, so that it is more visible and robust (1); depressed ventrally, so that it is less visible and somewhat obscures the acetabulum (2). *A. defossor* was coded as 1 based on AMNH 7300. *D. hawkinsi* was coded as 1 based on AMNH 7427.
264. Acetabular ilium, lateral aspect, cranially oriented prominence on the cranial margin of the antitrochanter, status: absent (0); present (1). *A. defossor* was coded as 1 based on AMNH 7300. *D. hawkinsi* was coded as 1 based on AMNH 7427.
265. Acetabular ilium and ischium, lateral aspect, ilioischadic foramen, status and form: absent (0); oblong (1); essentially circular (2). *A. defossor* was coded as 2 based on AMNH 7300. *D. hawkinsi* was coded as 1 based on AMNH 7427. Livezey and Zusi (2006), character 1791.
266. Acetabular ilium and concavitas infracristalis caudal to acetabulum, lateral aspect, foramen ilioischadicum, craniocaudal extent within concavitas infracristalis (including foramen itself): limited to cranial one half but exceeding one third (1); encompasses at least one half of concavitas caudal to acetabulum (2); limited to cranial one third or less (3). Noncomparable for Tinamiformes. *A. defossor* was coded as 3 based on AMNH 7300. *D. hawkinsi* was coded as 1 based on AMNH 7427. Livezey and Zusi (2006), character 1790.
267. Pelvis. Postacetabular ilium, lateral face, lamina infracristalis ilii, margin of ilioischadic foramen (exclusive of vestigia of membrana ossificans ilioischadica, if present), status and form: absent, lamina infracristalis lacking (0); present, delimiting a deep (minor axis at least one half major axis)

- elliptical to circular margin (1); present, delimiting a subangular, ventrocaudally attenuated margin (2). *A. defossor* was coded as 2 based on AMNH 7300. *D. hawkinsi* was coded as 1 based on AMNH 7427. Livezey and Zusi (2006), character 1881.
268. Pelvis. Acetabular ilium, lateral face, obturator foramen, status and form: lost due to lack of caudal margin (1); rounded (2); lateromedially elongate, ovoid (3). *A. defossor* was coded as 1 based on AMNH 7300. *D. hawkinsi* was coded as 1 based on AMNH 7427. Livezey and Zusi (2006), character 1783.
269. Pelvis. Acetabular ilium, lateral face, caudal margin of obturator foramen, form: oriented dorsally (1); oriented ventrally (2). Not comparable for taxa without a fully formed obturator foramen.
270. Pelvis. Postacetabular ilium, dorsal face, extreme bilateral compression of elements resulting in the caudal portion of the pelvis being lateromedially narrower than the preacetabular ilium, status: absent (0); present (1). *A. defossor* was coded as 0 based on AMNH 7300. *D. hawkinsi* was coded as 0 based on AMNH 7427. Livezey and Zusi (2006), character 1860.
271. Pelvis. Postacetabular ilium and synsacrum, dorsal face, vestigial iliosynsacral suture, status: absent (0); present (1). *A. defossor* was coded as 1 based on AMNH 7300. *D. hawkinsi* was coded as 0 based on AMNH 7427. Livezey and Zusi (2006), character 1760.
272. Pelvis. Postacetabular ilium, lateral face, crista dorsolateralis ilii, caudolateral angle (where present), form: marked by a comparatively small, rounded, laterally directed prominence (1); marked by a comparatively prominent, ventrally curved flange, undercut by a deep concavitas infracristalis (2). Not comparable for taxa with an extremely bilaterally compressed pelvis. *A. defossor* was coded as 1 based on AMNH 7300. *D. hawkinsi* was coded as 2 based on AMNH 7427. Livezey (1998), character 286.
273. Pelvis. Postacetabular ilium and ischium, lateral face, fusion, status: unfused posteriorly (0); fused posteriorly, ilioischiatric fenestra closed (1). *A. defossor* was coded as 1 based on AMNH 7300. *D. hawkinsi* was coded as 1 based on AMNH 7427. Cracraft and Clarke (2001), character 27.
274. Pelvis. Postacetabular ilium, lateral face, lamina infracristalis ilii, concavitas infracristalis, status: absent or barely discernable (0); present (1). *A. defossor* was coded as 1 based on AMNH 7300. *D. hawkinsi* was coded as 1 based on AMNH 7427. Livezey and Zusi (2006), character 1880.
275. Postacetabular ilium and ischium, lateral aspect, synchondrosis ilioischiadica, form: extremely smooth, barely visible or absent (1); linelike and distinctly etched craniocaudally or cranioventrally (2). *A. defossor* was coded as 2 based on AMNH 7300. *D. hawkinsi* was coded as 1 based on AMNH 7427. Livezey and Zusi (2006), character 1952.
276. Postacetabular ilium and ischium, lateral aspect, deep incisura in caudal margin, status: absent (0); present (1). Not comparable for Tinamiformes. *A. defossor* was coded as 0 based on AMNH 7300. *D. hawkinsi* was coded as 0 based on AMNH 7427. Livezey and Zusi (2006), character 1787.
277. Postacetabular ilium and ischium, lateral aspect, incisura in caudal margin of pelvis, dorsoventral height relative to diameter of acetabulum, status and form: absent or obsolete where incisura width less than that of acetabulum (0); present, narrow, maximal dorsoventral height equal to the diameter of acetabulum (1); present, wide, maximal dorsoventral height greater than diameter of acetabulum (2). Not comparable for Tinamiformes. *A. defossor* was coded as 1 based on AMNH 7300. *D. hawkinsi* was coded as 0 based on AMNH 7427. Livezey and Zusi (2006), character 1806.
278. Postacetabular ilium and ischium, lateral aspect, caudal margin, caudal extent of ilium relative to that of ischium, form: ilium distinctly cranial to ischium, characterized by distinct angular indentation proximate to the terminus caudalis of ilioischadic suture (1); ischium distinctly cranial to ilium, collectively defining an obliquely sloping caudal margin of pelvis exclusive of spina dorso-

- lateralis ilii and incisura marginis caudalis, if present (2); subequal (3). Not comparable for Tinamiformes. *A. defossor* was coded as 3 based on AMNH 7300. *D. hawkinsi* was coded as 2 based on AMNH 7427. Livezey and Zusi (2006), character 1892.
279. Preacetabular synsacrum, ventral aspect, large spine protruding from cranial portion, status: absent (0); present (1). *A. defossor* was coded as 1 based on AMNH 7300. *D. hawkinsi* was coded as 0 based on AMNH 7427.
280. Acetabular synsacrum, ankylosis of acetabular transverse process (often synostotic) to acetabular area beyond lateral margin of synsacrum, status and site: absent, transverse process does not ankylose to acetabular area (0); present, ankyloses to dorsal margin of acetabulum, often within dorso-caudal margin of the acetabulum (1); present, ankyloses to craniodorsal margin of ilioischadic foramen with variable separation between acetabulum and ankylosis, accompanied by sessile concavity between ankylosis and margin of acetabulum (2); present, ankyloses to ventral site between caudal acetabular margin and cranial margin of ilioischadic foramen, ankylosed to pila that extends from ankyloses between the ilioischadic foramen toward the dorsal margin of the obturator foramen (3). Noncomparable for Tinamiformes. *A. defossor* was coded as 2 based on AMNH 7300. *D. hawkinsi* was coded as 2 based on AMNH 7427.
281. Preacetabular synsacrum, ventral aspect, degree of fusion of two caudalmost transverse processes of synsacrum ankylosing with preacetabular ilium, form: last (caudalmost) one to two processes not fully fused, vestigial linelike suture site of ankylosis apparent (1); all processes completely fused, no linelike sutures discernable (2). *A. defossor* was coded as 2 based on AMNH 7300. *D. hawkinsi* was coded as 1 based on AMNH 7427.
282. Preacetabular and acetabular synsacrum, ventral aspect, ventral sulcus of synsacrum, status: present (1); lost or barely discernable (2). *A. defossor* was coded as 1 based on AMNH 7300. *D. hawkinsi* was coded as 2 based on AMNH 7427.
283. Postacetabular ischium, ventral aspect, foramen in oblique iliac crest, status: present (1); lost (2). *A. defossor* was coded as 2 based on AMNH 7300. *D. hawkinsi* was coded as 2 based on AMNH 7427.
284. Postacetabular synsacrum and fossa renalis, ventral aspect, degree of depression: postacetabular portion of synsacrum depressed dorsally, fossa renalis shallow (1); postacetabular portion of synsacrum raised ventrally, fossa renalis distinctly deeper (2). *A. defossor* was coded as 2 based on AMNH 7300. *D. hawkinsi* was coded as 2 based on AMNH 7427. Livezey and Zusi (2006), character 1793.
285. Postacetabular synsacrum, ventral aspect, processus transverses, at articulation with ala postacetabularis ilii, medial margin, status and form: no vertebrae modified as in states 2–4 (1); three or more vertebrae craniocaudally broadened, ventrally prominent, accommodating dorsally (with medial margin) a caudal extension of fossa renalis, recessus iliacus (2); two vertebrae craniocaudally broadened, ventrally prominent, accommodating dorsally (with medial margin) a caudal extension of fossa renalis, recessus iliacus (3); one vertebrae craniocaudally broadened, ventrally prominent, accommodating dorsally (with medial margin) a caudal extension of fossa renalis, recessus iliacus (4). Note: count does not include cranialmost, variably synostotic vertebra caudalis. *A. defossor* was coded as 2 based on AMNH 7300. *D. hawkinsi* was coded as 4 based on AMNH 7427. Livezey (1998), character 125.
286. Postacetabular ilium and ischium, ventral aspect, fossa renalis and recessus caudalis fossae, form: absent (0); relatively shallow, not extending beyond caudal margin of ilium (1); deeply recessed, extending beyond caudal margin of ilium (2). *A. defossor* was coded as 1 based on AMNH 7300. *D. hawkinsi* was coded as 0 based on AMNH 7427. Livezey (1998), character 1802.

287. Postacetabular ilium, ventral aspect, caudal margin, ovoid groove along medial margin of ilium, status: absent (0); present (1). *A. defossor* was coded as 1 based on AMNH 7300. *D. hawkinsi* was coded as 0 based on AMNH 7427.
288. Postacetabular ilium, ventral aspect, especially caudal margin, degree of lateromedial compression: somewhat lateromedially compressed, creating a narrow medial fenestra with modestly bowed ilii, typically creating a semicircular fenestra (1); extremely laterally splayed, so that medial fenestra wide due to laterally bowed caudal margin of ischium (2); extremely lateromedially compressed, creating a narrow medial fenestra constrained by almost 180° caudal margins of the ala ilii more or less in line with the caudal portion of the synsacrum (3). *A. defossor* was coded as 3 based on AMNH 7300. *D. hawkinsi* was coded as 2 based on AMNH 7427.
289. Postacetabular synsacrum and ischium, ventral aspect, caudal margin of ischium, in relation to caudal portion of synsacrum, form: caudal portion of synsacrum separating from and continuing caudally past caudal margin of ischium and splaying laterally towards apex (1); caudal portion of synsacrum fused to caudal margin of ischium completely, ending with the ischium (2); caudal portion of synsacrum separating from and continuing caudally past caudal margin of ischium and tapered toward apex (3). *A. defossor* was coded as 3 based on AMNH 7300. *D. hawkinsi* was coded as 2 based on AMNH 7427.
290. Postacetabular synsacrum, ventral aspect, caudalmost portion of synsacrum, foramen, status and form: large and ovoid (1); small and circular (2); foramen lost (3). *A. defossor* was coded as 2 based on AMNH 7300. *D. hawkinsi* was coded as 1 based on AMNH 7427. Livezey and Zusi (2006), character 956.
291. Postacetabular ilium, ventral aspect, processus marginis caudalis, status and form: absent or obsolete (0); present, of varying prominence, often present as rounded eminentia (1); present, prominent, but imbedded as pila within membrana ossificans (2). *A. defossor* was coded as 1 based on AMNH 7300. *D. hawkinsi* was coded as 1 based on AMNH 7427. Livezey and Zusi (2006), character 1808.
292. Postacetabular ilium, ventral aspect, processus marginis caudalis delimited by raised crest on most caudal portion of postacetabular region and accompanying depression, form of laterocaudal portion: essentially absent, no extraneous demarcation apparent (0); semicircular depression delimited by shallow crest on dorsal face of postacetabular ilium, oriented superioinferiorly (1); semicircular depression delimited by shallow crest on medioventral face of postacetabular ilium, oriented medio-laterally (2); semicircular depression delimited by shallow crest on laterodorsal face of postacetabular ilium, oriented lateromedially with varying cranial expansion (3); acuminate depression delimited by shallow crest on laterodorsal face of postacetabular ilium (4). *A. defossor* was coded as 3 based on AMNH 7300. *D. hawkinsi* was coded as 0 based on AMNH 7427.
293. Scapus pubis, lateral aspect, fusion to postacetabular ischium, status and form: pubis separated significantly from postacetabular ischium, remaining completely unfused (1); maintains extreme proximity to postacetabular ischium, typically fused to it completely along the length of the ischium (2); remains largely fused as in state 2 but with a significant medial portion unfused, creating an elongate fenestra (3). *A. defossor* was coded as 1 based on AMNH 7300. *D. hawkinsi* was coded as 1 based on AMNH 7427.
294. Scapus pubis, exclusive of marked departures in apex, dorsal margin, dorsoventral form: recurved, dorsal margin variably concave (1); essentially straight or sigmoid, approximately aligned with major axis of apex of pubis (2); decurved, dorsal margin convex (3). *A. defossor* was coded as 1 based on AMNH 7300. Livezey and Zusi (2006), character 1928.

295. Scapus and apex of pubis, length of extension beyond pubis: pubis not extending beyond caudal portion of ischium or, if it does, makes up less than one third of entire length of pubis (1); portion extending beyond caudal portion of ischium makes up at least one third that of entire length of pubis or more (2). *A. defossor* was coded as 1 based on AMNH 7300. Livezey and Zusi (2006), character 1901.
296. Apex of pubis, form: projecting dorsally (1); projecting ventrally (2). *A. defossor* was coded as 1 based on AMNH 7300. *D. hawkinsi* was coded as 1 based on AMNH 7427. Livezey and Zusi (2006), character 1945.
297. Apex of pubis, dorsomedial form, status: dorsoventrally spatulate (1); spatulation negligible, scapus pubis and apex pubis subparallel along ventral and dorsal margins (2). *A. defossor* was coded as 2 based on AMNH 7300. Livezey and Zusi (2006), character 1940.

HINDLIMBS

298. Femur and tibiotarsus, intratendinous ossification, status: absent (0); present (1). Bertelli et al. (2011), character 80.

FEMUR

299. Proximal femur, crista trochanteris, projection: markedly projected cranially (1); shallow, somewhat projected cranially (2); shallow, laterally flattened (3). *A. defossor* was coded as 2 based on AMNH 7300. *D. hawkinsi* was coded as 1 based on AMNH 7428. Mayr and Clarke (2003), character 97.
300. Proximal femur, caudal aspect, crista trochanteris, distal to facies articularis antitrochantericus, form: thickening weakly developed (1); lacking distinct, distal thickening (2). *A. defossor* was coded as 1 based on AMNH 7300. *D. hawkinsi* was coded as 1 based on AMNH 7428. Livezey (1998), character 301.
301. Proximal femur, fossa trochantericus, status: lost or shallow (1); present, deep, extending across entire width of facies articularis antitrochantericus (2). *A. defossor* was coded as 2 based on AMNH 7300. *D. hawkinsi* was coded as 1 based on AMNH 7428. Livezey and Zusi (2006), character 1978.
302. Proximal femur, caudal aspect, impressiones obturatoriae, form: craniocaudally oriented, elongate, deep (1); circular, most cranial impression larger than caudal impression(s) (2); large, lateromedially elongate, especially most cranial impression (3); small, circular, impression sizes subequal (4); essentially obsolete (5). *A. defossor* was coded as 3 based on AMNH 7300. *D. hawkinsi* was coded as 4 based on AMNH 7428.
303. Proximal femur, collum femoris, facies articularis antitrochanterica, caudal margin, form: located at 90° angle to femoral body (1); projecting proximally (2). *A. defossor* was coded as 1 based on AMNH 7300. *D. hawkinsi* was coded as 1 based on AMNH 7428. Livezey and Zusi (2006), character 1975.
304. Shaft of femur, caudal aspect, lineae intermuscularis, delimitation of subtriangular planum or depressio suprapoplitea between linea intermusculares distal to bifurcatio linea, status: shallow or absent (0); present (1). *A. defossor* was coded as 0 based on AMNH 7300. *D. hawkinsi* was coded as 0 based on AMNH 7428. Livezey and Zusi (2006), character 2004.
305. Distal femur, cranial aspect, Sulcus patellaris, proximal region, ovate accessory subfossa, status: absent (0); present (1). *A. defossor* was coded as 0 based on AMNH 7300. *D. hawkinsi* was coded as 0 based on AMNH 7428. Livezey and Zusi (2006), character 2039.

306. Distal femur, caudal aspect, fossa poplitea, form: shallow, weakly delimited (1); deep (2). *A. defossor* was coded as 2 based on AMNH 7300. *D. hawkinsi* was coded as 1 based on AMNH 7428. Livezey and Zusi (2006), character 2047.
307. Distal femur, caudal aspect, fossa poplitea, foramen pneumaticum, form: small, round (1); large, craniocaudally elongate (2). *A. defossor* was coded as 1 based on AMNH 7300. *D. hawkinsi* was coded as 2 based on AMNH 7428. Livezey and Zusi (2006), character 2048.
308. Distal femur, caudal aspect, tuberculum m. gastrocnemius pars lateralis, form: smooth, shallow (1); sharp, anteriorly oriented semicircular crest (2). *A. defossor* was coded as 1 based on AMNH 7300. *D. hawkinsi* was coded as 1 based on AMNH 7428. Livezey and Zusi (2006), character 2029.
309. Distal femur, caudal aspect, impressio ansae m. iliofibularis, site: located caudally and more distally (1); located laterally and more anteriorly (2). *A. defossor* was coded as 2 based on AMNH 7300. *D. hawkinsi* was coded as 1 based on AMNH 7428. Worthy and Scofield (2012), character 127.
310. Distal femur, caudal aspect, impressio ansae m. iliofibularis, form: ovoid (1); circular (2). *A. defossor* was coded as 2 based on AMNH 7300. *D. hawkinsi* was coded as 1 based on AMNH 7428. Worthy (2012), character 127.
311. Distal femur, cranial aspect, epicondylus medialis, cranioproximal terminus on corpus femoris, site: prominently elevated, typically tubercular (1); not prominently elevated, with smooth gradation (2). *A. defossor* was coded as 2 based on AMNH 7300. *D. hawkinsi* was coded as 2 based on AMNH 7428. Livezey (1998), character 308.
312. Distal femur, caudal aspect, condylus lateralis, crista tibiofibularis, distal extent relative to condylus medialis, magnitude: subequal to condylus medialis (1); distal to condylus medialis (2). *A. defossor* was coded as 2 based on AMNH 7300. *D. hawkinsi* was coded as 2 based on AMNH 7428. Livezey and Zusi (2006), character 2012.
313. Distal femur, caudal and distal aspects, condylus lateralis, trochlea fibularis, entire trochlea of greater caudal prominence and lateromedial divergence from corpus than condylus medialis, status: absent (0); present (1). *A. defossor* was coded as 0 based on AMNH 7300. *D. hawkinsi* was coded as 0 based on AMNH 7428. Livezey and Zusi (2006), character 2017.
314. Distal femur, caudal aspect, condylus lateralis, lateromedial width relative to that of condylus medialis, form: subequal (1); condylus lateralis significantly wider (2); condylus lateralis significantly narrower (3). *A. defossor* was coded as 3 based on AMNH 7300. *D. hawkinsi* was coded as 3 based on AMNH 7428. Livezey and Zusi (2006), character 2027.
315. Distal femur, caudal aspect, condylus lateralis, relative proximodistal position of the proximal termini of the crista tibiofibularis and trochlea fibularis, form: proximal terminus of crista tibiofibularis located more proximally than that of trochlea fibularis (1); subequal (2). *A. defossor* was coded as 1 based on AMNH 7300. *D. hawkinsi* was coded as 1 based on AMNH 7428. Livezey and Zusi (2006), character 2010.
316. Distal femur, caudal aspect, condylus medialis, general form: spherical, distal portion greatly rounded, extremely convex (1); triangular, distal portion somewhat rounded (2). *A. defossor* was coded as 2 based on AMNH 7300. *D. hawkinsi* was coded as 2 based on AMNH 7428. Livezey and Zusi (2006), character 2030.
317. Distal femur, medial and cranial aspects, condylus medialis, proximal terminus, form: abrupt, sub-perpendicular or acuminate (1); comparatively gradual (2). *A. defossor* was coded as 1 based on AMNH 7300. *D. hawkinsi* was coded as 1 based on AMNH 7428. Livezey and Zusi (2006), character 2032.

318. Distal femur, medial and caudal aspects, condylus medialis, crista supracondylaris medialis, form relative to condylus medialis and facies caudalis corporis: absent or rudimentary, condylus not extended by crista, caused by one distinct (often abrupt) angle or incision above the condylus medialis, rarely also a second one present (comparatively proximal), interrupting an otherwise gradual curving crest (1); present and prominent, condylus medialis continued by crest without interruption by angle or incision above the condylus medialis (2). *A. defossor* was coded as 2 based on AMNH 7300. *D. hawkinsi* was coded as 2 based on AMNH 7428. Livezey and Zusi (2006), character 2042.
319. Distal femur, cranial aspect, fovea tendineus m. tibialis cranialis, form: large, round or ovoid (1); small, ovoid (2); small, circular (3). *A. defossor* was coded as 2 based on AMNH 7300. *D. hawkinsi* was coded as 2 based on AMNH 7428.
320. Distal femur, cranial aspect, site of fovea tendineus m. tibialis cranialis: anterior (1); posterior (2). *A. defossor* was coded as 1 based on AMNH 7300. *D. hawkinsi* was coded as 1 based on AMNH 7428.

TIBIOTARSUS

321. Proximal tibiotarsus, head, fossa retropatellaris, status: present, shallow (1); present, deep (2); lost (3). *A. defossor* was coded as 2 based on AMNH 7300. *D. hawkinsi* was coded as 1 based on AMNH 7429. Livezey and Zusi (2006), character 2112.
322. Proximal tibiotarsus, head, fossa retropatellaris or homologous site, ostia pneumatica—recess and/or foramina (pori) pneumatici, status and form: present, limited to foramina and/or pori (1); lost, neither recess nor separate foramina/pori evident (2). *A. defossor* was coded as 1 based on AMNH 7300. *D. hawkinsi* was coded as 1 based on AMNH 7429. Livezey and Zusi (2006), character 2113.
323. Proximal tibiotarsus, caudal aspect, head of tibiotarsus, interarticular area, incisura in caudal aspect of interarticular area delimiting facies articularis medialis, status: present (1); lost (2). *A. defossor* was coded as 2 based on AMNH 7300. *D. hawkinsi* was coded as 1 based on AMNH 7429.
324. Proximal tibiotarsus, caudal aspect, foramen pneumaticum underneath jugum between facies articularis lateralis and area interarticularis, status and number: present, 1 (1); present, 2 or more (2); lost (3). *A. defossor* was coded as 2 based on AMNH 7300.
325. Proximal tibiotarsus, head, cristae cnemiales, substantial reduction or virtual absence of both cristae (typically in both proximal and craniocaudal dimensions), status: absent (0); present (1). *A. defossor* was coded as 0 based on AMNH 7300. *D. hawkinsi* was coded as 0 based on AMNH 7429. Livezey and Zusi (2006), character 2069.
326. Proximal tibiotarsus, head, cristae cnemiales cranialis and lateralis, exceptional, proximodistally extensive cranial prominence and lateral concavity of crista cnemialis cranialis, status: absent (0); present (1). *A. defossor* was coded as 0 based on AMNH 7300. *D. hawkinsi* was coded as 0 based on AMNH 7429. Livezey and Zusi (2006), character 2076.
327. Proximal tibiotarsus, head, cristae cnemiales cranialis and lateralis, cranial and lateral margins, respectively, reinforced with thickened jugae, status: absent (0); present (1). *A. defossor* was coded as 0 based on AMNH 7300. *D. hawkinsi* was coded as 0 based on AMNH 7429. Livezey and Zusi (2006), character 2077.
328. Proximal tibiotarsus, head, crista cnemialis cranialis and lateralis, crista cnemialis lateralis, dorsal margin of cristae, lateral to intersection with crista cnemialis cranialis, marginal form: sigmoidal, convex laterally and concave medially (1); linear and variably sloping throughout (2); convex essentially throughout (3). *D. hawkinsi* was coded as 1 based on AMNH 7429. Livezey and Zusi (2006), character 2078.

329. Proximal tibiotarsus, head, crista cnemialis cranialis, pronounced lateral curvature especially proximally, status: present (1); lost (2). *A. defossor* was coded as 1 based on AMNH 7300. *D. hawkinsi* was coded as 1 based on AMNH 7429. Livezey and Zusi (2006), character 2082.
330. Proximal tibiotarsus, cnemial crest jugum relative to proximal terminus of fibular crest, form: proximal terminus well within margin of cnemial crest (1); proximal terminus located distal to most distal portion of cnemial crest jugum (2); proximal terminus in line with distal terminus of cnemial crest jugum (3). *A. defossor* was coded as 2 based on AMNH 7300. *D. hawkinsi* was coded as 2 based on AMNH 7429. Livezey and Zusi (2006), character 2085.
331. Proximal tibiotarsus, head, crista cnemialis lateralis, lateral prominence relative to articulated fibula: not lateral to fibular head (1); lateral to fibular head (2). Livezey and Zusi (2006), character 2094.
332. Proximal tibiotarsus, head, cristae cnemiales cranialis and lateralis, comparative distal extents on body of tibiotarsus, form: cristae cnemiales cranialis terminating distal to crista lateralis (1); cristae subequal in distal extent (typically truncated), both lacking jugae (2). Not comparable for *Phaethon* and Caprimulgiformes. *A. defossor* was coded as 1 based on AMNH 7300. *D. hawkinsi* was coded as 2 based on AMNH 7429. Livezey and Zusi (2006), character 2099.
333. Proximal fibula, head, form and position relative to head of tibiotarsus: elongate and extending past interarticular area (1); essentially circular, from proximal view not extending past interarticular area (2). *A. defossor* was coded as 2 based on AMNH 7300.
334. Proximal tibiotarsus, head, facies articularis fibularis, status and form: present, shallow incisura (1); present, short jugum extending distally from margin of the head and/or distinct lateral extension of the rim of the head (2). *A. defossor* was coded as 2 based on AMNH 7300. *D. hawkinsi* was coded as 2 based on AMNH 7429. Livezey and Zusi (2006), character 2108.
335. Shaft of tibiotarsus, lateral margin, foramen interosseum proximale, form: sublinear and incisurate, relatively narrow (1); approximately ovate, relatively spacious (2). Livezey and Zusi (2006), character 2128.
336. Shaft of tibiotarsus, lateral margin, foramen interosseum distale, length as compared with length of the tibiotarsus: more than one fourth the length of the tibiotarsus (1); less than one fourth the length of tibiotarsus (2); exactly one fourth the length of tibiotarsus (3). *A. defossor* was coded as 1 based on AMNH 7300. Livezey and Zusi (2006), character 2129.
337. Distal tibiotarsus, caudal aspect, epicondylus medialis, form: pronounced (1); lost or barely visible (2). *A. defossor* was coded as 1 based on AMNH 7300. *D. hawkinsi* was coded as 1 based on AMNH 7429. Livezey and Zusi (2006), character 2046.
338. Distal tibiotarsus, caudal aspect, trochlea cartilaginis tibialis, lateral and medial margins: splayed laterally (1); medially compressed (2). *A. defossor* was coded as 1 based on AMNH 7300. *D. hawkinsi* was coded as 2 based on AMNH 7429.
339. Distal tibiotarsus, caudal aspect, trochlea cartilaginis tibialis, height, form: craniocaudally short (1); craniocaudally elongate (2). *A. defossor* was coded as 1 based on AMNH 7300. *D. hawkinsi* was coded as 2 based on AMNH 7429.
340. Distal tibiotarsus, caudal aspect, trochlea cartilaginis tibialis, medial portion, rectangular, medially oriented projection on medial margin: absent (0); present (1). *A. defossor* was coded as 0 based on AMNH 7300. *D. hawkinsi* was coded as 0 based on AMNH 7429.
341. Distal tibiotarsus, lateral perspective, condylus lateralis, depressio epicondylaris lateralis, form: shallow, rim of condylus lateralis not raised much more than lateral epicondylar impression (1); deeply pitted, condylus lateralis distinctly protruding, like state 3, but no accessory depression present (2); shallowly depressed cranially with smaller, circular accessory located toward cranial margin, rim

typically raised (3). *A. defossor* was coded as 2 based on AMNH 7300. *D. hawkinsi* was coded as 1 based on AMNH 7429.

342. Distal tibiotarsus, cranial aspect, condylus medialis and condylus lateralis, relative positions: pulled in medially (1); splayed laterally (2). *A. defossor* was coded as 2 based on AMNH 7300. *D. hawkinsi* was coded as 2 based on AMNH 7429.
343. Distal tibiotarsus, cranial aspect, condylus medialis and condylus lateralis, relative size: condylus medialis distinctly smaller than condylus lateralis (1); subequal (2). *A. defossor* was coded as 1 based on AMNH 7300. *D. hawkinsi* was coded as 1 based on AMNH 7429. Livezey and Zusi (2006), characters 2144 and 2145.
344. Distal tibiotarsus, distal aspect, condylus medialis and condylus lateralis, incisura intercondylaris, foveae (sulcus) transcondylares medialis and lateralis, status: present (1); lost (2). *A. defossor* was coded as 1 based on AMNH 7300. *D. hawkinsi* was coded as 1 based on AMNH 7429. Livezey and Zusi (2006), character 2155.
345. Distal tibiotarsus, cranial aspect, tuberculum ligamenti tibiometatarsale intercondylare, status: absent (0); present (1). *A. defossor* was coded as 0 based on AMNH 7300. *D. hawkinsi* was coded as 1 based on AMNH 7429. Livezey and Zusi (2006), character 2137.

TARSOMETATARSUS

346. Proximal tarsometatarsus, dorsal aspect, cotyla lateralis and cotyla medialis, relative proximal elevation, site: cotyla lateralis distinctly distal to cotyla medialis (1); cotyla lateralis subequal to cotyla medialis (2); cotyla medialis distal to cotyla lateralis (3). *A. defossor* was coded as 1 based on AMNH 7300. Livezey and Zusi (2006), character 2250.
347. Proximal tarsometatarsus, fossa parahypotarsalis lateralis, status: shallow or absent (0); deep (1). *A. defossor* was coded as 0 based on AMNH 7300. Livezey and Zusi (2006), character 2258.
348. Proximal tarsometatarsus, fossa parahypotarsalis medialis, status and form: shallow or barely visible (1); deep (2). *A. defossor* was coded as 1 based on AMNH 7300. Livezey and Zusi (2006), character 2257.
349. Proximal tarsometatarsus, plantar aspect, hypotarsus, lamina medialis hypotarsi (refers to total dorsoplantar lamina, including exposed crista, plantar to corpus tarsometatarsi, facies plantaris), plantar prominence relative to corpus tarsometatarsi, magnitude: greater than or equal to plantar prominence of lamina lateralis hypotarsi (1); less than plantar prominence of lamina lateralis hypotarsi (2). *A. defossor* was coded as 1 based on AMNH 7300. Livezey (1998), character 336.
350. Proximal tarsometatarsus, plantar aspect, crista medialis hypotarsi and crista lateralis hypotarsi, form: fused, so that foramina hypotarsi formed instead of just a sulcus (1); separated (2). *A. defossor* was coded as 1 based on AMNH 7300. Mayr and Clarke (2003), character 103; Livezey and Zusi (2006), characters 2284, 2285, and 2286.
351. Proximal tarsometatarsus, hypotarsus, sulcus and/or canalis hypotarsi, number: 2 (1); 1 (2); 3 (3). *A. defossor* was coded as 2 based on AMNH 7300. Livezey and Zusi (2006), character 2284.
352. Proximal tarsometatarsus, hypotarsus, hypotarsus tendon of musculus flexor perforatus digiti II furrow/canal for tendon of musculus flexor perforatus digiti II, form: medial hypotarsal crest of higher height than lateral crest (1); essentially equal in size (2); marked and laterally bordered by a proximodistally long and plantarly protruding crista lateralis (3). *A. defossor* was coded as 2 based on AMNH 7300. Bertelli et al. (2011), character 75.
353. Proximal tarsometatarsus, dorsal aspect, foramina vascularia proximalia, form: subequal in height (1); lateral foramina distal to medial foramina (2). *A. defossor* was coded as 1 based on AMNH 7300. Livezey and Zusi (2006), character 2264.

354. Proximal tarsometatarsus, dorsal aspect, fossa infracotyloidalis dorsalis, form: extremely deep and small, circular (1); significantly deeper than sulcus extensorius (2); coplanar with sulcus extensorius, depth is approximately equal (3). *A. defossor* was coded as 2 based on AMNH 7300. Livezey and Zusi (2006), character 2259.
355. Proximal tarsometatarsus, plantar aspect, foramina vascularia proximalia, form: each made up of one circular opening (1); lateral foramen made up of two circular openings (2). *A. defossor* was coded as 2 based on AMNH 7300. Livezey and Zusi (2006), character 2264.
356. Proximal tarsometatarsus, plantar aspect, foramina vascularia proximalia, form: lateral foramina distinctly distal to medial foramina (1); lateral and medial foramina about equal in height (2). *A. defossor* was coded as 2 based on AMNH 7300. Ksepka and Clarke (2012), character 78.
357. Shaft of tarsometatarsus, dorsal aspect, sulcus extensorius, status and form: present and delineated moderately by cristulae (1); lost or present but shallow (2); present, deep to cavernous cristulae on both sides (3). *A. defossor* was coded as 2 based on AMNH 7300. Livezey and Zusi (2006), character 2305.
358. Shaft of tarsometatarsus, plantar aspect, metatarsi I, status and form: lost and/or now a fossa, shaft of tarsometatarsus appears smooth and gracile (1); extremely prominent, located roughly halfway between proximal and distal end of the tarsometatarsus (2); present as jugum connecting metatarsi I to crista medialis hypotarsi (3). *A. defossor* was coded as 3 based on AMNH 7300. Livezey and Zusi (2006), character 2312.
359. Shaft of tarsometatarsus, plantar aspect, metatarsi I, fossa (if present), depth, form: shallow (1); deep (2). Not comparable for taxa with metatarsi I eminentia. *A. defossor* was coded as 2 based on AMNH 7300. Livezey and Zusi (2006), character 2312.
360. Distal tarsometatarsus, foramen vasculare distale, form sensu dorsoplantar orientation relative to major axis shaft, form: subperpendicular, essentially directly dorsoplantar, unobstructed perpendicular line of sight (1); oblique, distinctly ventrodorsal, obstructed perpendicular line of sight (2). Not comparable for Spheniscidae. *A. defossor* was coded as 1 based on AMNH 7300. Livezey and Zusi (2006), character 2317.
361. Distal tarsometatarsus, foramen vasculare distale, site in which foramen perforates tarsometatarsus relative to approximate major axis: lateral (1); central (2). Not comparable for Spheniscidae. *A. defossor* was coded as 1 based on AMNH 7300. Livezey and Zusi (2006), character 2320.
362. Distal tarsometatarsus, canalis and sulcus interosseus intertrochlearis tendineus distalis (foramen tendinis m. extensor brevis digiti IV), dorsal form: foramen continued distally by dorsoventrally exposed sulcus tendineus, including taxa lacking foramen distale (1); foramen continued distally by complete canalis tendineus (2). *A. defossor* was coded as 1 based on AMNH 7300. Livezey and Zusi (2006), character 2325.
363. Distal tarsometatarsus, plantar aspect, fossa supratrochlearis plantaris, status: absent or indistinct (0); present, distinctly concave (1). *A. defossor* was coded as 0 based on AMNH 7300. Livezey and Zusi (2006), character 2329.
364. Distal tarsometatarsus, metatarsal II trochlea, eminentia (medio) plantaris, status: absent (0); present (1). *A. defossor* was coded as 1 based on AMNH 7300. Livezey and Zusi (2006), character 2352.
365. Distal tarsometatarsus, dorsal aspect, metatarsal III trochlea, length as compared to that of body of tarsometatarsus: length from proximal to distal end less than one fifth length of entire tarsometatarsus from top of eminentia intercotylaris to extreme caudal end of metatarsal III trochlea (1); length from proximal to distal end one fifth or greater than length of entire tarsometatarsus from

- top of eminentia intercotylaris to caudal end of metatarsal III trochlea (2). *A. defossor* was coded as 2 based on AMNH 7300.
366. Distal tarsometatarsus, metatarsal IV trochlea, foveae ligamentorum collateralium, status and form in terms of depth and width: present, moderate depression (1); small, shallow, almost absent (2). *A. defossor* was coded as 1 based on AMNH 7300. Livezey and Zusi (2006), character 2349.
367. Distal tarsometatarsus, distal aspect, metatarsal II–IV trochleae, relative dorsal elevations: II<III ≥IV and II<IV (1); II<III>IV (2); II>III ≥IV (3); II=III=IV (4). *A. defossor* was coded as 1 based on AMNH 7300. Livezey and Zusi (2006), character 2363.
368. Distal tarsometatarsus, metatarsal II trochlea, facies articularis phalangealis, sulcus trochlearis (narrow groove between lateral and medial rims of trochlea), form: remains distinct on dorsal face (1); obsolete on dorsal face, terminating medially toward fovea ligamentorum collateralium at distal apex of trochlea (2). *A. defossor* was coded as 2 based on AMNH 7300. Livezey (1998), character 354.

All issues of *Novitates* and *Bulletin* are available on the web (<http://digitalibrary.amnh.org/dspace>). Order printed copies on the web from:

<http://shop.amnh.org/a701/shop-by-category/books/scientific-publications.html>

or via standard mail from:

American Museum of Natural History—Scientific Publications
Central Park West at 79th Street
New York, NY 10024

Ⓢ This paper meets the requirements of ANSI/NISO Z39.48-1992 (permanence of paper).